To the Graduate Council:

I am submitting herewith a thesis written by Matthew T. Dale entitled "The Novel Use of the Urbanski-Colburn Valve for Liquid Bi-Propellant Rocket Engines." I have examined the final paper copy of this thesis for form and content and recommend that it be accepted in partial fulfillment of the requirements for the degree of Master of Science, with a major in Aerospace Engineering.

_____

Dr. Evans Lyne, Major Professor

We have read this thesis
and recommend its acceptance:

_____

Committee Member 1

_____

Committee Member 2

_____

Committee Member 3

Accepted for the Council:

_____

Dixie L. Thompson

Vice Provost and Dean of the Graduate School

To the Graduate Council:
I am submitting herewith a thesis written by Matthew T. Dale entitled "The Novel Use of the Urbanski-Colburn Valve for Liquid Bi-Propellant Rocket Engines." I have examined the final electronic copy of this thesis for form and content and recommend that it be accepted in partial fulfillment of the requirements for the degree of Master of Science, with a major in Aerospace Engineering.

Dr. Evans Lyne, Major Professor

We have read this thesis
and recommend its acceptance:

Committee Member 1

Committee Member 2

Committee Member 3

Accepted for the Council:

Dixie L. Thompson

Vice Provost and Dean of the Graduate School

(Original signatures are on file with official student records.)

The Novel Use of the Urbanski-Colburn Valve for Liquid Bi-Propellant Rocket Engines

A Thesis Presented for the

Master of Science

Degree

The University of Tennessee, Knoxville

Matthew T. Dale

August 2025

© by Matthew T. Dale, 2025
All Rights Reserved.

This thesis is dedicated to my late grandfathers, Dr. John K. Altier and Paul T. Dale. They both supported my curiosity at a young age and encouraged me to pursue my dreams. I will always cherish my memories with them. They are missed.

Acknowledgements

I would like to thank my friends, family, coworkers, fellow students, and professors who have helped me throughout this journey. Thank you to the University of Tennessee for providing funding to the Student Space Technology Association which supported the development of this thesis. I would also like to thank the members of SSTA, along with the senior design classes of 2023 and 2024, for helping to make this thesis possible. A special thank you to Dr. Evans Lyne for providing guidance and instruction throughout my time as a graduate student. I would also like to recognize and thank Dr. Trevor Moeller and Dr. David Icove for their feedback and for serving on my committee. Finally, I would like to thank my parents, Tom and Mara, for their love and support over all these years; without you, this would never have been possible.

Abstract

Liquid bi-propellant rockets have been in use since the early 20th century, but their complexity and risk of bodily harm have kept all but the most advanced and well-funded institutions from attempting to design and build them. Liquid rockets are the most cost-effective and efficient source of transporting materials from the earth's surface to space. Typically, the infrastructure supporting these rockets is just as large, if not larger than, the rocket it is supporting. In this thesis a new, much less complex, and more cost efficient way to fuel a liquid bi-propellant rocket is designed and tested. Through the use of the Urbanski-Colburn valve, a floating injector baffle within the rocket, and nylon fill lines, the total infrastructure surrounding the liquid rocket can be greatly reduced.

A 3 inch diameter liquid-bipropellant rocket engine was developed to test this theory. The engine used a mixture of 70% ethanol and nitrous oxide as the fuel and oxidizer. The unlike-pentad injector design provided a 4:1 oxidizer to fuel mixture through the use of orifices and push-to-connect injectors. An igniter was developed to simultaneously burn away the fuel and oxidizer fill lines and begin the combustion process in the combustion chamber. After a year's long test fire campaign, it was found that the Urbanski-Colburn valve could be utilized in the case of liquid bi-propellant rockets. The final test fire of the campaign provided the following results: thrust: 188 pounds; specific impulse: 119 seconds; total impulse 810 pound-seconds.

Table of Contents

1 Introduction **1**

1.1 A Brief History of Rocketry 1

1.2 Umbilical Towers and Fuel Systems 2

1.3 Student Rocketry 3

2 Background **6**

2.1 The Inception of the Urbanski-Colbrun Valve 6

2.2 Prior Use of the UC Valve at the University of Tennessee 9

3 Methodology **15**

3.1 Quasi-One-Dimensional Flow 15

3.2 Injector Flow Characteristics 17

3.3 Rocket Equations 19

4 Design and Manufacturing **22**

4.1 Design Constraints 22

4.2 Fuel and Oxidizer Tank Design 25

4.3 Nozzle Design 27

4.4 Injector Design 29

4.5 Igniter Design 34

4.5.1 Igniter Cup Fabrication 34

4.5.2 Igniter Ignition 37

4.5.3 Igniter Safety Concerns . . . 40
4.5.4 Igniter Design Process . . . 40
4.6 Engine Simulation . . . 44

5 Component Testing and Test Stand Setup 46
5.1 Injector Testing . . . 46
5.2 Ignition Cup Testing . . . 50
5.3 Fuel and Oxidizer Tank Pressure Testing . . . 52
5.4 Engine Assembly . . . 55
5.5 Test Stand Assembly . . . 62
5.6 Data Acquisition . . . 67

6 Experimental Results 70
6.1 Liquid Motor Test Fire Sequence . . . 70
6.2 Test Fire Results . . . 72
6.2.1 May 2, 2023 Test Fire . . . 72
6.2.2 May 11, 2023 Test Fire . . . 77
6.2.3 February 27, 2024 Test Fire . . . 80
6.2.4 April 11, 2024 Test Fire . . . 85

7 Conclusion 90
7.1 Summary . . . 90
7.2 Future Work . . . 92

Bibliography 94

A Igniter Designs 99

B Post Test Fire Engine Disassembly Pictures 108

C Liquid Engine Data Analysis Code 117

Vita **126**

List of Tables

4.1 Initial Constraints 23
4.2 Simulation Data 45
5.1 Test Stand Bill of Materials 64
6.1 Sim Data vs. Test Fire Data 89

List of Figures

1.1 Legacy Umbilical Examples 4

2.1 Urbanski-Colburn Hybrid Rocket Design 8
2.2 Contrail Rockets 3 Inch Injector Baffle 10
2.3 3 Inch Injector Baffle for the 2018-2019 UTK Spaceport America Cup Rocket 10
2.4 UTK 2019 Competition Rocket Motor Assembly, Total length = 39 inches 12
2.5 UC Valve and Ignition Cup for UTK 2022 Spaceport America Cup Rocket 13

4.1 Exploded View of the Vega Rocket Engine 24
4.2 Aft Section of Fuel and Oxidizer Tanks 26
4.3 Forward Section of Fuel and Oxidizer Tanks 26
4.4 Original Graphite Nozzle Design 28
4.5 CHAMBERSAFE Nozzle Casting 30
4.6 Diverging Side of Test Fired Nozzle (left) vs. Newly Cast Nozzle (right) 31
4.7 Converging Side of Test Fired Nozzle (left) vs. Newly Cast Nozzle (right) 31
4.8 Gill and Nurick Injector Comparison Table 33
4.9 Vega Injector Baffle Drawing (all dimensions in inches) 35
4.10 Vega Injector Baffle SolidWorks Model 36
4.11 Machined Injector with NPT Fittings Installed 36

4.12 Model of bridge wire in Electronic Match 38
4.13 Umbrella Igniter Design 41
4.14 Final Igniter Design 43

5.1 Injector Testing Apparatus 47
5.2 Injector Testing Apparatus 2 49
5.3 Injector Flow Testing, Proof of Mixed Flow 49
5.4 Igniter Test Set Up 51
5.5 Igniter Design 7 Test Burn 51
5.6 Motor Assembly for Hydrostatic Testing 54
5.7 Nitrogen Assembly for Hydrostatic Testing 54
5.8 Inter-stage Assembly 56
5.9 Combustion Chamber Assembly with Igniter and Nitrous Fill Lines . 57
5.10 Combustion Chamber Assembly with Igniter, Taped Nitrous Fill Lines, and Phenolic Liner 58
5.11 Combustion Chamber Cutaway 60
5.12 Forward Closure 61
5.13 Test Stand Apparatus 63
5.14 Ground Control Box Labeled with Flow Path 65
5.15 Ground Control Box Valves, Vent, and Power 65
5.16 Rocket Fill Piping and Instrumentation Diagram 66
5.17 Data Acquisition Box 68
5.18 Circuit Diagram of Data Acquisition Box 69

6.1 Engine Test Fire 5/2/23 Thrust vs. Time Data 73
6.2 Engine Test Fire 5/2/23 Pressure vs. Time Data 74
6.3 Injector Plug Configuration for 5/2/23 Test Fire 76
6.4 Injector Plug Configuration for 5/11/23 Test Fire 76
6.5 Engine Test Fire 5/11/23 Thrust vs. Time Data 78
6.6 Engine Test Fire 5/11/23 Pressure vs. Time Data 79

6.7 Injector with Nylon Tube Plugging Unused Oxidizer Lines (not to scale) 81
6.8 Engine Test Fire 2/27/24 Thrust vs. Time Data 82
6.9 Engine Test Fire 2/27/24 Engine Firing 84
6.10 Engine Test Fire 4/11/24 Engine Firing 86
6.11 Engine Test Fire 4/11/24 Thrust vs. Time Data 87
6.12 All Engine Test Fires Thrust vs. Time Data 88

A.1 Igniter 1 Design, OD = 1.88 in., Height = 1.35 in. 100
A.2 Igniter 2 Design, OD = 1.88 in., Height = 0.65 in. 101
A.3 Igniter 3 Design, OD = 1.88 in., Height = 1.30 in. 102
A.4 Igniter 7 Design, OD = 1.88 in., Height = 1.91 in. 103
A.5 Igniter 8 Design, OD = 2.1 in., Height = 3.2 in. 104
A.6 Igniter 9 Design, OD = 2.1 in., Height = 3.2 in. 105
A.7 Igniter 10 Design, OD = 2.1 in., Height = 3.2 in. 106
A.8 Igniter 11 Design, OD = 2.1 in., Height = 3.02 in. 107

B.1 Combustion Chamber post 5/2/23 Test Fire 109
B.2 Injector Post 5/2/23 Test Fire 109
B.3 Oxidizer Tank Post 5/2/23 Test Fire 110
B.4 Combustion Chamber Post 5/11/23 Test Fire 111
B.5 Combustion Chamber Alternate View Post 5/11/23 Test Fire 112
B.6 Injector Post 5/11/23 Test Fire 112
B.7 Oxidizer Tank Post 5/11/23 Test Fire 113
B.8 Nozzle Inlet Post 5/11/23 Test Fire 114
B.9 Nozzle Outlet Post 5/11/23 Test Fire 115
B.10 Nozzle Carrier Inlet Post 5/11/23 Test Fire 115
B.11 Nozzle Carrier Inlet Post 5/11/23 Test Fire 116

Nomenclature

δ	angle between chamber axis and average resultant stream, *degrees*
$\dot{m}$	mass flow rate, $\frac{lb}{s}$
γ	angle between chamber axis and stream, *degrees*
$_f$	fuel condition
$_{in}$	inlet condition
$_{out}$	outlet condition
$_o$	oxidizer condition
$_{total}$	total condition
A	cross-sectional area, in^2
C	exhaust velocity, $\frac{ft}{s}$
C_d	discharge coefficient
C_p	constant pressure specific heat, $\frac{BTU}{lbm*R}$
C_v	constant volume specific heat, $\frac{BTU}{lbm*R}$
CS	control surface
CV	control volume

F	thrust, lb
h	enthalpy, $\frac{BTU}{lbm}$
n	outward normal unit vector
p	pressure, psi
Q	volumetric flow rate, $\frac{ft^3}{s}$
R	universal gas constant, $\frac{ft-lbf}{lb-mol*R}$
r	mixture ratio
T	temperature, R, F
t_{burn}	motor burn time, s
V	volume, $inch^3$
v	velocity, $\frac{ft}{s}$
Δp	change in pressure, psi
ρ	density, $\frac{slug}{ft^3}$

Chapter 1

Introduction

1.1 A Brief History of Rocketry

Since the inception of flight, engineers have tried to push the envelope of what could be achieved by the materials at their disposal. Konstantin Tsiolkovsky famously published his rocket equation in 1903 [1] which led to an explosion of research into the field of rocketry. Using Tsiolkovsky's equations, Robert Goddard developed and flew the first liquid fueled rocket on March 16th, 1926 [2]. Goddard spent his life advocating for the further development and use of liquid rockets to propel the human race into a multi-planetary species. Tsiolkovsky and Goddard's research set the groundwork for the development of rocketry as we know it today.

In the late 1930s Wernher von Braun continued the development of liquid rocketry for a much more sinister reason, the bombing of London. Von Braun and his team developed the V2 rocket. Using an engine powered by alcohol and liquid oxygen the V2 had a range of 200 miles and could reach an altitude of 55 miles [3]. Although almost 3,000 V2 rockets were launched during WWII they suffered from reliability issues and many missed their intended targets. After the war, American and Soviet military's scrambled to capture as many V2 rockets and German scientists as they

could. Von Braun was brought to the U.S. through Operation Paperclip to continue his work.

The Space Race saw another explosion in the development of liquid rockets through the design and production of Intercontinental Ballistic Missiles (ICBMs), and the first man made satellite, Sputnik. While the Soviets seemed to be winning the Space Race by a landslide Von Braun and the United States were about to end the race once and for all. On July 16th, 1969, the U.S. launched a Saturn V rocket, powered by five F1 engines fueled by RP-1 and liquid oxygen, into low Earth orbit. After four days of traveling in the vastness of space the command module landed on the moon. The U.S. had won the space race. However, rocket development did not stop there.

Over the next half a century rockets became lighter while their engines became more powerful. Countries moved away from competing with each other and towards partnerships that would see the greatest scientific and engineering feat that humanity has ever achieved. The first module of the International Space Station was launched on November 20th, 1998. Since November 2, 2000, humanity has been living among the stars, researching and developing new technologies for the betterment of our species.

In more recent years, the private space industry has flourished with the likes of SpaceX, Blue Origin, and Virgin Galactic carrying the torch forward. These companies have inspired a new generation of engineers to push their knowledge to the limits and continue the works of the great scientists and engineers that came before them. In the next half a century humanity may be able to achieve the dreams of Tsiolkovsky and Goddard by establishing colonies on the moon and beyond.

1.2 Umbilical Towers and Fuel Systems

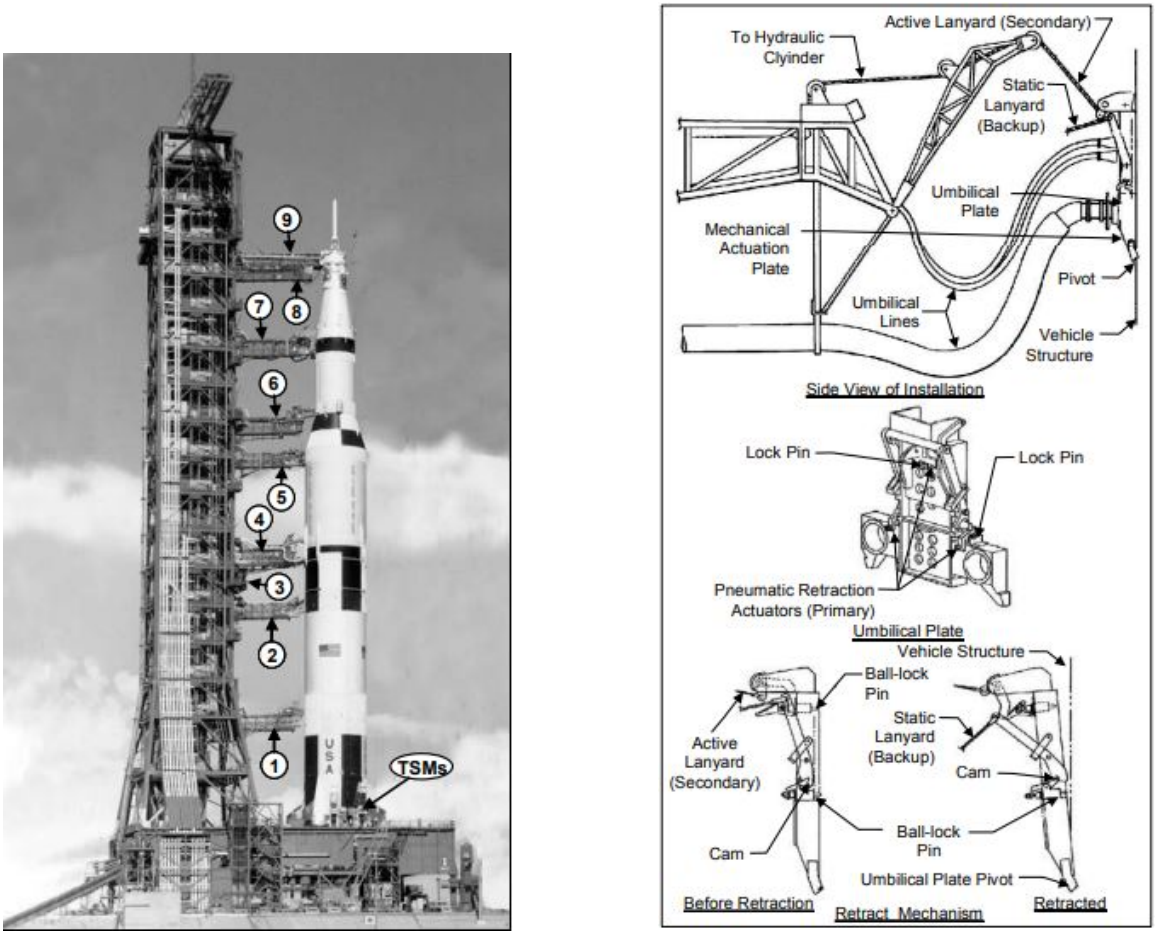
For the past 75 years rockets have used complex umbilical systems that require large amounts of infrastructure to fuel liquid rockets. The Saturn V Launch Umbilical

Tower was a 360-foot-tall tower that supplied fuel, hydraulics, electric power, water, and vital communications to and from the rocket [4]. The mobile launch tower had nine connection points (Fig. 1.1) to the rocket to provide all of the necessary vitals. The Space Shuttle launch tower (Fig. 1.1) iterated on the Saturn V tower, and was able to reduce the number of main connection lines needed to and from the launch tower down to five [4]. In more recent years, SpaceX has been able to further reduce the total number of connections from the ground support through their unique strong back launch tower. While these systems may be necessary for large scale rockets such as the Saturn V or Falcon 9 they are much too complex and expensive for amateur rocketeers or collegiate teams.

1.3 Student Rocketry

Liquid rocketry is extremely difficult even before considering the ground support necessary to control the fueling process or the rocket. Many amateurs, and even most highly ranked engineering colleges, used to stay away from liquid rocketry because of its complexity, cost, and the danger it poses to personnel and infrastructure. However, the past 20 years have seen increased interest in, and funding for, STEM education [5] [6]. This increased funding allowed for the establishment of many collegiate rocketry teams and competitions for those teams to compete in. Universities such as UCLA [7], MIT [8], Georgia Tech [9], UCF [10], and now, the University of Tennessee have begun to delve into liquid rocketry.

The main focus of the teams at these universities is twofold: design, build, test, and fly a rocket; allow students to gain precious hands-on experience that they can carry with them into the aerospace industry when they graduate. Competitions such as the Intercollegiate Rocket Engineering Competition (IREC) [11], NASA Student Launch [12], Argonia Cup Competition [13], and Friends of Amateur Rocketry's Dollar Per Foot [14] give students an avenue to exercise their engineering prowess. In these



(a) Saturn V Umbilical Tower

(b) Space Shuttle Retractable Arm

Figure 1.1: Legacy Umbilical Examples [4]

competitions, students are typically given a set of guidelines that they must follow when designing their rocket. Teams then design and test their rockets in the time frame set for the competition. The culmination of many of the competitions consists of a massive gathering of the teams in a single location where they can present their designs, launch their rockets, and win prizes based on how well their rocket performed.

Almost every major launch provider in the world uses a liquid bi-propellant rocket to launch payloads into orbit. Although the projects these students work on may not be as complex as the Space Shuttle [15], Falcon 9, or New Glenn, working with the components, materials, and fluids that those vehicles use(d) helps prepare them to enter the rocket launch industry. Whether students are working to obtain sponsorships, building avionics, designing nozzles, or running engine test fires, they will be better prepared for whatever opportunity presents itself after graduating because they were involved in a rocketry team.

Chapter 2

Background

2.1 The Inception of the Urbanski-Colbrun Valve

In the summer of 1995, two amateur rocketeers went into the Black Rock Desert with what they thought was a unique idea. Like many great engineering or mathematical discoveries they came to find out they had developed the same idea simultaneously but separately. Bill Colburn and John Urbanski were both in Black Rock to fly hybrid rockets and test their new idea when fate brought them together. While Bill was explaining his new idea to some fellow rocketeers that stopped by his tent, one told him that his idea sounded very similar to something they had heard a few tents over. Bill was very curious, since he believed to be the first to come up with this idea, and he went over to this other tent.

When Bill arrived at the tent, he found John's rocket with the same "new" idea implemented. Bill and John discussed hybrid rocketry and their idea and John even offered Bill some different tubing for him to try on his rocket.

What both Bill and John had discovered was when using the Korey-Pooley [16] method of fueling a rocket through the nozzle if the typically used metal tube was substituted with a plastic tube and a PrestoLoc^{TM} Fitting a valve was created in their rockets.

This valve was used to do the following:

> "1. Filled the tank with Nitrous Oxide.
> 2. Acted as a safety valve (bursting at 1000 to 1200 psi at 65 F).
> 3. Acted as a start valve by failing under pressure and heat at the injector face during ignition.
> 4. Act as an orifice when selecting it and/or drilling it slightly to match the motor flow rate needs." [16]

Bill went on to fly the first "M" hybrid motor from Aerocon during the event using the nylon tubing that John had given him. The launch went perfectly, but unfortunately Bill's rocket suffered a burn through. Later that year, John and Bill met up again at the MudRoc launch, and Bill demonstrated a perfect launch with the new valve set up. Graciously, Bill and John have left the design in the public domain for all amateur rocketeers to use, but request that the valve be called the Urbanski-Colburn or UC valve. While there are no drawings or pictures of the original design, a detailed schematic of a typical Urbanski-Colburn rocket design can be seen in Figure 2.1.

The UC valve has since been used by many amateur hybrid rocketeers, rocketry teams, and even some companies such as Contrail Rockets [17]. The simplicity of the system allows for the easy assembly, filling, and launch of hybrid rockets. In the case of Contrail Rockets push-to-connects are used to insert the fill lines into the injectors and the oxidizer is filled through the lines and injectors. When the oxidizer tank is deemed filled the ignition sequence is started. The ignition sequence consists of the lines being burned away from the injectors which, in turn, allows for the oxidizer to flow into the combustion chamber. When combustion begins, the lines are forced out of the rocket from the initial ignition of the rocket motor. Once the lines are forced out of the motor the rocket is free to complete its burn and the lines are typically found on the ground near the launch site.

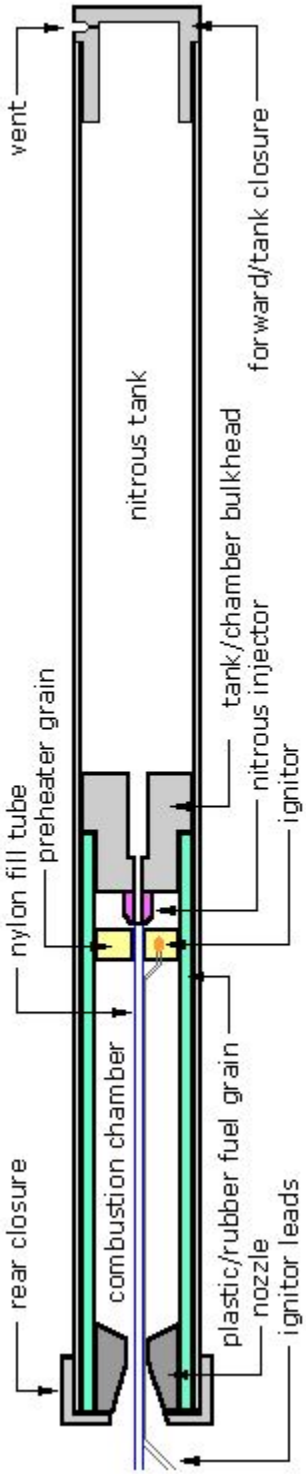


Figure 2.1: Urbanski-Colburn Hybrid Rocket Design [18]

2.2 Prior Use of the UC Valve at the University of Tennessee

The University of Tennessee has a rich history of rocket motors dating back to 1999. Initial research focused on the use of bio-derived fuels for hybrid rockets [19] [20] [21]. With the rise of additive manufacturing, research focus shifted to the possibilities that the new technology could bring about. Liquid-cooled 3-D printed nozzles [22], 3-D printed polymer filled matrices [23], and powder filled ABS matrices [24] are a few examples of research topics studied. The culmination of years of research came a head when, in 2018, students decided to enter into the Spaceport America Cup [25].

Since 2018 the University of Tennessee's rocketry club, the Student Space Technology Association, has been experimenting with and implementing the UC Valve in hybrid rockets. The idea to use the UC valve came from its relative simplicity and low volume taken up in the rocket. SSTA realized they could increase the total volume of oxidizer while simultaneously reducing the complexity of the filling and ignition system by using the UC valve. The club started out by studying the design of commercial UC valves, such as those implemented by Tom Sanders and his company Contrail Rockets [17] (Fig. 2.2). The 29mm and 75mm hardware were purchased and used multiple times to understand the design and construction of the motor.

After using the UC valve multiple times and understanding its functionality, SSTA decided to make their own for their 3 inch competition motor that would fly in the 2019 Spaceport America Cup competition. The design consisted of four $\frac{1}{4}$ inch injectors, two of which acted as oxidizer fill lines, and a single $\frac{1}{8}$th inch vent line. Fig. 2.3 shows the a model of the injector baffle without injectors installed. The four outer holes are the oxidizer injectors and the single, internal, hole is the vent line. When the nitrous tank was full, the ignition sequence began and the lines were severed. The motor now had four active injectors that would spray nitrous into the combustion chamber.

A new design for motor ignition was also introduced with the use of the in-house UC valve. A 3D printed cup was filled with a compound and placed at the top of



Figure 2.2: Contrail Rockets 3 Inch Injector Baffle

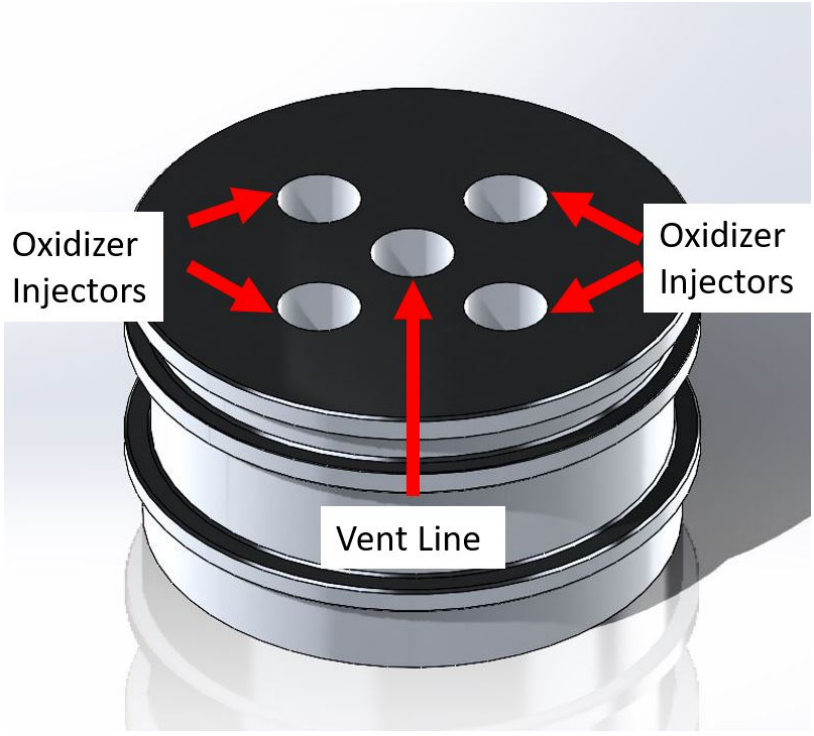


Figure 2.3: 3 Inch Injector Baffle for the 2018-2019 UTK Spaceport America Cup Rocket

the combustion chamber to help initiate combustion of the ABS/coal compound and nitrous. The compound would only burn for a few seconds, but it was hot enough to guarantee ignition of the engine. The exact chemical makeup and geometry of the ignition cup will be discussed later in this paper.

After successful flight and recovery in the 10,000 foot (10k) category of the 2019 Spaceport America competition (Fig. 2.4), SSTA decided to move up to the next category, 30,000 feet (30k). It was understood that the new rocket, and engine, would need to be larger than their 10k entry. In 2019, work began on developing new fuels and motor geometry.

Fuel testing began on the university's horizontal test stand. Sorbitol, plastisol, and paraffin were all considered as the main fuel for the 30k motor. After many horizontal firings, sorbitol was chosen because of its low regression rate and high thrust. The next step was to increase the size of the grains from the horizontal stand to the 3 in. motor for the vertical stand.

A duplicate 3 in. motor was made for use on the vertical test stand to help further characterize the sorbitol fuel grain. No changes were made between the competition motor and the test stand motor. Multiple test fires of the sorbitol fuel grain happened without issue, but when the 3 in. motor was being used to help characterize another fuel type a catastrophic anomaly occurred. The vent at the top of the chamber was closed prematurely, and a back pressure wave cause the top enclosure to be ejected from the motor. This was a fatal flaw in the design of the motor and would be changed for the next iteration.

SSTA would use the 3 inch motor as a stepping stone to create a new 5 in. diameter motor for the 30k competition. With knowledge gained from the explosion on the test stand, a new top enclosure of the motor was designed to be ensure the same failure would not happen again.

The 5 inch motor was designed to have four injectors, just like the 3 inch design, but they would be $\frac{1}{2}$ inch to allow for more flow (Fig. 2.5). The entire motor assembly would work much like the 3 inch predecessor, just on a larger scale.

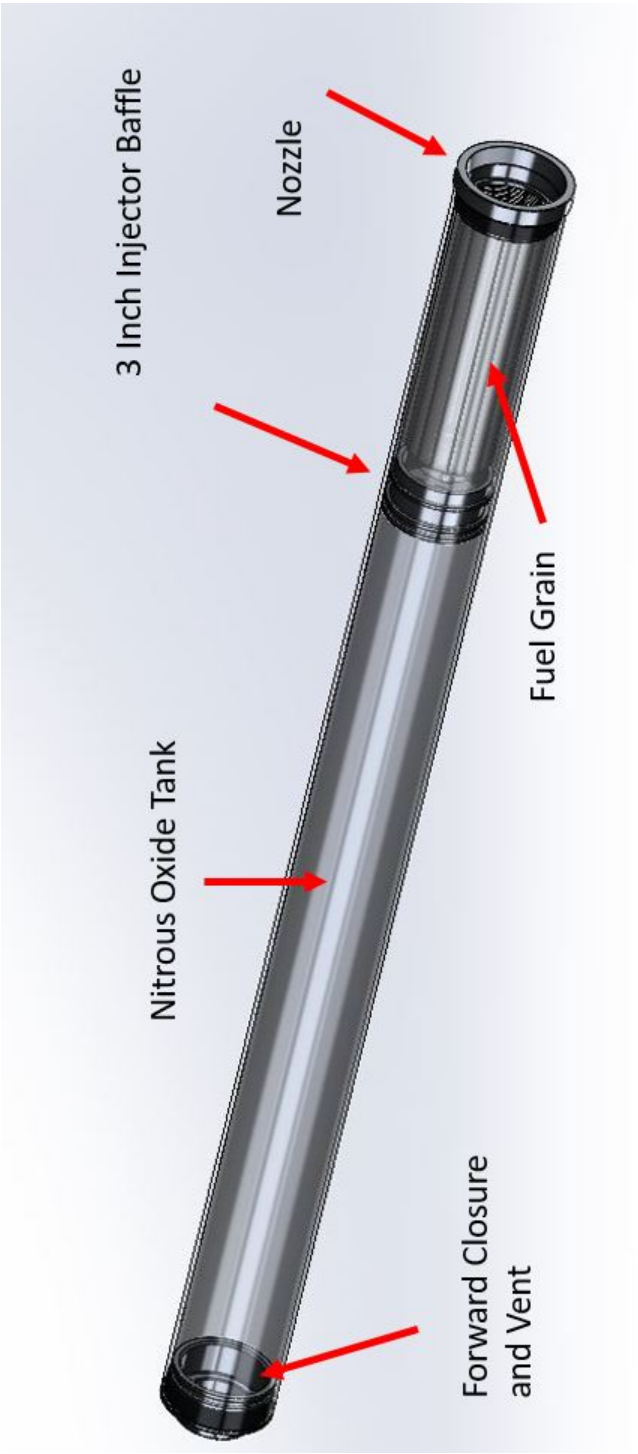


Figure 2.4: UTK 2019 Competition Rocket Motor Assembly, Total length = 39 inches

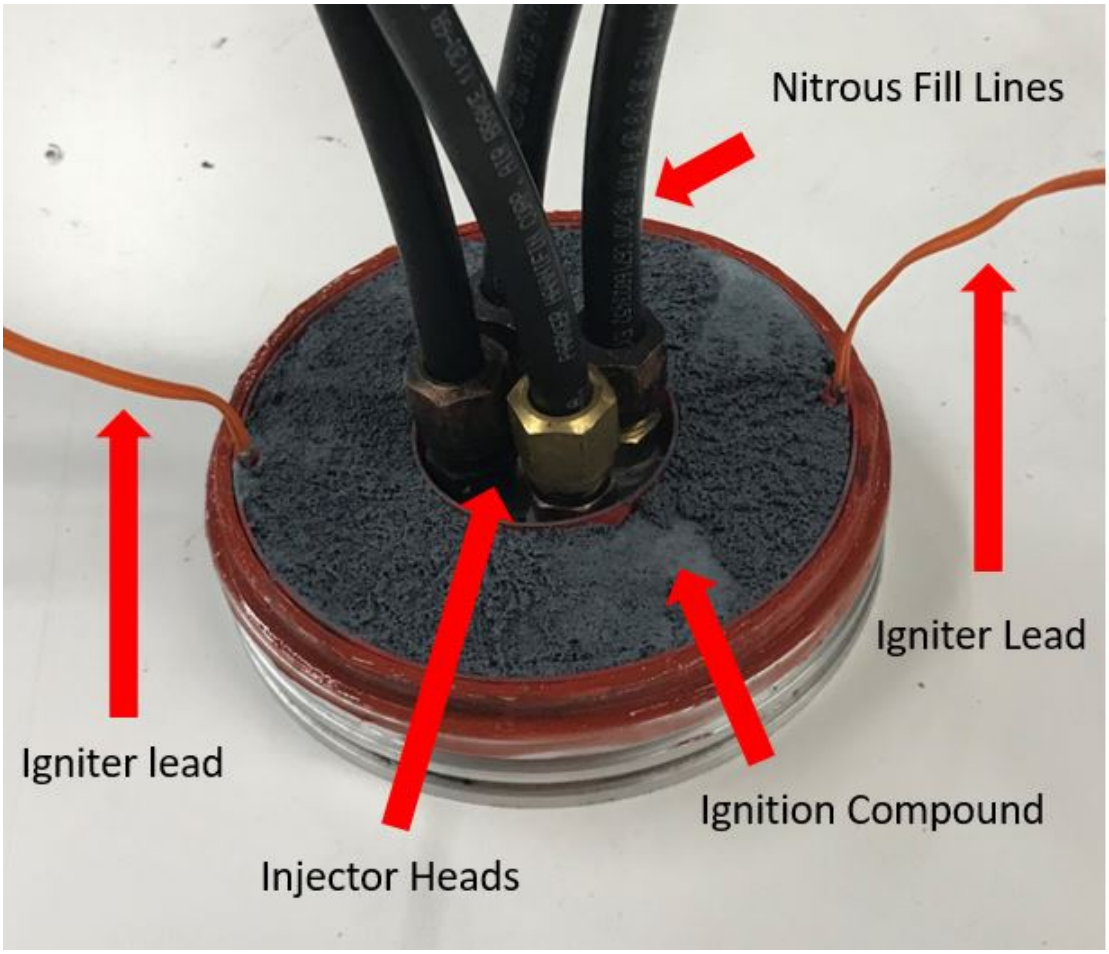


Figure 2.5: UC Valve and Ignition Cup for UTK 2022 Spaceport America Cup Rocket

New O-rings would need be used to ensure no nitrous leaked, and a new ignition cup was designed to fit in the new motor.

The motor was hydro-tested to ensure no leaks occurred and to meet regulations of the Spaceport competition. This process consisted of capping the injectors on the injector baffle, inserting the injector baffle into the motor hardware, filling the upper portion of the motor with water, and securing the forward closure to the motor. A fitting was secured onto the forward closure and a K-bottle of nitrogen was connected to the fitting. Through the use of a regulator on the K-bottle, pressure was slowly introduced to the motor assembly. The motor was pressurized to 1150 psi, or just over 1.5 times the mean operating pressure of the motor. The motor was then left to hold the pressure for 24 hours. After the 24 hour hold the pressure was checked in the motor to ensure no decaying had occurred. The pressure was slowly, and safely, released from the motor assembly, the water was removed from the motor casing, and having passed hydrostatic testing, the motor was disassembled and left to dry.

Multiple fuel grains were cast in preparation of the test fires to come. The motor was assembled, placed on the vertical test stand, and fired twice over the course of two months. The motor flew at competition without issue, and the team won the 2022 Student Researched and Developed 30k category.

After returning from the desert SSTA began to plan their next endeavor as a club. The possibility of designing, building, and flying a liquid bi-propellant rocket had been on the mind of the club's members for the past few years, and now, with more experienced team members that possibility transitioned into a reality. Through late summer and early fall of 2022, the design of a liquid bi-propellant rocket began to come to fruition.

Chapter 3

Methodology

3.1 Quasi-One-Dimensional Flow

The combustion chamber and nozzle for the liquid bi-propellant rocket will be analyzed as a quasi-one dimensional flow problem. Control volume analysis has been conducted for centuries with dozens of textbooks covering the subject. The brief review to follow is from White's book Fluid Mechanics Eighth Edition [26].

The equation of state used to describe the gaseous particles in the combustion chamber is the perfect gas law. This law relates the pressure, temperature, and density of the fluid. The law requires that the fluid behaves as an ideal gas, i.e. it has a constant heat capacity. This assumption is accurate as long as the fluid is not at an extremely low pressure or temperature or at extremely high temperature where gas dissociates and R changes.

$$p = \rho RT \tag{3.1}$$

$$R = C_p - C_v = \text{gas constant} \tag{3.2}$$

Where C_p and C_v are defined as the specific heat at constant pressure and constant volume, respectively, for a gas. Each gas has its own gas constant, R, defined by the universal gas constant divided by the molecular weight of the gas in question. While there is no "perfect liquid law" many fluids are nearly incompressible and have a reasonably constant specific heat. Therefore, an idealized state relation for a liquid can be written as

$$\rho \approx \text{constant} \quad C_p \approx C_V \approx \text{constant} \quad dh \approx C_p dT \tag{3.3}$$

The conservation of mass of a fixed control volume can be described as:

$$\int_{CV} \frac{\partial \rho}{\partial t} dV + \int_{CS} \rho(v \cdot n) dA = 0 \tag{3.4}$$

For a control volume with multiple one dimensional inlets and outlets equation 3.4 can be written as:

$$\int_{CV} \frac{\partial \rho}{\partial t} dV + \sum_i (\rho_i A_i v_i)_{out} - \sum_i (\rho_i A_i v_i)_{in} = 0 \tag{3.5}$$

This equation can be further reduced by stating the flow across the control volume is steady; and $\frac{\partial \rho}{\partial t} = 0$, and equation 3.4 reduces to

$$\int_{CS} \rho(v \cdot n) dA = 0 \tag{3.6}$$

Therefore, equation 3.5 reduces to:

$$\sum_i (\rho_i A_i v_i)_{in} = \sum_i (\rho_i A_i v_i)_{out} \tag{3.7}$$

In equations 3.5 and 3.7 ρAV is most commonly defined as the mass flow rate or $\dot{m}$.

Therefore,

$$\sum_i (\dot{m}_i)_{in} = \sum_i (\dot{m}_i)_{out} \tag{3.8}$$

The volumetric flow rate is defined as:

$$\sum_i (A_i v_i)_{in} = \sum_i (A_i v_i)_{out} \tag{3.9}$$

Or more commonly,

$$\sum Q_{in} = \sum Q_{out} \tag{3.10}$$

3.2 Injector Flow Characteristics

For a fluid mixture to combust at a given pressure and temperature the mixture must be in a state that easily allows for heat transfer into the fluid. As the temperature increases in the fluid mixture it will begin to evaporate. When the fluid evaporates it creates a dense region of either fuel or oxidizer, and combustion can occur. The conditions for the fuel to be rapidly heated and evaporated depends heavily on the injector type and geometry of impingement when using multiple injectors, such as in this case. The best-case scenario is what is referred to as the "atomization" [27] of the fuel. In this case the droplets of fuel and oxidizer are on the order of micrometers in diameter. Sutton provides great insight on the characteristics of injectors in his book Rocket Propulsion Elements [27].

For a given thrust, F, and effective exhaust velocity, c, the propellant mass flow rate, $\dot{m}$, can be found:

$$\dot{m} = \frac{F}{c} \tag{3.11}$$

In equation 3.11 $\dot{m}$, consists of the total mass flow rate of fuel and oxidizer. In order to proceed we must take a step back and look at the mixture ratio, the ratio of

fuel to oxidizer present in the combustion chamber. The mixture ratio is defined by the equation below:

$$r = \frac{\dot{m}_o}{\dot{m}_f} \tag{3.12}$$

It is quite obvious that the total mass flow into the combustion chamber must equal the respective mass flow of the fuel and oxidizer combined.

$$\dot{m} = \dot{m}_o + \dot{m}_f \tag{3.13}$$

Substituting equation 3.11 into 3.12 it can be shown that:

$$\dot{m}_o = \frac{r\dot{m}}{r+1} \tag{3.14}$$

and

$$\dot{m}_f = \frac{\dot{m}}{r+1} \tag{3.15}$$

Finally, the equation for the volumetric flow rate and mass flow rate across the injector orifice can be stated as follows.

$$Q = C_d A \sqrt{2\frac{\Delta p}{\rho}} \tag{3.16}$$

$$\dot{m} = Q\rho = C_d A \sqrt{2\rho\Delta p} \tag{3.17}$$

Where rho is the density of the fluid, C_d is the dimensionless discharge coefficient of the injector, Δp is the pressure drop across the injector, and A is the cross-sectional area of the injector.

From this equation the time to inject all fuel and oxidizer can be determined.

$$t_{burn} = \frac{m_{total}}{\dot{m}} \tag{3.18}$$

From equations 3.12 and 3.17 the mixture ratio can be defined as:

$$r = \frac{(C_d)_o}{(C_d)_f}\left(\frac{A_o}{A_f}\right)\sqrt{\frac{\rho_o}{\rho_f}\frac{\Delta p_o}{\Delta p_f}} \tag{3.19}$$

When the oxidizer and fuel jets impinge in the combustion chamber the momentum of the resultant jet can be calculated by the following:

$$\tan\delta = \frac{\dot{m}_o v_o \sin\gamma_o - \dot{m}_f v_f \sin\gamma_f}{\dot{m}_o v_o \cos\gamma_o + \dot{m}_f v_f \cos\gamma_f} \tag{3.20}$$

Where γ_o is defined as the angle between the oxidizer jet and the chamber axis, γ_f is defined as the angle between the fuel jet and the chamber axis, and δ is defined as the the angle between the chamber axis and the average resultant stream. It is typically best for the resultant moment of the impinging jets to be approximately axial. Therefore, if $\delta = 0$ and $\tan\delta = 0$ equation 3.20 becomes:

$$\dot{m}_o v_o \sin\gamma_o = \dot{m}_f v_f \sin\gamma_f \tag{3.21}$$

In physical terms, equation 3.20 and 3.21 state that the sum of the momentum of the fuel and oxidizer jets should all be axial with no radial component.

3.3 Rocket Equations

Rockets are typically defined by a few major characteristics, thrust, total impulse, specific impulse, mass ratio, and exhaust velocity. Depending on the mission profile that is intended for the rocket, the engine will be designed to maximize some of these characteristics. In the case of this thesis the following equations were used to design the engine to limit the thrust in order to stay under the maximum limit of the load cell used on the test stand. These equations come from Sutton's Rocket Propulsion Elements [27].

The total impulse of a rocket I_t is found from the thrust force F integrated over the time it is applied, t:

$$I_t = \int_0^t F dt \tag{3.22}$$

For constant thrust with short start and stop transients, equation 3.22 reduces to

$$I_t = Ft \tag{3.23}$$

Arguable the most important metric to define a rocket is the specific impulse, I_s. The specific impulse is described as the thrust per unit weight of propellant flow rate. As stated in equation 3.13, $\dot{m}$ is defined as the total mass flow rate of propellant. g_0 is the standard acceleration of gravity on earth, 9.8066 $\frac{m}{s^2}$ or 32.174 $\frac{ft}{s^2}$

$$I_s = \frac{\int_0^t F dt}{g_0 \int_0^t \dot{m} dt} \tag{3.24}$$

This equation gives a time averaged specific impulse value in units of seconds. In order to find the specific impulse for the transient start up and shutdown periods of an engine equation 3.24 or the following equation may be used. In the following equation, m_p is defined as the total effective mass of propellant.

$$I_s = \frac{I_t}{m_p g_0} \tag{3.25}$$

For constant mass flow rate $\dot{m}$, constant thrust F, and negligible start and stop transients 3.24 simplifies to:

$$I_s = \frac{F}{\dot{m} g_0} = \frac{F}{\dot{w}} = \frac{I_t}{w} \tag{3.26}$$

where the product of $m_p g_0$ is the effective weight of propellant, w, at or near the Earth's surface, and the rate of change of that weight is $\dot{w}$.

To determine the expected thrust output of the rocket, the exhaust velocity must be calculated. As a note, in real rocket engines the exhaust is not uniform across the outlet of the nozzle. However, in order to simplify the calculations it is safe to assume a uniform exhaust velocity called the effective exhaust velocity, c.

$$c = I_s g_0 = \frac{F}{\dot{m}} \tag{3.27}$$

Chapter 4

Design and Manufacturing

4.1 Design Constraints

Certain design constraints must be covered before discussing the methodology of the design process of the UC valve for the liquid rocket. As discussed above, the design will be used in tandem with the design of SSTA's liquid bi-propellant rocket. Although the rocket was developed with this thesis in mind, many of the decisions made about the design were based on cost. The objective of the design of this rocket was to use the UC valve to greatly simplify the filling of both the fuel and oxidizer into the rocket. This would be the first time the Urbanski-Colburn valve was used in this way, at least at the University of Tennessee. The dimensions of the rocket can be seen below in Table 4.1. An exploded and cross sectional view of the rocket can be seen in Figure 4.1.

Another design consideration that must be taken into account for this UC valve is the use of ethanol as the fuel. Ethanol was chosen as the fuel for the rocket because of a partnership that was planned with a local Knoxville company that would provide high-grade ethanol. Past experience using nitrous oxide throughout hybrid motor test campaigns as part of SSTA played a major role in the decision to use nitrous oxide as the oxidizer. Finally, the relatively high density of nitrous oxide and fairly safe

Table 4.1: Initial Constraints

Rocket Part	Outer Diameter (inches)	Wall Thickness (inches)	Inner Diameter (inches)	Material Selection.
Airframe/Oxidizer Tank	3	0.125	2.75	6061-T6 Aluminum
Fuel Tank	1.37	0.0625	1.245	6061-T6 Aluminum
Combustion Chamber Structural Support	3.0	0.125	2.75	A-36 Steel
Ablative Liner (A)	2.75	No Data	No Data	In House Phenolic
Ablative Liner (B)	2.75	0.25	2.25	Franklin Fiber Phenolic

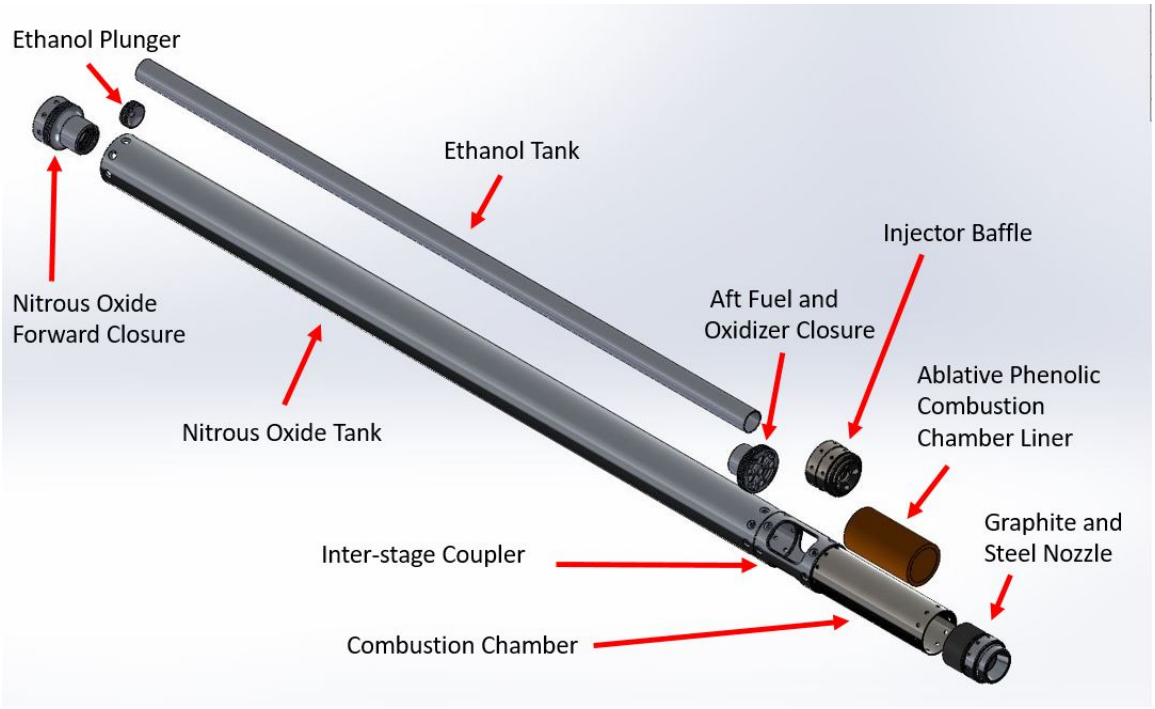


Figure 4.1: Exploded View of the Vega Rocket Engine

handling properties, compared to liquid oxygen or hydrogen peroxide [28][29][30], cemented it as the oxidizer for this rocket engine. Many liquid rocket designs use pumps or turbines to feed the fuel and oxidizer into the combustion chamber. However, in the case of this rocket, safety factors and cost prevented the use of pumps.

The final design constraint to be discussed is the use of the inter-stage coupler. A former SSTA member, who acted as a mentor to the club, was concerned about the over-pressurization of the combustion chamber during test fires that could potentially lead to catastrophic failure of the engine. The suggested solution to this problem was the use of an inter-stage, separating the combustion chamber from the fuel and oxidizer tanks. The rationale being that if the combustion chamber overpressurized the nylon fill lines in the inter-stage would separate from the push to connects and flow into the combustion chamber would cease.

4.2 Fuel and Oxidizer Tank Design

The fuel and oxidizer tanks were designed as concentric tanks, with the fuel tank being the inner tank and the oxidizer tank being the outer. Concentric tanks would allow simultaneous pressurization of both tanks through a special design of the forward closure and a plunger at the forward end of the fuel tank. The fuel tank would be slotted into the aft fuel and oxidizer closure (Fig. 4.2), and that assembly would sit inside the oxidizer tank. The plunger, outfitted with two o-rings to protect from cross-contamination, sat at the top of the fuel tank. The forward oxidizer closure was designed to secure the forward part of the fuel tank by sliding around the outer diameter of the fuel tank (Fig. 4.3). Holes drilled concentrically in the forward oxidizer closure allowed the nitrous oxide in the oxidizer tank to also press on the plunger at the top of the fuel tank (Fig. 4.3). This design allowed the oxidizer and fuel tank to be at nearly the same pressure at the time of ignition. The forward most

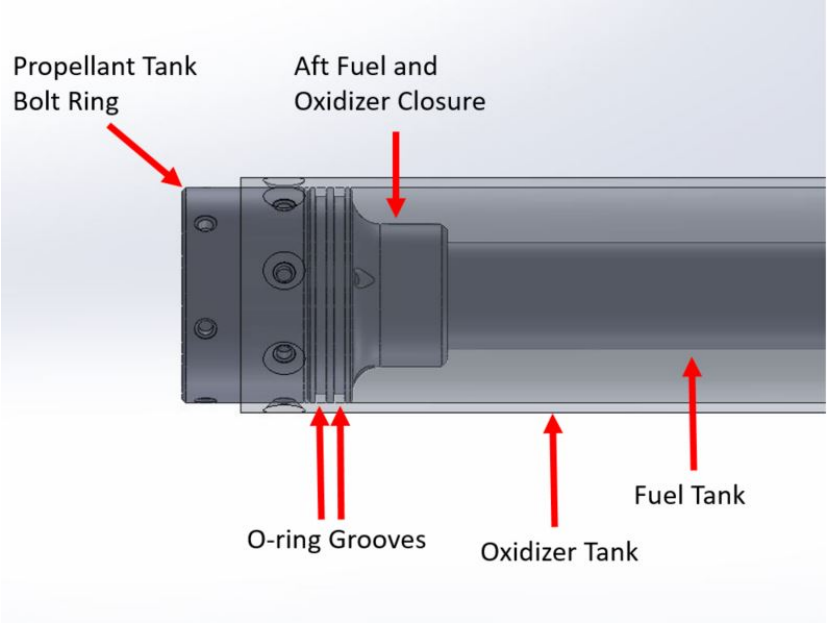


Figure 4.2: Aft Section of Fuel and Oxidizer Tanks

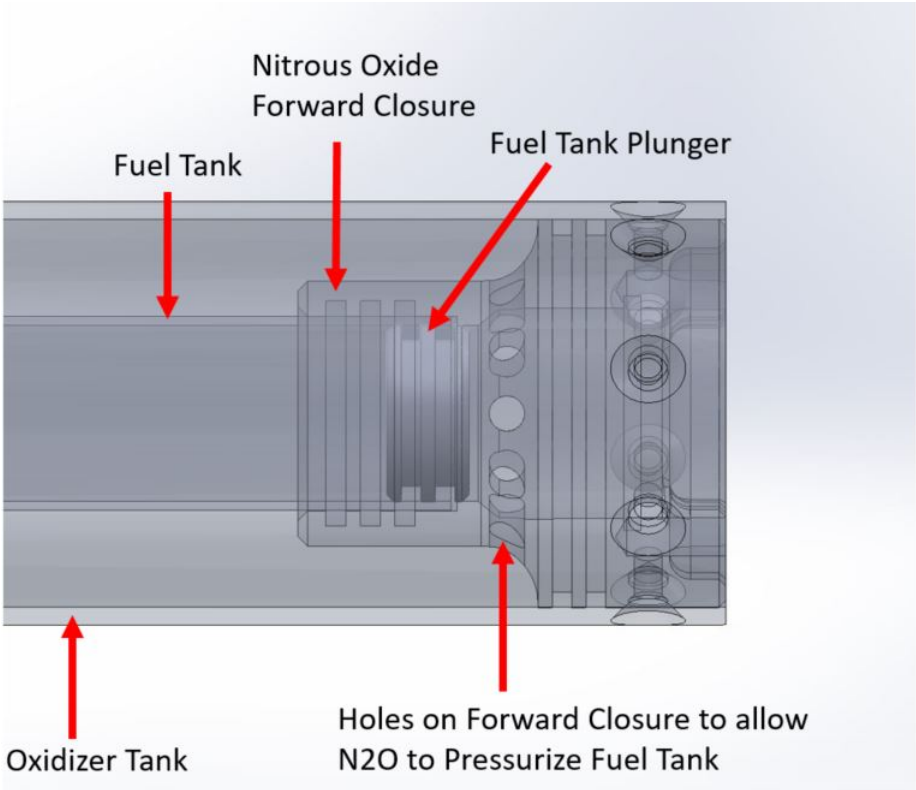


Figure 4.3: Forward Section of Fuel and Oxidizer Tanks

section of the oxidizer tank and oxidizer forward closure had bolt holes and were secured to each other. It should be noted that the concentric tank design and the design for the forward closure were conceptualized to support this thesis, but the exact dimensions and manufacturing were completed by students in SSTA.

4.3 Nozzle Design

The expected combustion pressure of the combustion chamber was in 350 psi range, thus the nozzle was designed with a 2.1 inch diameter converging section, 0.8 inch diameter throat, and 1.73 inch diameter diverging section. These dimensions gave a contraction area ratio (A_C/A_t) of 6.9 and an expansion area ratio (A_e/A_t) of 4.68.

The nozzle of this rocket engine was originally designed to be a single piece of machined graphite (Fig. 4.4), much like the ones that had been used previously for the Andromeda and Redshift rockets launched at the Spaceport America Cup in 2019 and 2022. However, lead times for a professionally machined nozzle were much too long. Thus, the decision was made to use single use, in house fabricated, nozzles. These nozzles would be made by casting a mixture in a 3-D printed mold. This idea came after reading about fellow collegiate liquid rocket enthusiasts at the University of Central Florida. These enthusiasts, dubbed Half Cat Rocketry, had developed a process of mixing epoxy, microballoons, and sodium bicarbonate (baking soda) into a material they called CHAMBERSAFE [31]. Half Cat Rocketry had demonstrated multiple successful nozzle castings and test fires using their CHAMBERSAFE material [31]. Half Cat Rocketry graciously allowed for the use CHAMBERSAFE provided credit was given to them for the development of the material [31].

With the help of 2023 graduate Calvin Eckerman, an inverse of the nozzle CAD model was made and multiple molds were printed. The CHAMBERSAFE recipe was slightly altered from Half Cat Rocketry's original 63.3% epoxy, 31.7% baking soda,

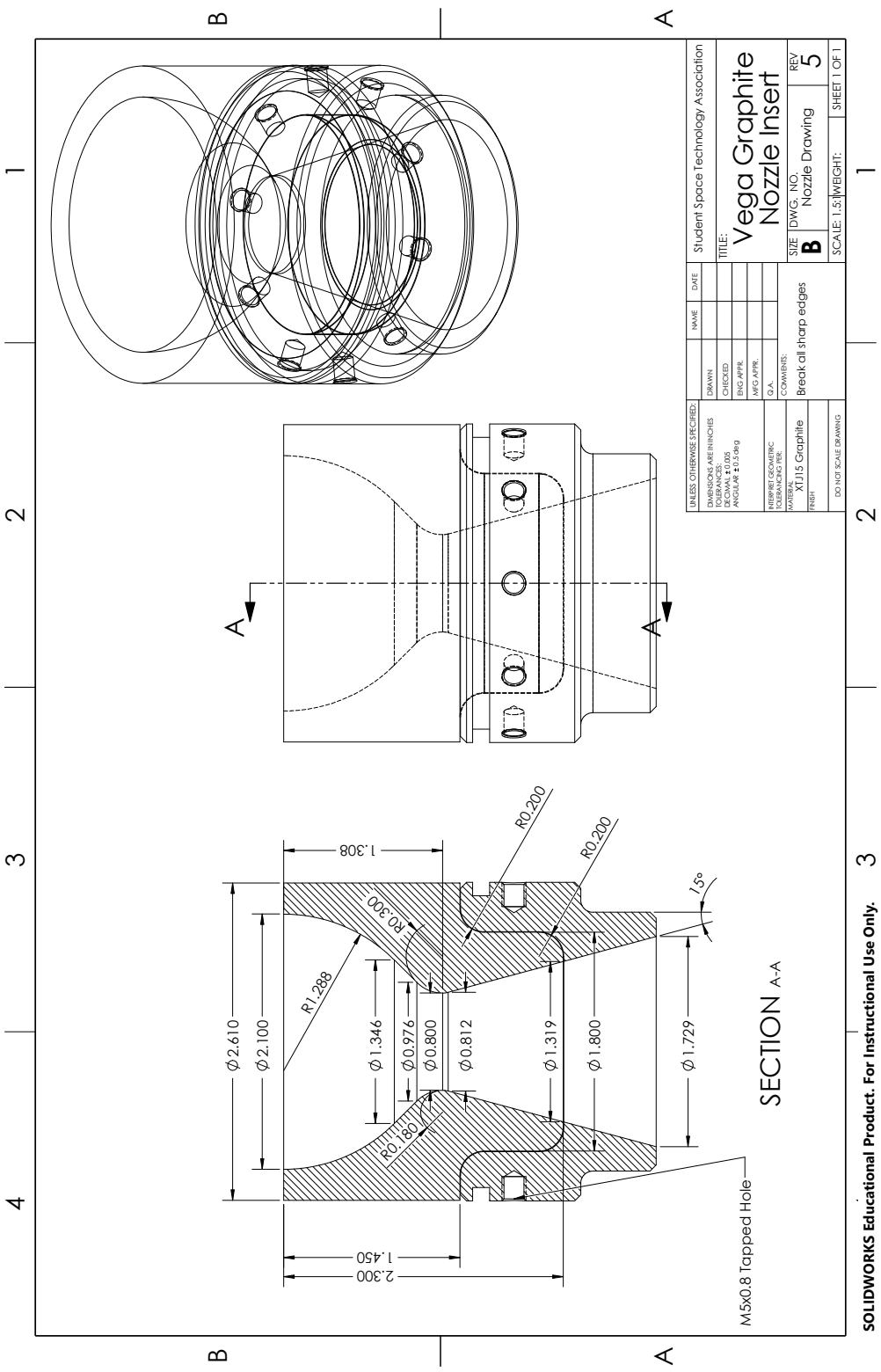


Figure 4.4: Original Graphite Nozzle Design

and 5% microballoons [31], to 65% epoxy, 30% baking soda, and 5% microballoons to make the measurement of the constituents easier. As this was the first attempt,three nozzles were cast (Fig. 4.5), left to cure for 24 hours, then removed from the molds. Two of the three nozzles were easily extruded from the 3-D printed mold and the third was damaged in the removal process. The two surviving nozzles were sanded down to fit the nozzle carrier, and the better of the two was chosen to be used for the first test fire of the liquid engine.

The first few test fire attempts utilized the CHAMBERSAFE material. However, degradation and expansion of the nozzle throat area was much too high, nearly twice the original diameter (Fig. 4.6 and 4.7). In the past, SSTA had demonstrated nominal use of Delrin® nozzles, and thus, the decision was made to change to a machined Delrin® nozzle.

4.4 Injector Design

As stated above, injector design is one of the most important factors in facilitating combustion in a rocket engine. The injectors must atomize the fuel and oxidizer well enough to allow heat transfer into the droplets to ensure their evaporation and subsequent combustion. The injector baffle was designed to allow for the fuel to inject directly into the combustion chamber, and the oxidizer will impinge on the fuel jet at a 20 degree angle (from the combustion chamber wall). The streams will intersect at approximately one inch from the injectors and allow for proper atomization of the fuel.

The initial design for the injector baffle consisted of a single fuel jet and three oxidizer jets set 120 degrees apart. This design would allow for three oxidizer jets to impinge on one central fuel jet. In theory, this would allow for proper fuel to oxidizer mixing and for the momentum of the resulting spray to continue axially into the combustion chamber. However, lack of literature on the three-on-one style injector brought this design decision into question. Gill and Nurick's report on liquid rocket

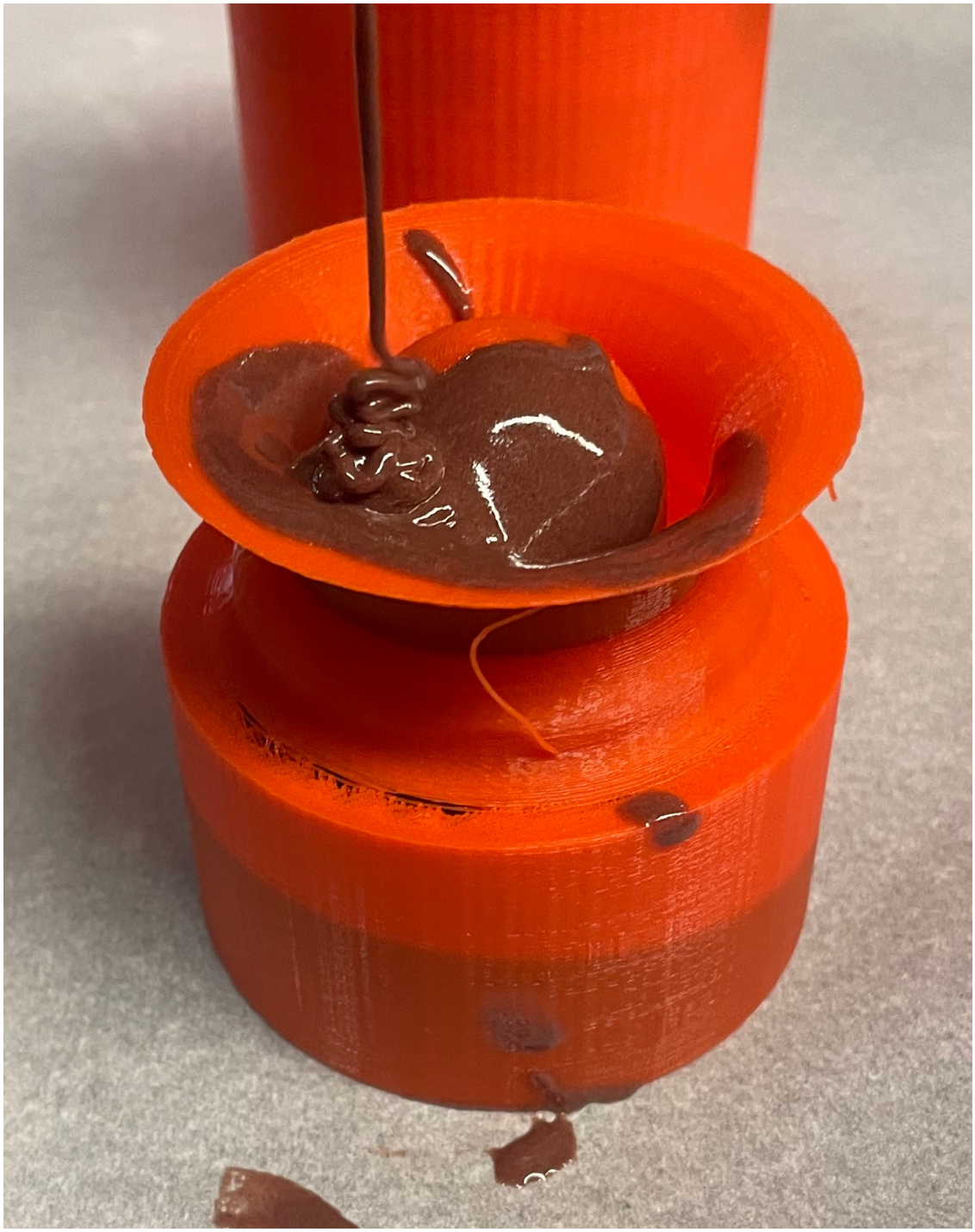


Figure 4.5: CHAMBERSAFE Nozzle Casting



Figure 4.6: Diverging Side of Test Fired Nozzle (left) vs. Newly Cast Nozzle (right)



Figure 4.7: Converging Side of Test Fired Nozzle (left) vs. Newly Cast Nozzle (right)

injectors [32] provides further insight on the advantages and disadvantages of injector design. The designs discussed in this paper that are most similar to the original three on one design are the unlike triplet and the unlike pentad. The unlike triplet design (Fig. 4.8) consists of a single fuel jet in the center of two oxidizer jets set 180 degrees apart while the unlike pentad (Fig 4.8) consists of one central fuel jet surrounded by a ring of oxidizer jets set 90 degrees apart. The following describes the details of the two injector types.

The heat transfer to the wall of the ablative phenolic liner was a major concern in the design of this rocket engine. The unlike triplet is described to have "extremely large variations in mixture ratio occur in the outer portions of the spray fan [32]." Phenolic liners were the primary combustion chamber liner used in the hybrid rockets previously discussed, Andromeda and Redshift. However, the liners used in the hybrids were thicker than the one planned to be used in the liquid engine. The hybrid rocket design also allowed the motor grain to carry heat away from the phenolic liner as the grain burned away.

Gill and Nurick go on to say "the triplet may not be desirable for use near the chamber walls." [32] From these statements it seemed plausible that burn through in the combustion chamber was possible. A burn through in the combustion chamber would be catastrophic to not only the engine and the test stand, but could also potentially shut down the rocketry club at the university.

While the unlike-impinging pentad has not been used in many, if any production engines, it has been tested thoroughly on test beds [32]. Gill and Nurick claim that "This element is extremely attractive for engines operating at mixture ratios much different than one [32]." This is great because the mixture ratio for nitrous oxide to ethanol is 5.7:1 [33]. Gill's paper also reports that the "unlike-impinging pentad results in more nearly uniform mixing than the doublet or triplet. In the case of the pentad high heat to the injector face was a cause of concern. While this may be the case for production rockets with burn times of dozens or even hundreds of seconds, this will not be a concern for a six second burn time motor that uses a stainless steel

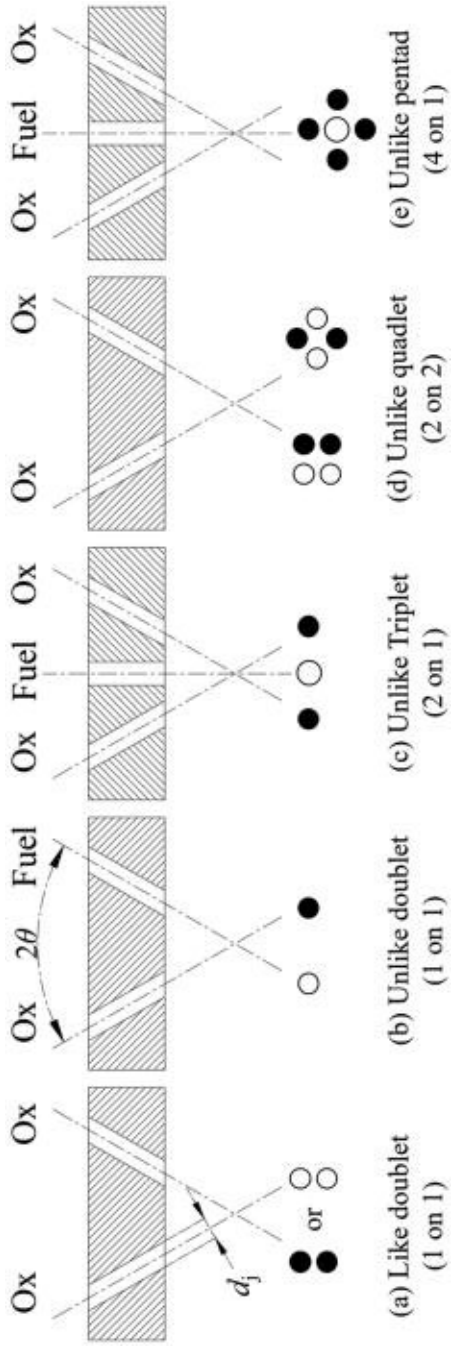


Figure 4.8: Injector Comparison Table [34]

injector. While both the unlike triplet and unlike pentad were viable options, the unlike pentad had better overall qualities, and thus, was chosen as the design for the injector.

The injector baffle is designed such that it can accept $\frac{1}{16}$ and $\frac{1}{8}$ in. orifices in the push to connects. This is to allow for testing between the different size injectors to determine the difference in mass flow rate and thrust output by the engine. While the stoichiometric ratio of nitrous oxide to ethanol is 5.7:1 [33], Youngblood's research [35] shows that O/F ratios as low as 2.5 are theoretically possible. It should also be noted that Youngblood completed a successful test fire at an O/F ratio as low as 3.91 $\pm$0.2 [35]. For simplicity's sake, an O/F ratio of 4 was chosen for this engine. Calculations show that $\frac{1}{8}$ in. orifices will allow for an initial mass flow rate of 2.8 lb/s (oxidizer) and 0.7 lb/s (fuel) into the combustion chamber. These flow rates can be expected to decrease during the burn as the pressure in the oxidizer tank decreases.

Figure 4.9 shows a drawing of the injector, Figure 4.10 shows the injector modeled in SolidWorks, and Figure 4.11 shows the final machined injector assembly. It should be noted that the unlike pentad injector design was chosen to support this thesis, but the exact dimensions and manufacturing were completed by students in SSTA.

4.5 Igniter Design

4.5.1 Igniter Cup Fabrication

Figure 2.5 shows the design of the ignition cup used for the Spaceport America Cup competition rocket used by SSTA. The ignition cup was 3D printed using acrylonitrile butadiene styrene (ABS). ABS provides a solid foundation for the ignition compound to be placed in while also melting at around 200 degrees Celsius. The ABS melting away ensures that neither the injectors nor the nozzle are clogged after combustion begins. The ignition compound, initially developed by students who previously attended UTK and been involved with SSTA, is a mixture of ammonium perchlorate

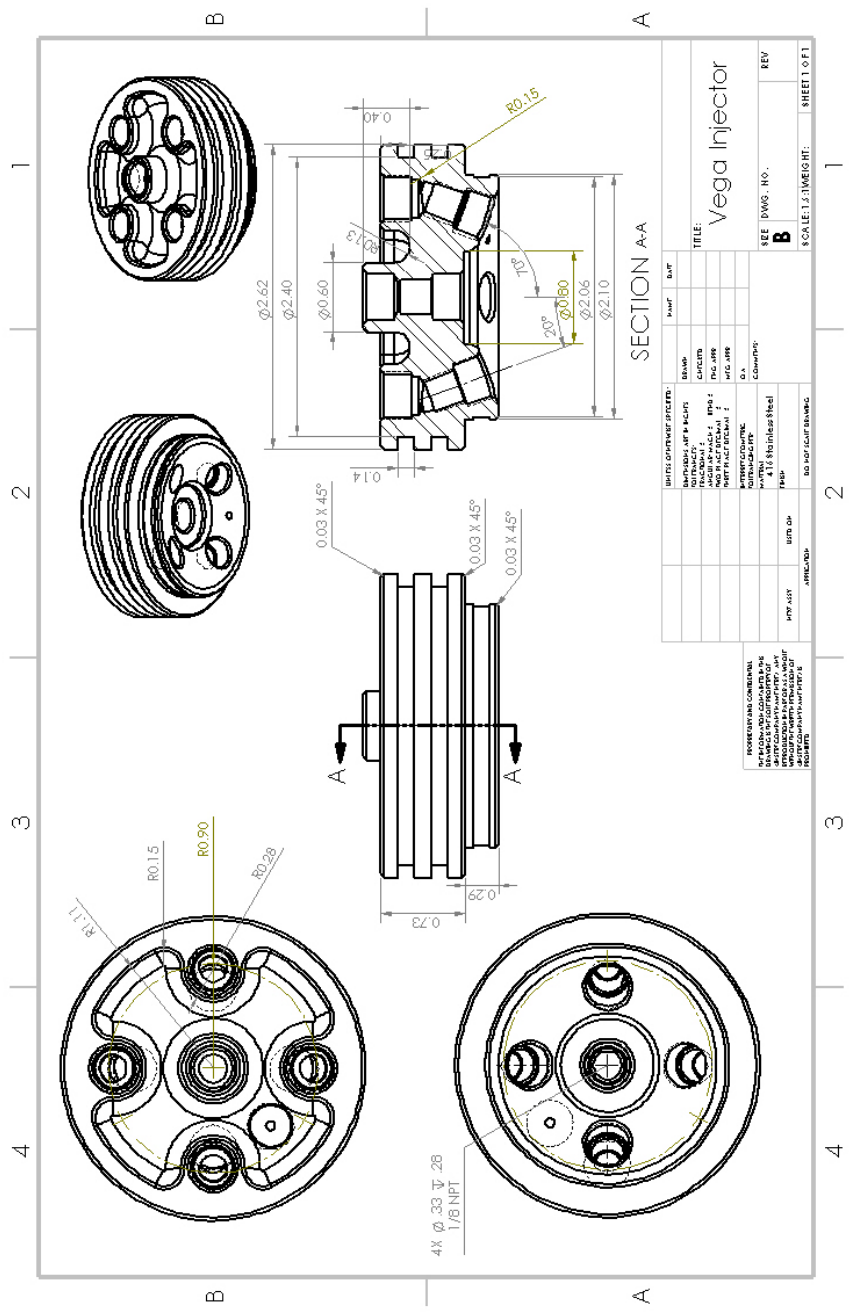


Figure 4.9: Vega Injector Baffle Drawing (all dimensions in inches)

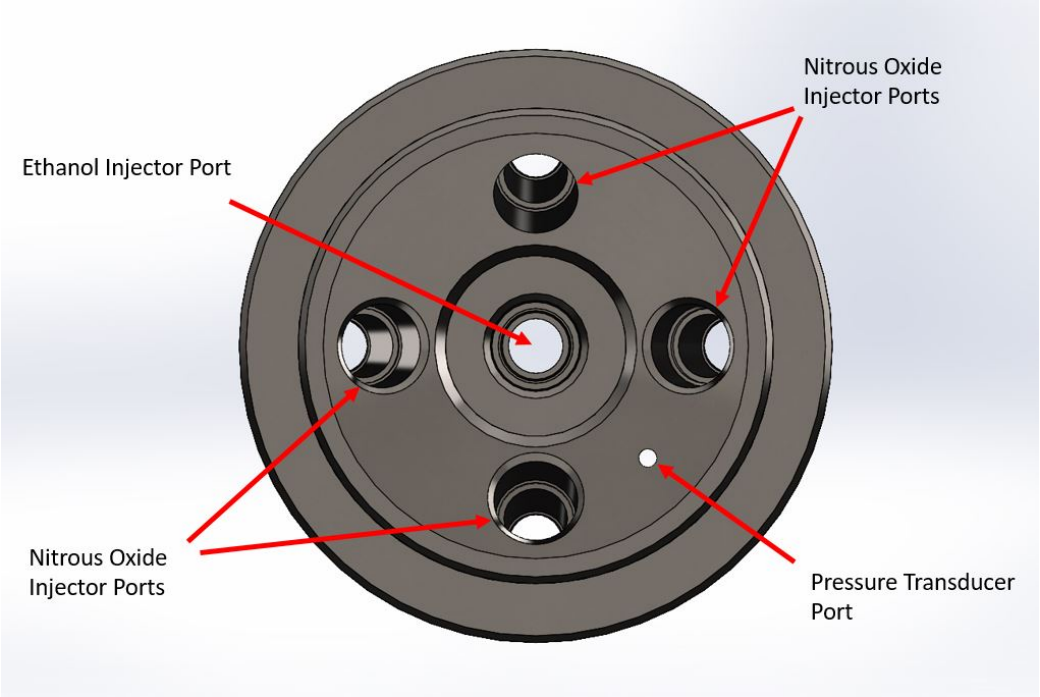


Figure 4.10: Vega Injector Baffle SolidWorks Model



Figure 4.11: Machined Injector with NPT Fittings Installed

(AP), copper thermite, and Flex Seal^{TM}. AP and copper thermite are used to ensure the temperature of combustion of the reactants is reached. Coper thermite typically burns at roughly 2500 degrees Celsius [36], more than enough to begin the ignition of ethanol and nitrous oxide. Flex Seal acts as the binder for the AP and copper thermite, and allows for the application of the mixture to the surface of the ABS ignition cup .

The dry ingredients, AP and copper thermite, are carefully measured, 280 grams and 40 grams respectively, and added to a plastic bowl. In order to minimize the chance of a spark igniting the compound , a wooden mixing stick is used to thoroughly mix the dry ingredients. Once the AP and copper thermite are mixed, 80 grams of Flex Seal^{TM} is added. Again, using a wooden mixing stick, the compound is thoroughly stirred to ensure that the Flex Seal is incorporated into the mixture. After mixing for three to five minutes the compound has about an hour before it begins to dry and harden onto the application surface.

Typically, the same wooden mixing stick is used to apply the compound to the surfaces of the igniter. The compound is scooped out of the mixture bowl and placed on the surface of the ABS ignition cup. The flat surface of the mixing stick is used to compress the compound to ensure the highest density of ignition compound in the available volume. Once the total volume available has been taken up by ignition compound, the igniter is placed in a flammable safe cabinet and left to dry for twelve hours. After the twelve hour drying period the igniters are ready to use and must be handled with caution.

4.5.2 Igniter Ignition

The igniter is typically lit using electronic matches (E-match), also known as a low-voltage electroexplosive device (EED), that are embedded into the igniter compound after the drying period. Electronic matches consist of a bridge wire surrounded by a pyrogen as shown in (Fig. 4.12). To light the pyrogen within the E-match, a low

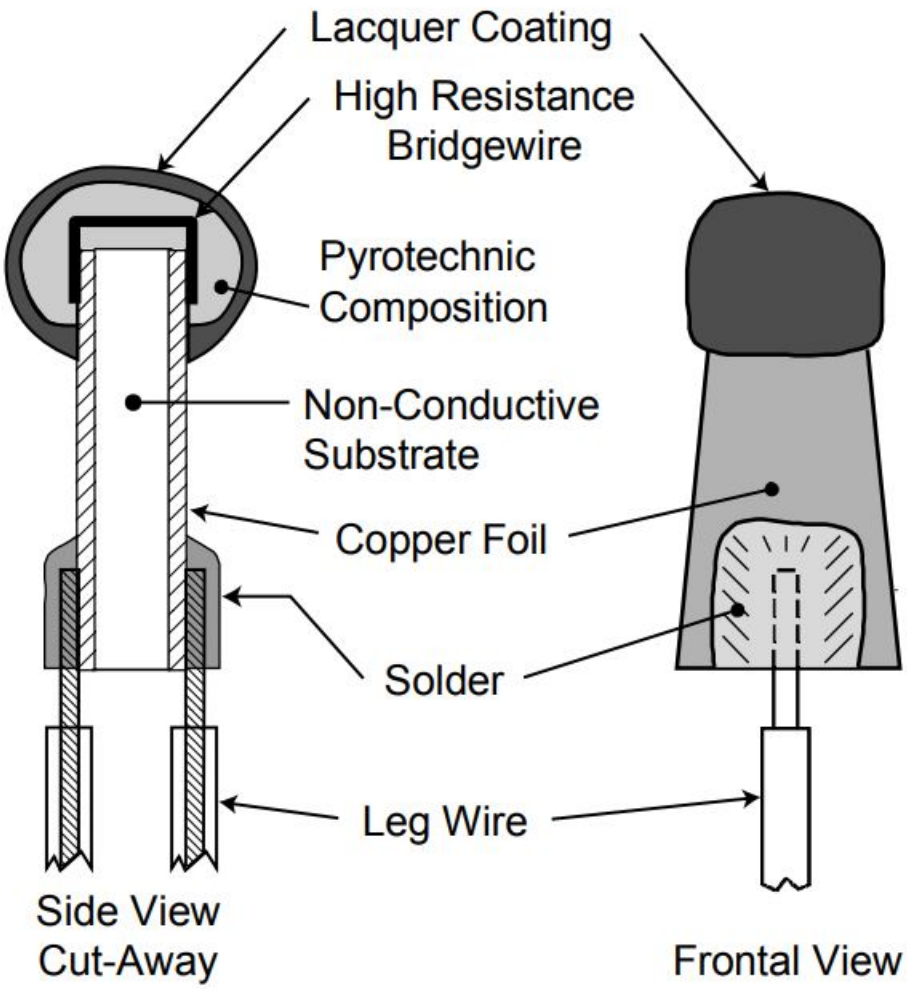


Figure 4.12: Model of bridge wire in Electronic Match [37]

current, typically between 0.1 and 5 amps [38], is applied to the lead wires. The current travels through the lead wires to the bridge wire. The bridge wire is a resistive element, typically a coil or very thin wire, that heats up when current is applied. When the bridge wire is sufficiently heated it will ignite the small amount of pyrogen that it is encased in [38]. A more in depth analysis of the E-match/EED can be found in NASA's 1971 report "Solid Rocket Motor Igniters" [38] as well as P.J. Rae and P.M. Dickson's 2019 article "A review of the mechanism by which exploding bridge-wire detonators function" [39].

The pyrogen burns, producing hot particles that collide with the igniter compound. These particles provide enough heat to begin the combustion process in the ignition compound. E-matches are made specifically not to create a shockwaves when lit. Shockwaves from an ignition source could cause cracks in the igniter compound and uneven heating of the fuel in the combustion chamber leading to combustion instability.

Another, less common, source used to light ignition sources is firework sparklers combined with E-matches. There have been cases in the past, when testing hybrid rockets on the test stand, in which the E-matches did not provide enough heat to ignite the rocket engine. In this case, an E-match was taped to a sparkler and the sparkler end was either laid on or inserted into the surface level of fuel grain or ignition compound. When it was time to test the hybrid motor, the E-match was supplied with a current causing the sparkler to ignite.

The extreme heat from the magnesium, typically around 5,500 degrees Fahrenheit or 3,100 degrees Celsius [40], in the sparkler was more than enough to ignite the igniter and begin the combustion process between the hybrid fuel grain and nitrous oxide. As a note, this style of ignition was not attempted on this liquid rocket engine, but it was considered as a suitable backup plan.

4.5.3 Igniter Safety Concerns

The following is a brief note on the safe handling of the igniter and igniter compound. Handling the igniter with caution is a safety precaution to ensure that no one is accidentally harmed by the extreme heat and light the igniter emits when lit. The igniter compound is resistant to shock and low levels of heat, and can even be manipulated with hand tools or handheld drills on low settings. However, sparks from welding equipment, holding the igniter over open flame, or sufficient current passing through a source of resistance could cause the igniter to light. The igniters are kept in a fire resistant cabinet at all times until it is time to insert the E-matches and then install the igniter into the motor casing. Prior to inserting the E-matches into the igniter compound, the leads are shorted. This is accomplished by twisting the leads together and wrapping the leads in electrical tape. This step ensures that no electrical current can pass through the wires to the bridge wire while the E-match is inserted into the compound. Small holes are drilled into the dry igniter compound and the pyro bulb of the E-matches are inserted into the holes. If, for some reason, the E-matches were installed into the igniter and the igniter was not immediately installed into the rocket, extra electrical tape was used to further secure the E-match leads. The igniter was then immediately placed back into the fire resistant cabinet until it was time to install the igniter into the motor. Knowledge gained from experience with the hybrid igniter proved that he method described above achieved the best chance of igniting the compound. Previous attempts at laying the compound onto the pyro bulbs proved not only difficult to accomplish but also degraded the coating around the pyro bulb and prevented them from working properly.

4.5.4 Igniter Design Process

The igniter for the liquid rocket went through an iterative design process that saw three major designs throughout testing. The initial design (Fig. 4.13) for the ignition source of the liquid rocket follows the precedent set by previous igniters used in the

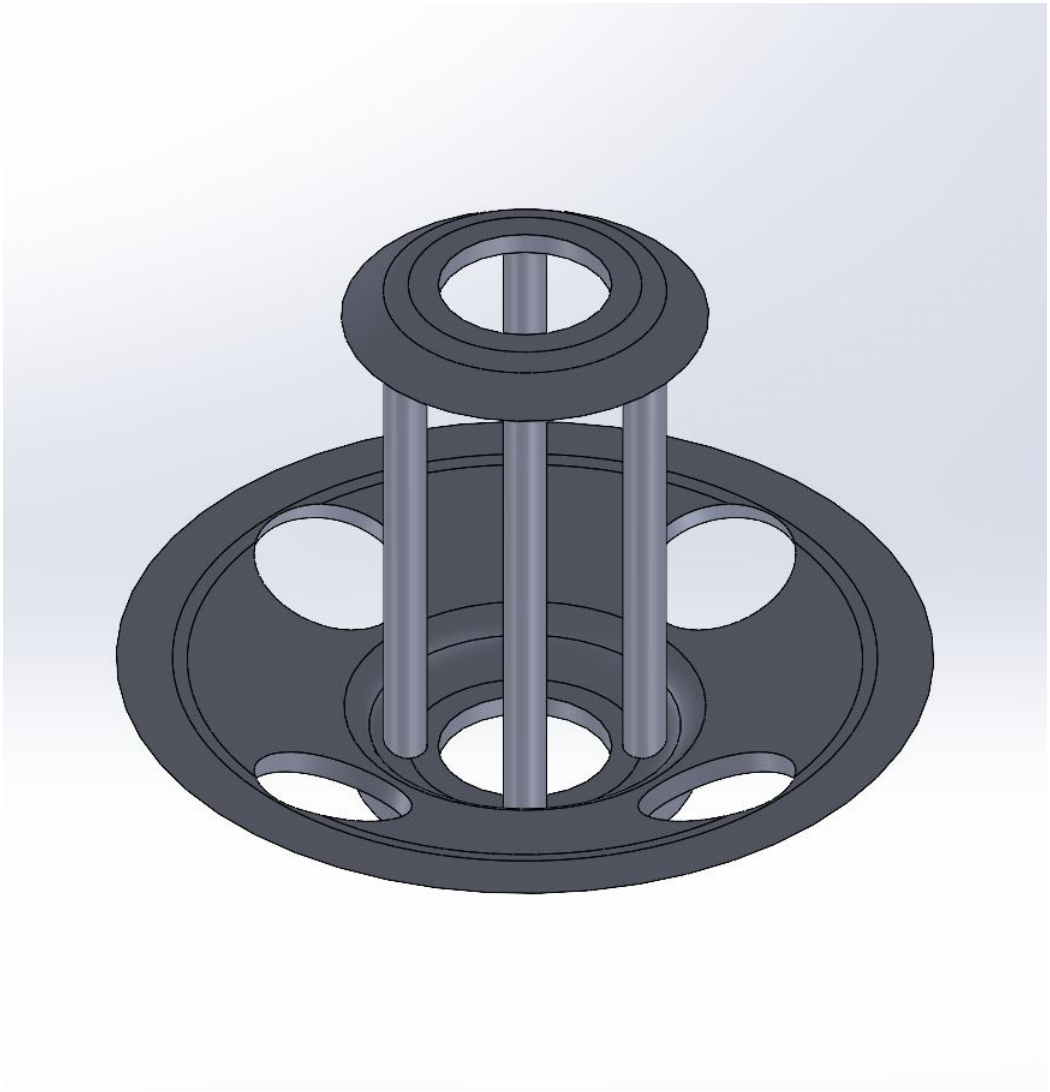
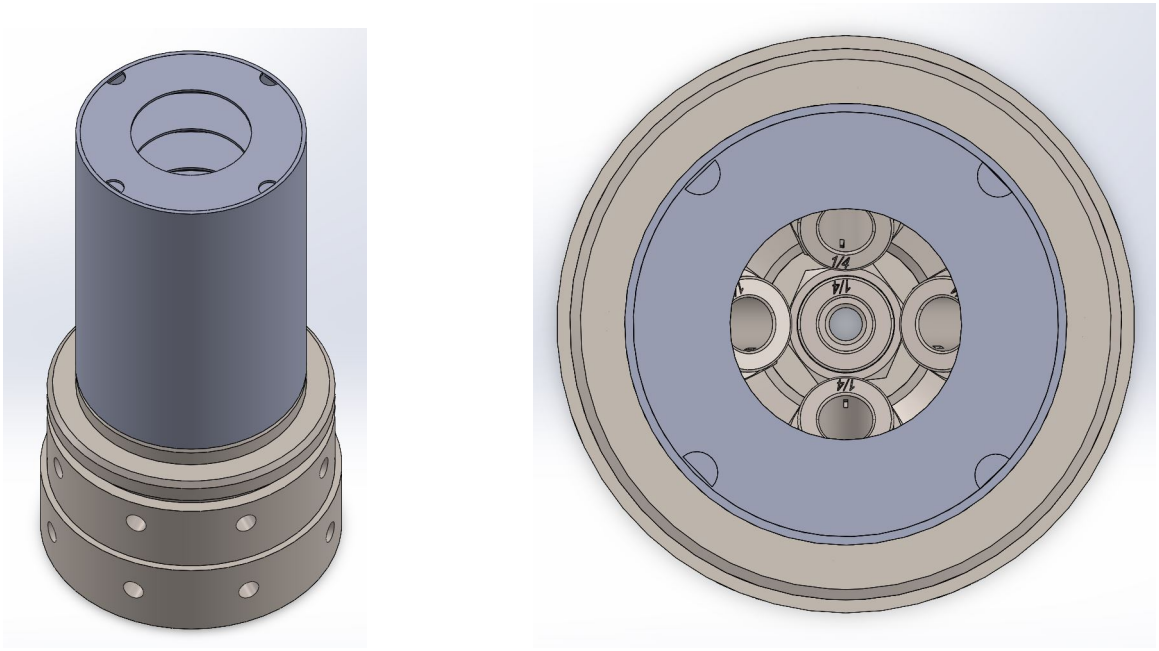


Figure 4.13: Umbrella Igniter Design

hybrid rockets at the University of Tennessee. The geometry was designed such that the top of the igniter sat flush against the curvature of the injector. Five holes were designed to allow the injectors to fit through the surface of the igniter. A second umbrella-like ignition cup was raised from the surface of the primary cup near the fuel and oxidizer impingement location. The rationale behind this design was that the igniter compound on the primary cup that laid on the surface of the injector would burn through the fuel and oxidizer lines, and the secondary "umbrella" cup would initiate combustion between the fuel and oxidizer. However, after testing of this initial design it was determined that there was not enough igniter compound to burn through the nylon fill lines.

The second major design changed the shape of the igniter to a cylinder with space removed at the top of the igniter to allow the injectors to sit inside the igniter itself. It was believed that the additional surface area from the cylinder shape would have a better chance of burning away the fill lines while also having enough excess igniter compound to begin the combustion process. This design also mitigated assembly issues that were seen with the first design. However, further testing showed that there still was not enough igniter compound in the igniter to burn away the nylon fill lines and start combustion. The final design of the igniter (Fig. 4.14) saw the removal of the tabs at the top of the previous edition and the addition of four ribs throughout the igniter. These ribs helped to increase the total surface area of the igniter to 38.75 square inches, allowing for nearly 180 grams of igniter compound to be inserted into the igniter. Four slots were extruded through the ribs such that the E-matches could slide all the way to the top of the igniter. This ensured that the igniter started burning closest to where the nylon fill lines inserted into the injectors. Testing showed that there was now enough igniter compound to burn through the nylon fill lines and initiate combustion. All igniter iterations can be seen in Appendix A.



(a) Final Igniter Isometric

(b) Final Igniter Top-Down

Figure 4.14: Final Igniter Design

4.6 Engine Simulation

Utilizing commercially available simulation environments, Rocket Propulsion Analysis (RPA) [41] and Half Cat Rocketry's HalfCatSim [42], the rocket engine was simulated. Both of these softwares have their own caveats that must be considered. RPA does not allow the user to specify the type or number of injectors feeding the combustion chamber, but it does allow the user to specify a multitude of different propellant types. Since RPA does not allow users to specify the mass of oxidizer and propellant, it does not provide a thrust curve. HalfCatSim is unique in the fact that it allows users to specify that fuel and oxidizer tanks are concentric. HalfCatSim also allows users to provide dimensions for the feed system and injectors, thus allowing for a more accurate model of this rocket engine.

The combustion chamber, nozzle dimensions, and expected initial conditions were entered into RPA, and the estimated optimum expansion performance came out to be 1.1 kN or about 248 lbf. A note should be made here that the engine was going to initially use 100% ethanol, but RPA simulations estimated the temperature at the nozzle throat in the range of 4780 to 4830 Fahrenheit. A mixture of 70% ethanol and 30% water lowered the estimated temperatures at the throat to between 4130 and 4165 Fahrenheit. Concerns about durability of the phenolic liner in the combustion chamber and the CHAMBERSAFE nozzle at these extreme temperatures drove the decision to use the 70% ethanol 30% water mixture as the fuel. The results of multiple simulations can be seen in Table 4.2. The simulations HAlfCat 2 and RPA 2 most closely matched the objectives set by SSTA and this thesis. The key takeaways are the initial thrust of 246 lbf., burn time around 5.5 seconds, specific impulse of 114 seconds, and O/F ratio of 3.8. With the simulations completed, the expected thrust of the engine was in the range of 225-275 lbf. The next steps were to test the individual components.

Table 4.2: Simulation Data

Data Set	Thrust (lbs.)	ISP (sec.)	Chamber Pressure (psi)	O/F Ratio	$\dot{m}_o$ (lb/sec)	$\dot{m}_f$ (lb/sec)	Area Ratio
HalfCatSim 1	226	112	409	4.0	1.55	0.38	4.68
RPA 1	207	203	300	4	No data	No Data	4.68
HalfCatSim 2	246	114	442	3.8	1.67	0.44	4.68
RPA 2	248	209	350	4	No data	No Data	4.68
HalfCatSim 3	267	116	473	3.2	1.78	0.49	4.68
RPA 3	287	213	400	4	No data	No Data	4.68

Chapter 5

Component Testing and Test Stand Setup

In order to confirm the validity of the proposed valve and rocket motor a multitude of tests was performed. The main aspects of the motor that had to be tested before assembling the entire design for a test fire were the injector baffle, Igniter cup, and the fuel and oxidizer tanks. The test apparatus and sequence of events during each test will be discussed.

5.1 Injector Testing

The injector baffle was tested to ensure proper atomization of fuel and oxidizer within the combustion chamber. However, due to budget limitations, a previous test set up was used that was not designed for the exact dimensions of this injector baffle. This led to leaks and an incomplete characterization of the flow from the injector baffle. However, after the test was completed, it was determined that the baffle would work as intended.

A PVC tripod stand was utilized to hold an aluminum tube that would act as the test oxidizer and fuel tank (Fig. 5.1). The aluminum tube was watertight sealed

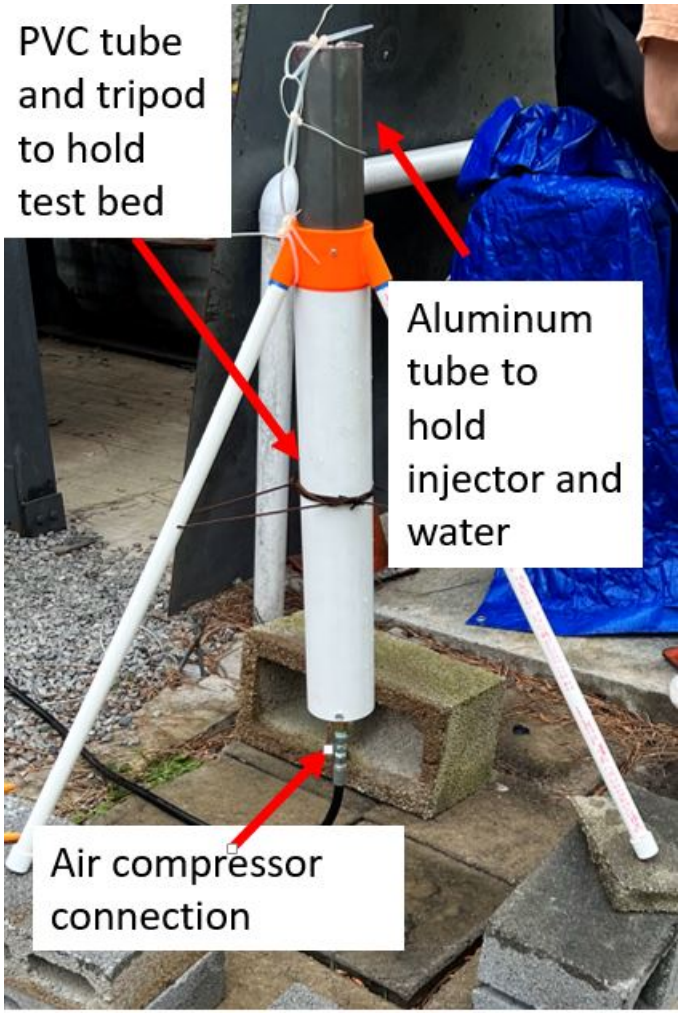


Figure 5.1: Injector Testing Apparatus

on one end (the end facing the ground) with a piece of circular composite material secured in place with a snap ring. The composite piece had a hole in it that allowed for a pneumatic quick disconnect coupler to be inserted and secured within it. This coupler would accept a connection from the standard air compressor that was to be used during the testing of the injectors. The opposite end of the aluminum tube would hold the injector baffle during testing.

The injector baffle was assembled at the workshop. Oxygen tape was wrapped around the threads of the $\frac{1}{4}$ in push-to-connects and then the push connects were secured into their threaded holes in the baffle. An industrial lubricant, Red "N" Tacky, was applied to the O-ring grooves and the O-ring was inserted into the groove. The testing of the injector baffle took place at the rocket test stand.

The PVC tripod stand was placed on concrete blocks to create an even surface. The aluminum tube, with composite cap and snap ring, was placed in the tripod. Next, the air compressor quick connect was attached to the connection point on the composite cap. The aluminum tube was filled with approximately 1 gallon of water. The injector baffle was inserted into the top of the aluminum tube and a snap ring was placed in a groove at the top of the aluminum tube to keep the injector from flying out (Fig. 5.2). Finally, the air compressor was charged, and the switch flipped to allow for the air to flow from the compressor into the aluminum tube.

Three tests were conducted using the process described above. Each test was conducted at a different compressor pressure to ensure that the push-to-connects would work as intended. The tests were conducted at 50, 100, and 150 psi., and it was observed that the push-to-connect injectors worked exactly as intended (Fig. 5.3). The stream from the four oxidizer injectors impinged on the single fuel jet approximately 1.45 inches above the surface of the fuel injector. The flow created by the impinged jets was a single jet that was well mixed. Unfortunately, due to the aluminum tube being designed for a slightly different size injector baffle there were

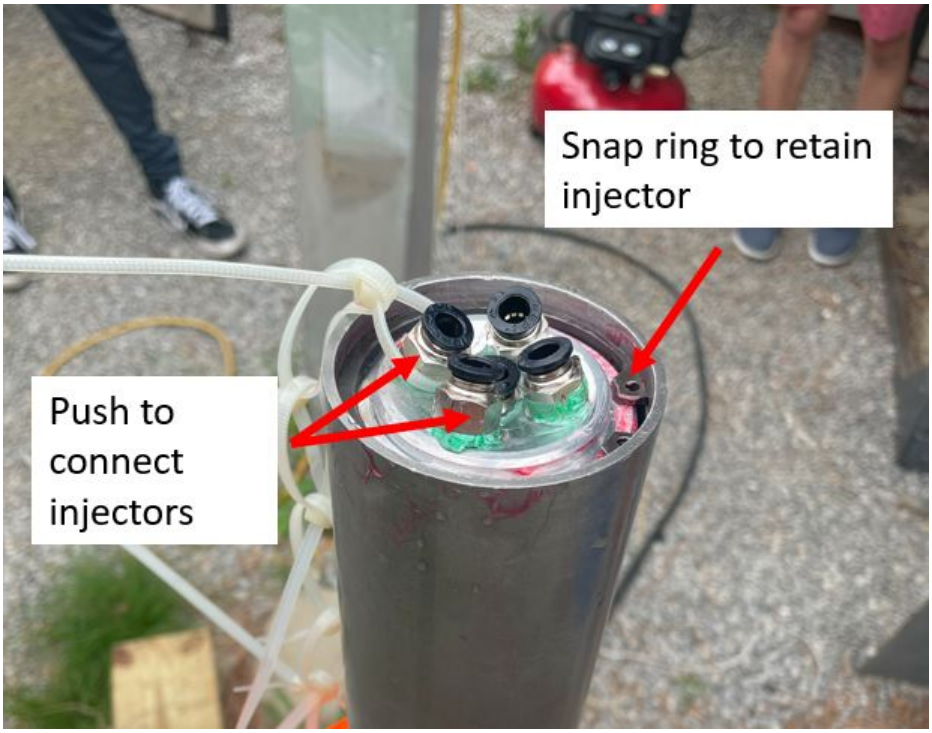


Figure 5.2: Injector Testing Apparatus 2

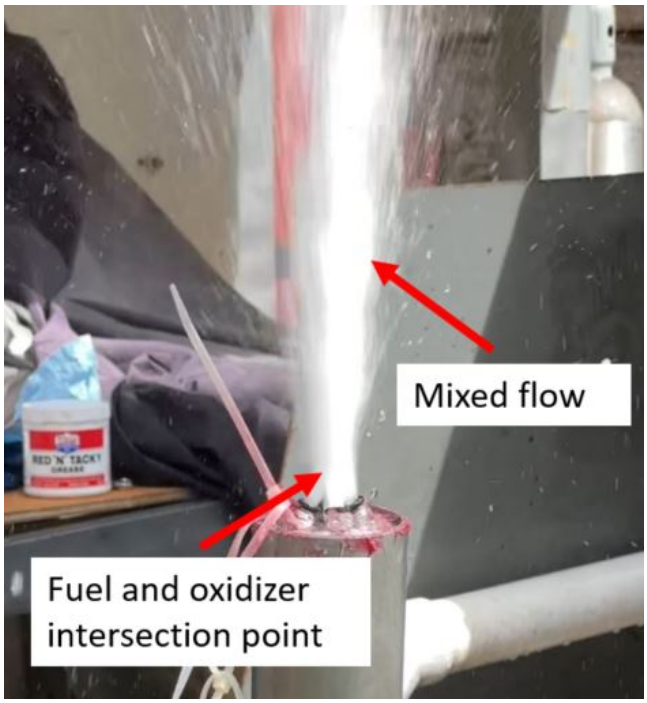


Figure 5.3: Injector Flow Testing, Proof of Mixed Flow

leaks during the testing and the coefficient of discharge could not be determined from the injector testing.

5.2 Ignition Cup Testing

As discussed above, many different versions of the ignition source were designed, printed, and test fit to the injector and combustion chamber. However, it was not until the seventh iteration of igniter that ignition compound was made, and the igniter tested. A batch of six igniters was made, all from the same batch of igniter compound to help reduce any deviation in compound makeup. The testing was conducted at the rocket test stand in a safe and secure area with fire extinguishers ready in case of any anomaly. A small pit was made from concrete blocks and the igniters placed within the pit to help ensure no accidental spread of fire (Fig. 5.4). This pit also provided an easy place to aim fire extinguishers if anything went wrong.

Two tests were conducted and recorded for review after. The igniters burned for an average of 17 seconds. From the videos, there are three clear phases that the igniter goes through while burning: initial ignition, full burn, and post-burn. The initial ignition lasts approximately one to two seconds and is categorized by the pop of the e-match and initial combustion of the igniter compound. The second phase, full burn, begins when the flames of the initial ignition reach the exit of the igniter cup. By this point the entire igniter cup has lit, and a majority of the heat energy from the igniter compound is being released. Figure 5.5 shows the igniter in the full-burn phase. The full burn lasted ten seconds on average. While the exact temperature of the flames were not measured, it would not be unreasonable to estimate the temperature of the full burn flames to range between 2,000 and 2,500 degrees Celsius [36]. The final phase, post-burn, is defined by the weakening of the flame exiting the igniter cup. At this point most of the igniter compound had burned away, but there was still flame present on and exiting the igniter cup. The post-burn lasted an average of five to six seconds.

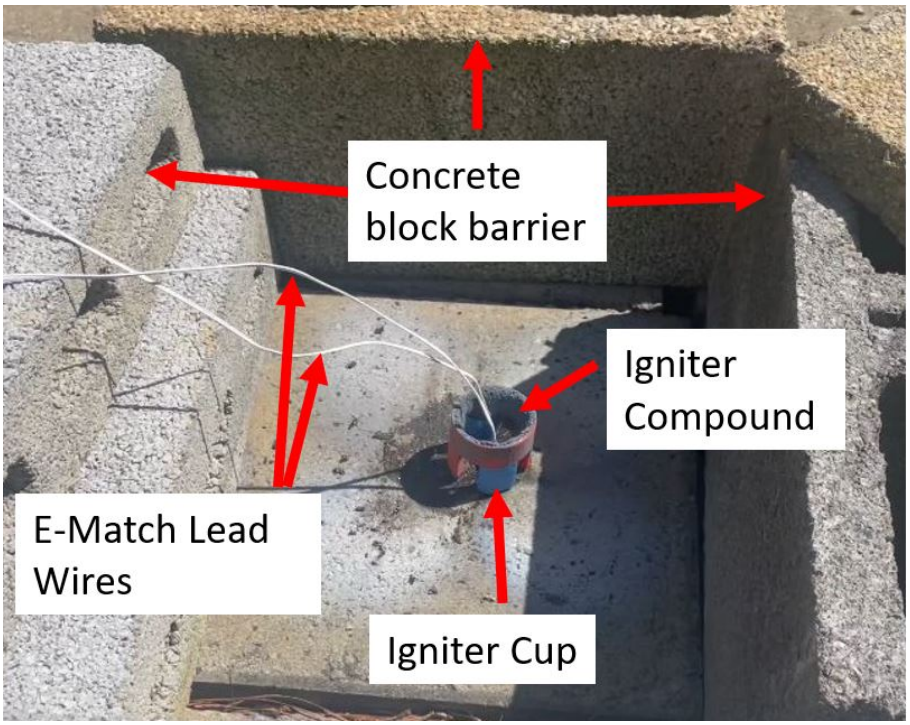


Figure 5.4: Igniter Test Set Up

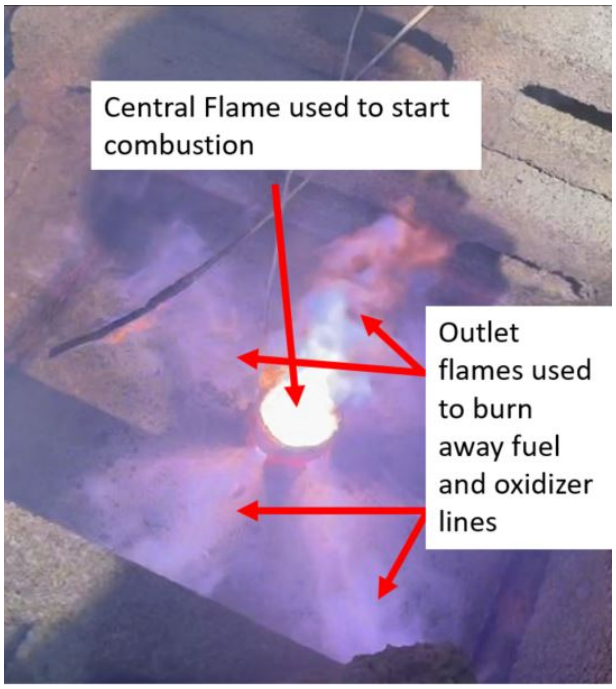


Figure 5.5: Igniter Design 7 Test Burn

Another series of igniter tests took place after the first two test fires to validate the final igniter design could burn through the nylon fill lines. The rocket was configured for a nominal test fire, but instead of their normal constituents, the fuel and oxidizer tanks were filled with water. The fuel and oxidizer tanks remained unpressurized for this test. The igniter leads were touched to a battery and the igniter started to burn. After two to three seconds the igniter reached peak burn, and shortly after water could be seen coming out of the nozzle outlet. At the conclusion of the test, the combustion chamber was disassembled and inspected. Multiple nylon fill lines had been completely severed in the test. While the test did not result in all the fill lines being severed there was confidence that when the fuel and oxidizer tanks were pressurized, the additional pressure on the nylon fill lines would help them burst or sever when heated by the igniter.

5.3 Fuel and Oxidizer Tank Pressure Testing

To ensure that both the fuel and oxidizer tanks could withstand operational pressures, a hydrostatic test was conducted. A hydrostatic test was chosen because in the event of a catastrophic failure of the pressure vessels the energy released from a hydrostatic test is much less than that of a pneumostatic test [43]. The fuel and oxidizer tank were assembled in their concentric configuration. All O-ring grooves and O-rings were covered in Krytox GPL 206 grease to help ensure a proper seal in the respective tanks. The injector baffle was plugged with threaded brass caps that were rated for a working pressure of 1200 PSI. When assembling the tanks for the test, the water in the fuel tank was dyed a dark red and the plunger was placed in its operating position. The oxidizer tank was then filled with clear unaltered water. The red dye was used to make it easier to determine if there was a leak between the two tanks. If any red was found in the oxidizer tank, it would be obvious that a leak between the tanks was present.

The tank assembly was taken to the rocket test stand to complete the pressurization test. The assembly was placed on a cinder block with one side against a structural beam of the test stand and strapped to the beam with two ratchet straps (Fig. 5.6). A braided metal hose was connected to the metal nipple that was screwed into the forward closure. The other end of the metal hose was connected to a regulator that was then connected to a high-pressure nitrogen tank (Fig. 5.7). The fuel and oxidizer tank would be charged to 1200 PSI, or just over 1.5 times the mean operating pressure of the tanks.

The process in which the fuel and oxidizer tank were pressure tested is as follows. After the metal hose was secured to the motor, the regulator valve to the nitrogen tank was opened very slightly. A leak check was performed on the regulator, metal hose, and fuel and oxidizer tanks. After it was determined that there were no active leaks, all personnel present at the hydro test moved behind the blast wall for safety purposes. The nitrogen valve on the K-bottle was slowly opened all the way.

Over seven minutes the regulator was used to slowly increase the pressure applied to the fuel and oxidizer tanks up to 1200 PSI. A maximum pressure of 1207 PSI was applied to the fuel and oxidizer tanks, but was reduced back down to 1200 to complete the test. Once the regulator was maintaining 1200 PSI the instrumentation was left untouched for five minutes. This was done to ensure that both the fuel and oxidizer tank would maintain their structural integrity in the event of extended over pressurization.

After the five minutes had passed, the regulator was used to reduce the pressure back down to ambient pressure. The flex hose was removed from the nipple of the forward closure and the tanks were inspected. Both tanks performed exceptionally well. After disassembling the tanks it was determined that there were no leaks between the fuel and oxidizer tanks and no damage was caused by the pressure test of the tanks.

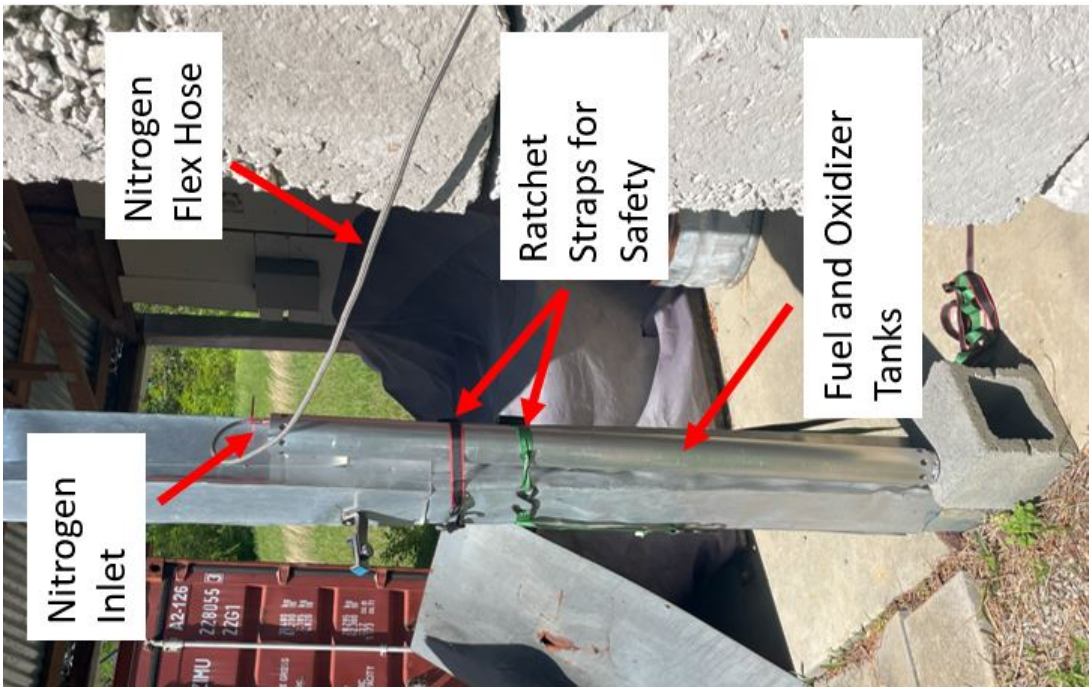


Figure 5.6: Motor Assembly for Hydrostatic Testing

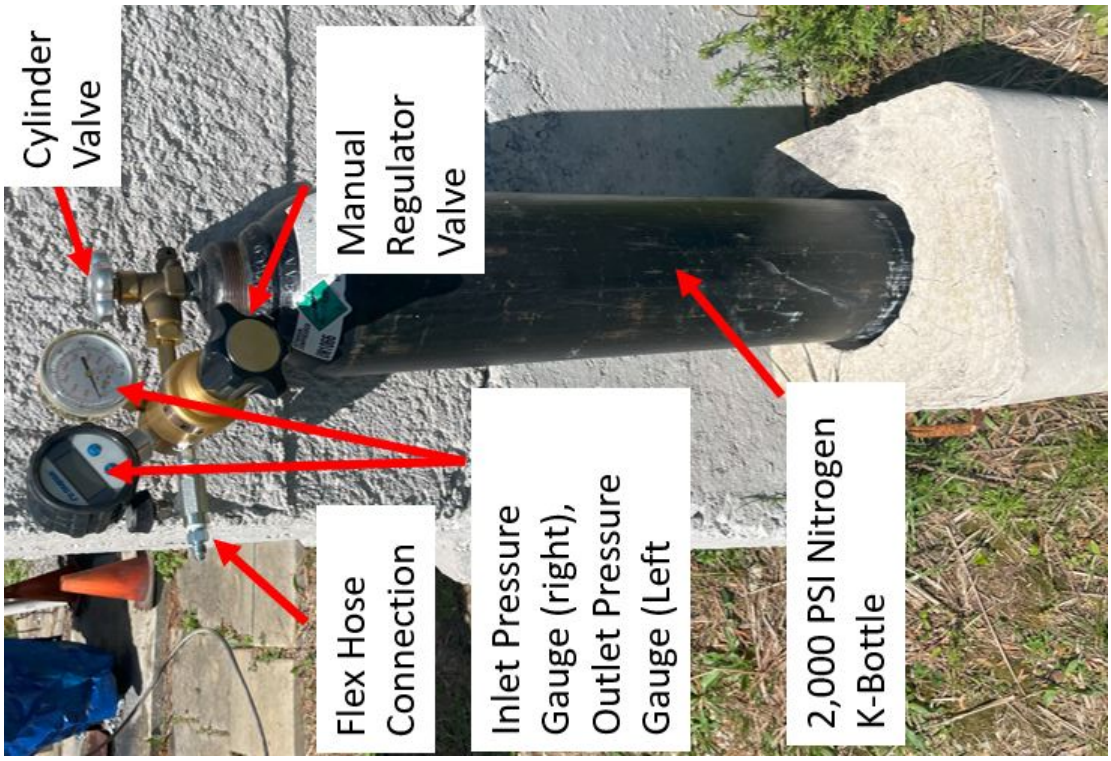


Figure 5.7: Nitrogen Assembly for Hydrostatic Testing

5.4 Engine Assembly

The final task to complete before going to the test stand was the assembly of the liquid bi-propellant engine. The most difficult part of assembly was the inter-stage, and thus, that is where assembly began. Push-to-connects were installed on the aft fuel and oxidizer closure and injector baffle. The aft closure was inserted into the inter-stage coupler and secured with screws. The injector baffle was inserted into the aft end of the inter-stage coupler but was not yet secured. Nylon tubing, to connect the aft closure and injector, was cut to length and test fitted. When the proper length of nylon tubing was determined, the injector was removed from the inter-stage. Five tubes were cut to the determined length and inserted into the aft closure. The injector was again inserted into the inter-stage coupler, and the nylon tubes coming from the aft closure were inserted into the push-to-connects on the forward end of the injector. The injector baffle was then secured to the inter-stage coupler with screws. The assembled inter-stage can be seen in Figure 5.8. The combustion chamber was then assembled.

Push-to-connects were installed on the aft end of the injector, and plugs and the fill line tubing were inserted into the push-to-connects. The igniter was installed on the aft end of the injector (Fig 5.9). The igniter leads and nylon tubing were secured together using electrical tape (Fig. 5.10). This was done to make the rest of the combustion chamber assembly easier and to ensure that the fill lines did not kink in the loading phase. Phenolic tubing was cut to approximately five inches in length and slid over the fill lines and igniter. The outside of the phenolic tubing was greased with Red "N" Tacky ^{TM} and the steel sleeve of the combustion chamber was slid all the way up to the forward section of the injector baffle. The steel liner was secured to the forward part of the injector baffle with screws. The nozzle was inserted into the nozzle carrier, and then both were slid into the aft of the steel liner. The forward part of the nozzle sat flush against the aft end of the phenolic liner while the aft end of the nozzle carrier was flush with the aft end of the steel liner. The nozzle carrier

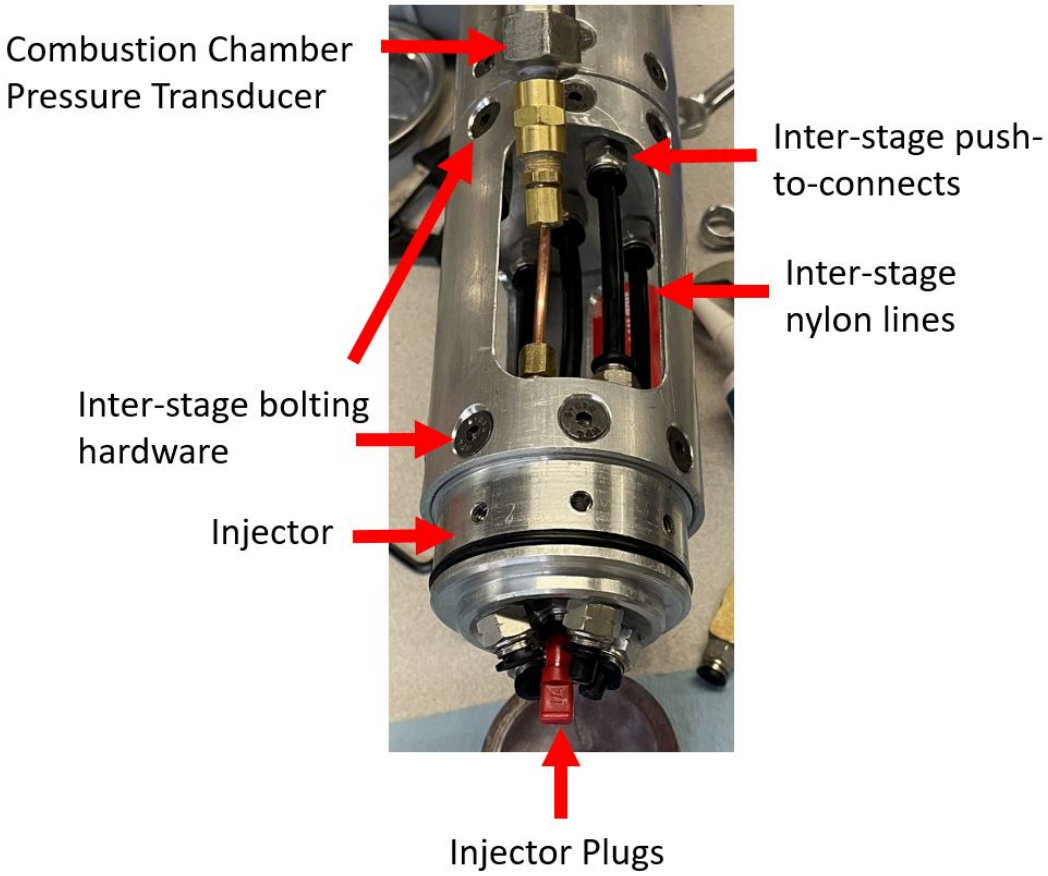


Figure 5.8: Inter-stage Assembly

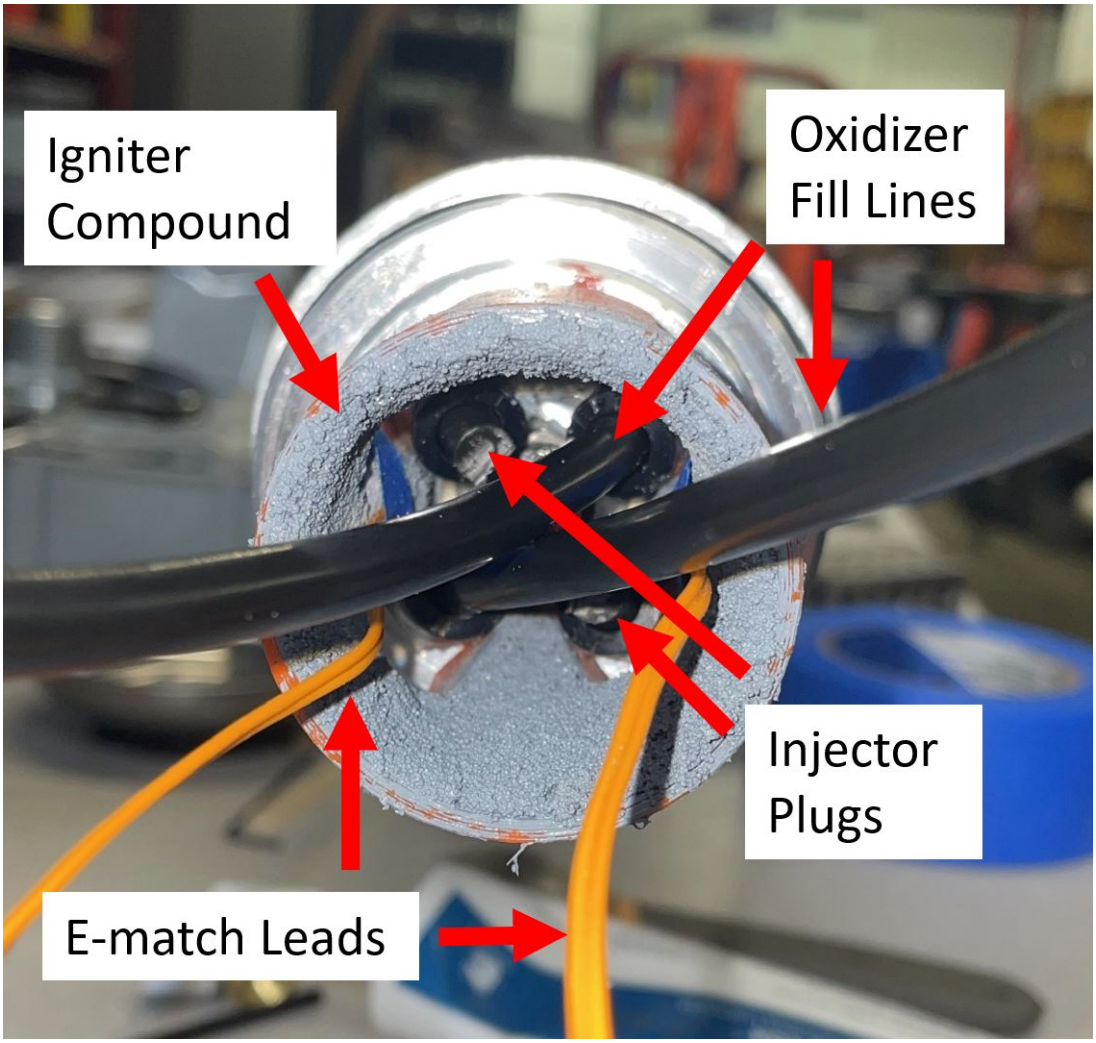


Figure 5.9: Combustion Chamber Assembly with Igniter and Nitrous Fill Lines



Figure 5.10: Combustion Chamber Assembly with Igniter, Taped Nitrous Fill Lines, and Phenolic Liner

was secured to the steel liner with screws. A cutaway of the combustion chamber assembly, sans nylon tubing, can be seen in Figure 5.11.

The first step in assembling the fuel and oxidizer tanks was to insert the ethanol tank into the top of the aft fuel and oxidizer closure (Fig. 4.3). The ethanol tank and aft closure were then slid into the nitrous oxide tank. The aft closure was then secured to the nitrous tank with screws. With the final two pieces left to install, the ethanol plunger and forward closure, it was time to fill the ethanol tank. The fuel, a mixture of 70% ethanol and 30% water by mass, was measured and mixed in a glass beaker. The entire motor assembly was stood vertically, and the ethanol was poured into the fuel tank via funnel. A small copper tube was screwed into the ethanol plunger. This tube would allow any air in the fuel tank to be removed as the plunger was being inserted. The plunger was inserted into the fuel tank and pushed down until the ethanol was at the very top of the copper tube. The copper tube was then capped and any ethanol that had spilled was cleaned as to not cause any cross contamination issues with the oxidizer tank. The forward closure was installed and secured to the oxidizer tank with screws. Just above the forward closure, a snap ring was installed to ensure the forward closure was not forced out of the assembly by the pressure from the nitrous oxide. Finally, the forward vent line, forward pressure transducer, and combustion chamber pressure transducer were installed (Fig. 5.12).

It should be noted that all O-rings on the combustion chamber, injector baffle, inter-stage, ethanol plunger, and forward closure were greased with a small amount of Krytox GPL 206 to help maintain their seals. All screws on the rocket assembly were also greased to help prevent galling.

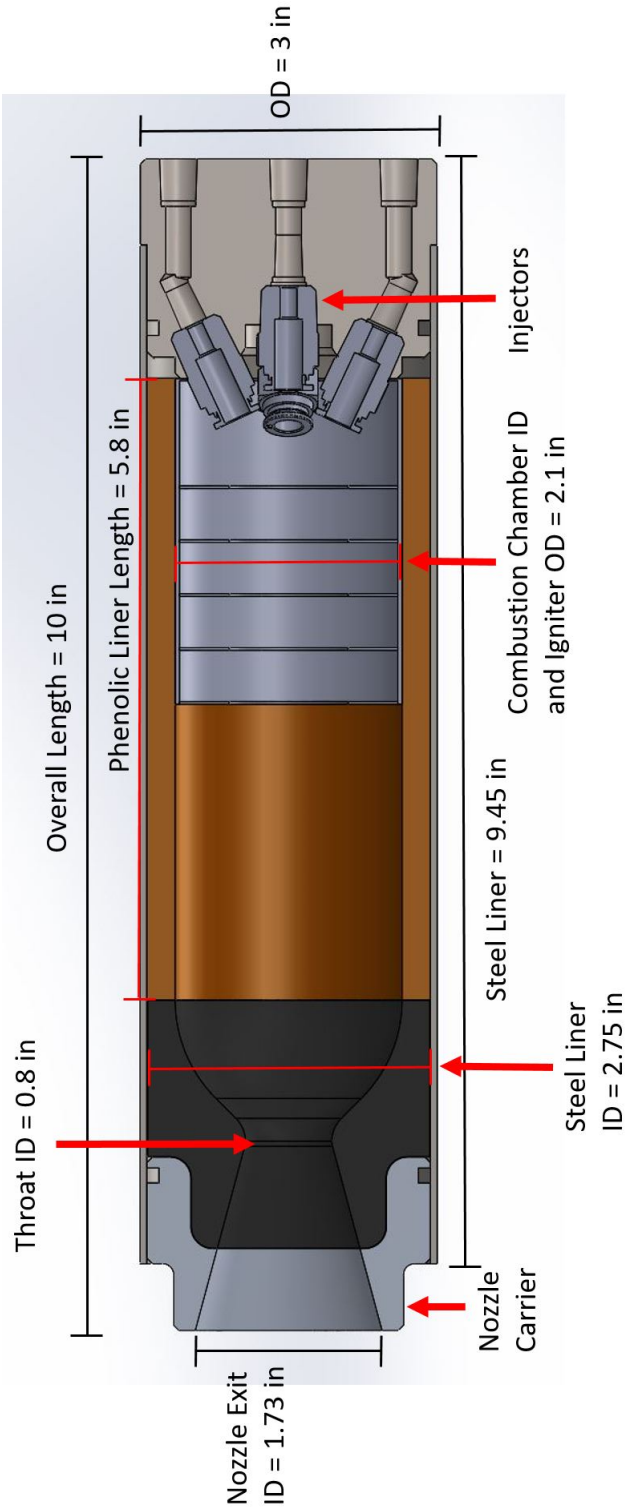


Figure 5.11: Combustion Chamber Cutaway

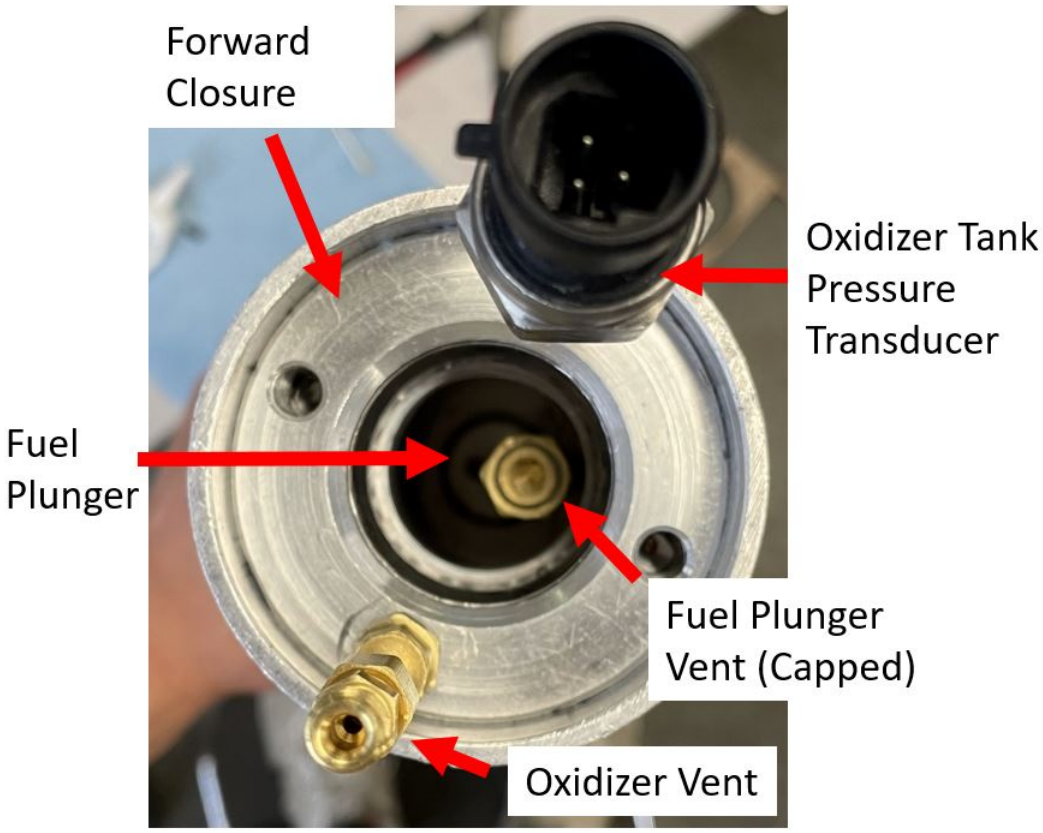


Figure 5.12: Forward Closure

5.5 Test Stand Assembly

Once at the test stand, the motor carriage was slid onto the carriage rails on the test stand mount. The top of load cell was bolted to the cross beam on the test stand, and the bottom was bolted to the top of the motor carriage, securing the motor carriage to the test stand. The rocket motor was then slid into the motor carriage. Aluminum machine blocks were placed on the forward closure of the motor to ensure the force of the motor would transfer directly to the load cell, and to protect the motor from being damaged by the bolt connecting the load cell to the cross beam. U-bolts in the motor carriage were tightened to ensure the motor would not move out of plane. Figure 5.13 shows the motor installed at the test stand while Table 5.1 describes the individual parts of the test stand.

After the motor install was complete, the nitrous oxide fill lines were connected with an NPT t-fitting. The t-fitting was then connected to a stainless steel flex hose. The flex hose was then routed from the t-fitting to the ground control box, and another flex hose was routed from the ground control box to the nitrous oxide K-bottle.

The ground control box can be seen, labeled with the flow of nitrous oxide, in Figure 5.14. The following figure, Fig. 5.15, numbers the main components of the control box. The components are as follows: 1, power connections to actuate the fill and vent solenoid valves; 2, solenoid valve that allows nitrous oxide flow from the K-bottle to the oxidizer tank on the rocket, also known as the fill control solenoid valve; 3, solenoid valve that is a bleed vent valve or can act as an emergency vent valve for the vehicle oxidizer tank; 4,vent path. A piping and instrumentation diagram can be seen in Figure 5.16.

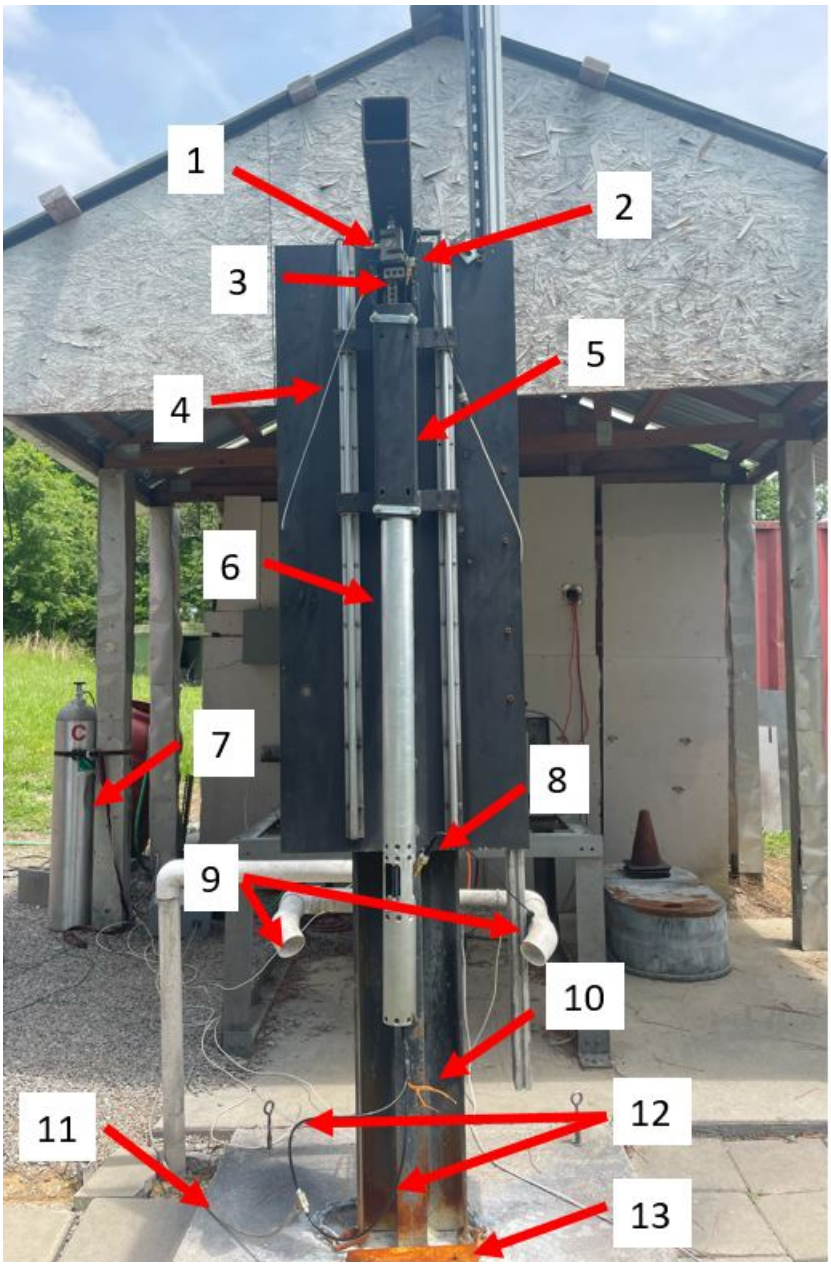


Figure 5.13: Test Stand Apparatus

Table 5.1: Test Stand Bill of Materials

Bill of Materials Number	Material/Item Description
1	500 lb. load cell
2	Oxidizer tank pressure transducer
3	Machine blocks
4	Oxidizer tank vent line
5	Motor carriage
6	Liquid bi-propellant motor
7	Nitrous oxide K-bottle
8	Combustion chamber pressure transducer
9	Water deluge system outlets
10	Igniter leads
11	Oxidizer flex hose
12	Oxidizer fill lines
13	Steel blast plate

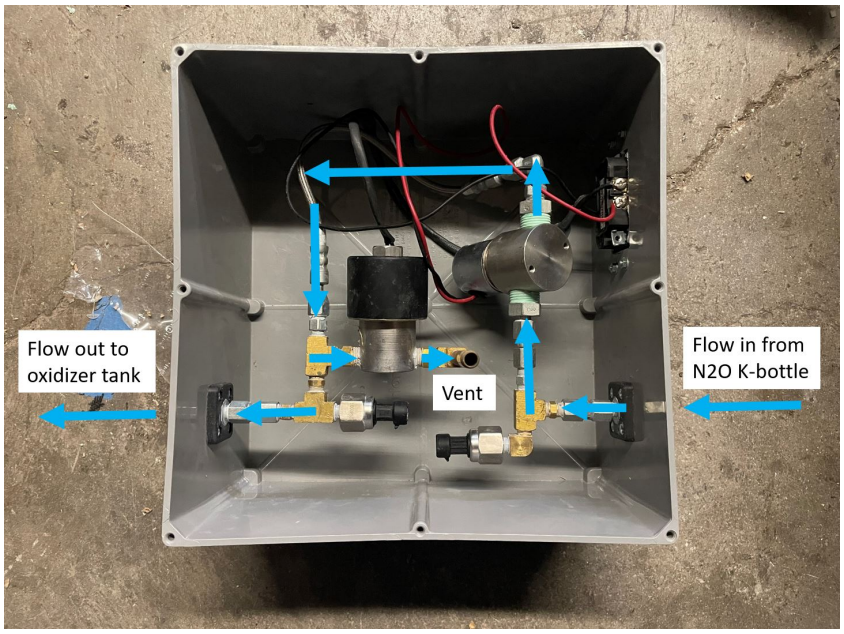


Figure 5.14: Ground Control Box Labeled with Flow Path

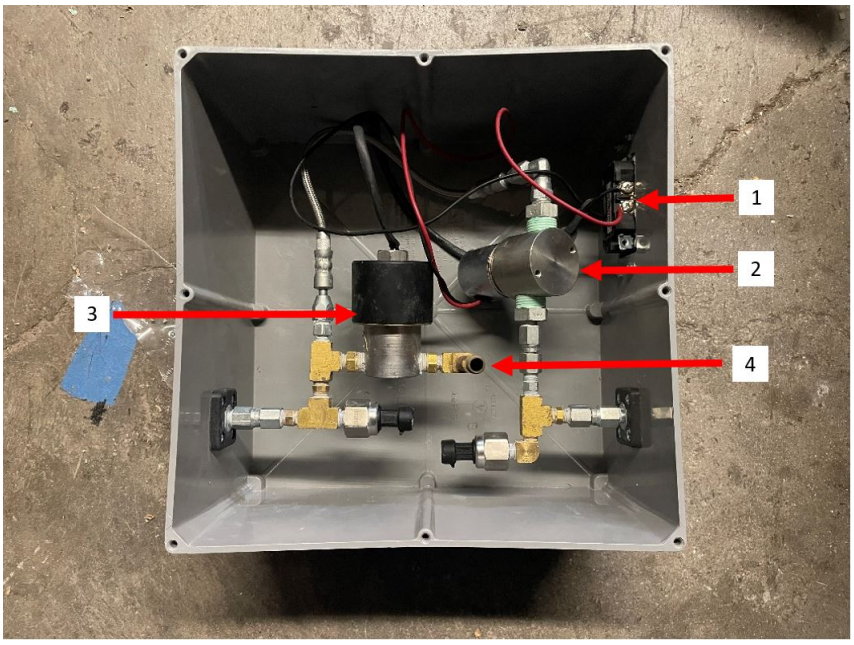


Figure 5.15: Ground Control Box Valves, Vent, and Power

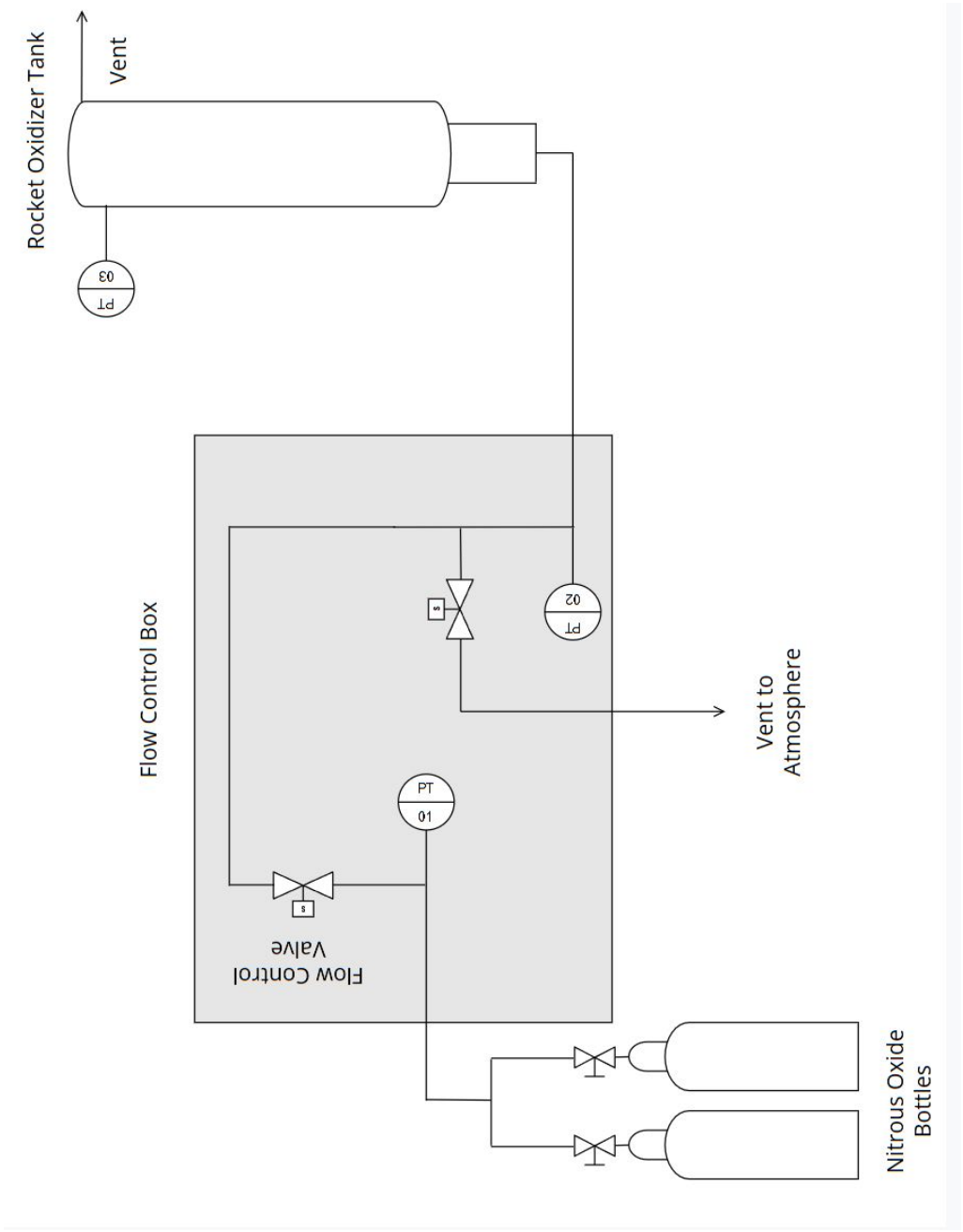


Figure 5.16: Rocket Fill Piping and Instrumentation Diagram

5.6 Data Acquisition

The data acquisition system (DAQ) (Fig. 5.17) used throughout the testing of this rocket engine was developed in the 2023 academic year by James Cooper. The system was developed to be used for both this liquid engine and SSTA's hybrid rocket, Davy Rocket. It was designed to be small, yet robust, containing the following breakout boards: ESP32-WROOM Module (38pin version) - Microprocessor, HX711 - Load Cell Amplifier, ADS1115 - Analog to Digital Converter (Pressure Data), XBee3 - Radio Module (Data Transmitting), SSD1306 - Display Module, Micro SD Card Reader - Data Logging, MP1584EN DC-DC Buck Converter - Voltage Regulator (Fig. 5.18). The data acquisition box received voltage inputs from the load cell, combustion chamber pressure transducer, and oxidizer tank pressure transducer. Those inputs would be converted from analog to digital within the DAQ and be sent out over WiFi signal via XBee3. A corresponding XBee3 plugged into a laptop would receive the data packages sent out from the DAQ. Thomas Scott developed a software program to convert the digital data packets from the Xbee3 into engineering units. This software was also useful in that it could be used to perform calibrations on the sensors used for testing. Both the load cell and the pressure transducers follow a linear curve fit. To calibrate the system, a known weight or pressure could be applied to one of the instruments, the raw data output was recorded, a linear fit was made, and calibration adjustments could be input into the software.



Figure 5.17: Data Acquisition Box

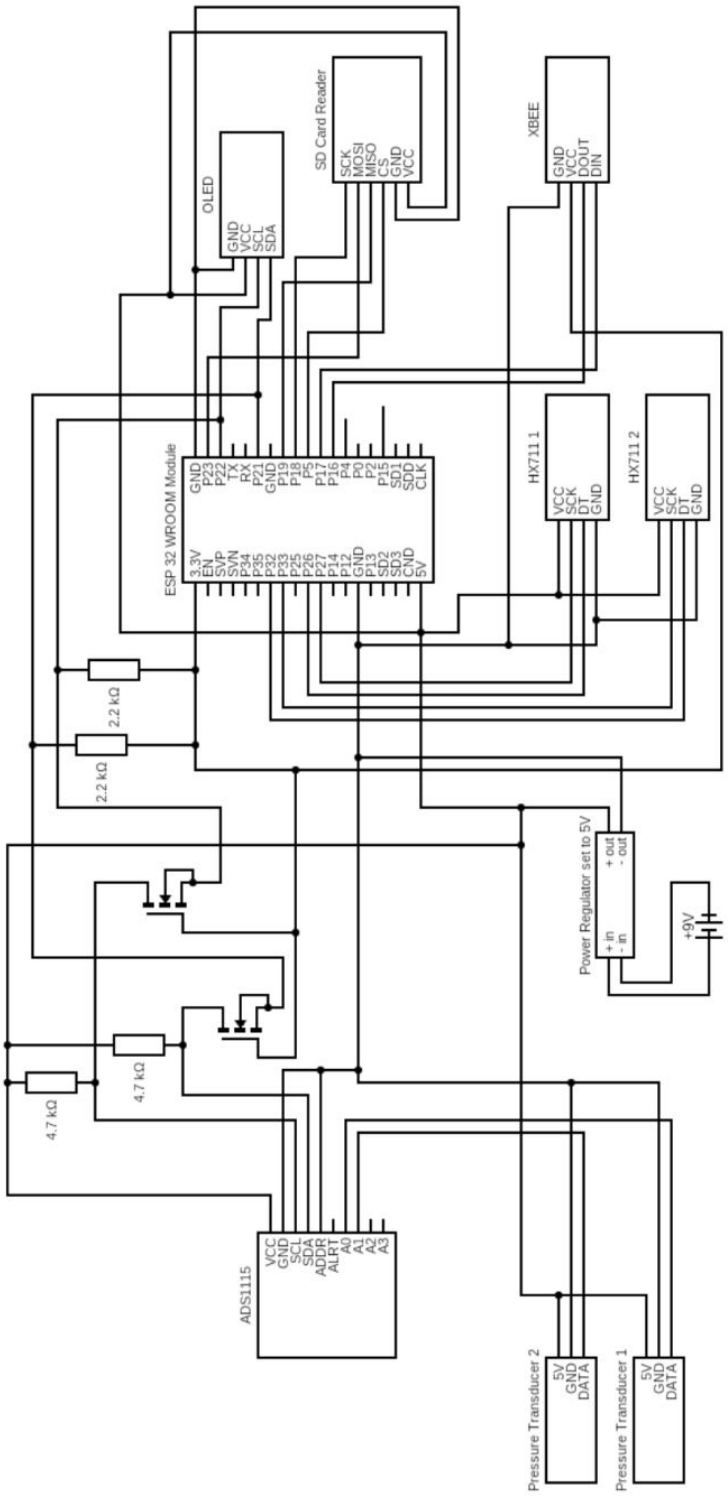


Figure 5.18: Circuit Diagram of Data Acquisition Box

Chapter 6

Experimental Results

6.1 Liquid Motor Test Fire Sequence

Once the oxidizer flex hoses were connected to the K-bottle all non-essential personnel were cleared to a safe distance (at least 1000 feet) from the test stand. Checkouts were performed in the bunker control room to confirm that the proper data would be logged from the test fire. The load cell readouts were checked to ensure the load cell had been zeroed. Oxidizer tank and combustion chamber pressure transducers readings were checked to confirm that they were reading within acceptable ranges. Cameras were checked to ensure proper visualization of the motor during test fire and recording software was enabled to allow for video review post-test fire.

After confirmation of good telemetry the final two set up steps were ready to be complete. After confirmation that all personnel were a safe distance from the pad, the electrical connections to the igniter leads were made and continuity was checked on the control box in the bunker control room. The nitrous oxide K-bottle was then opened to allow nitrous oxide to flow up to the solenoid valve in the ground control box. All personnel then fell back to either the bunker control room or the designated safe distance.

The motor loading and test fire sequence is as follows:

1. Final confirmation that all personnel have been cleared of the pad and are either in the bunker control room or at the minimum safe distance via radio call out and visual check from control room cameras.

2. Final checkouts of all telemetry: load cell, oxidizer tank pressure transducer, combustion tank pressure transducer, igniter continuity check, control room cameras, drone operated camera (if applicable).

3. A radio callout was made to all personnel that loading would begin in 30 seconds.

4. After 30 seconds a command was sent to open the fill control solenoid valve in the ground control box and the solenoid valve was opened.

5. Data from the oxidizer pressure transducer was observed and the control room cameras were watched to ensure no anomalies could be seen.

6. When the oxidizer tank pressure read 750 PSI a command was sent to close the fill control solenoid valve.

7. Pressure was monitored for 30 seconds after the fill control valve was closed to ensure it was within the desired range of 750 $\pm$ 15 PSI. After confirmation of good pressure range a radio callout was made that loading was complete.

8. Another radio callout was made that the motor would be test fired in 30 seconds. At 10 seconds a countdown was begun on the radio.

9. At zero seconds the fire button on the fire control box was pushed and the electrical signal was sent to the igniter.

10. Throughout the duration of the test fire the pressures in the oxidizer tank and combustion chamber were observed and the cameras were monitored for any anomalies.

6.2 Test Fire Results

6.2.1 May 2, 2023 Test Fire

The inaugural test fire of the liquid rocket engine did not go as well as one would have liked. After the fire button was pressed on the control box, the spark of the igniter could be seen coming out of the end of the nozzle, and, shortly after, the flow of nitrous oxide could be seen as well. The engine lit for a brief, 1.3 seconds, was extinguished by the flow of nitrous oxide for six seconds, relit for two seconds, and finally flamed out. The thrust and pressure data can be seen below in Figures 6.1 and 6.2. A peak thrust of 220 lbs. was recorded with a total impulse of 162 lb.-s.

After the test fire was complete the motor was disassembled to investigate what happened during the test fire, pictures can be seen in Appendix B. After the combustion chamber was removed, it was discovered that only a small hole had burned through the plug used in the ethanol injector. It is believed that this small hole allowed for a minuscule amount of ethanol to enter the combustion chamber which correlated to the brief, 1.3 second burn that could be seen at the beginning of the test. However, with the high pressure flow of nitrous oxide into the combustion chamber, the fuel to oxidizer ratio became too oxidizer rich and combustion stopped. As the nitrous tank emptied, pressure lowered, and ethanol leaked from the hole in the injector plug into the combustion chamber, the chemical makeup within the combustion chamber swung back to that of a more stable fuel-oxidizer mixture. There was still enough heat being produced from the igniter cup to ignite the nitrous oxide vapor and ethanol mixture, and hence, the secondary two second burn. It should be noted that there was no increase in measurable thrust in the secondary burn.

While disassembling the engine it was also observed that the nitrous oxide fill lines did not burn through as intended. In fact, some portion of the fill lines were still connected to the push-to-connect injectors. Holes had been burned through the

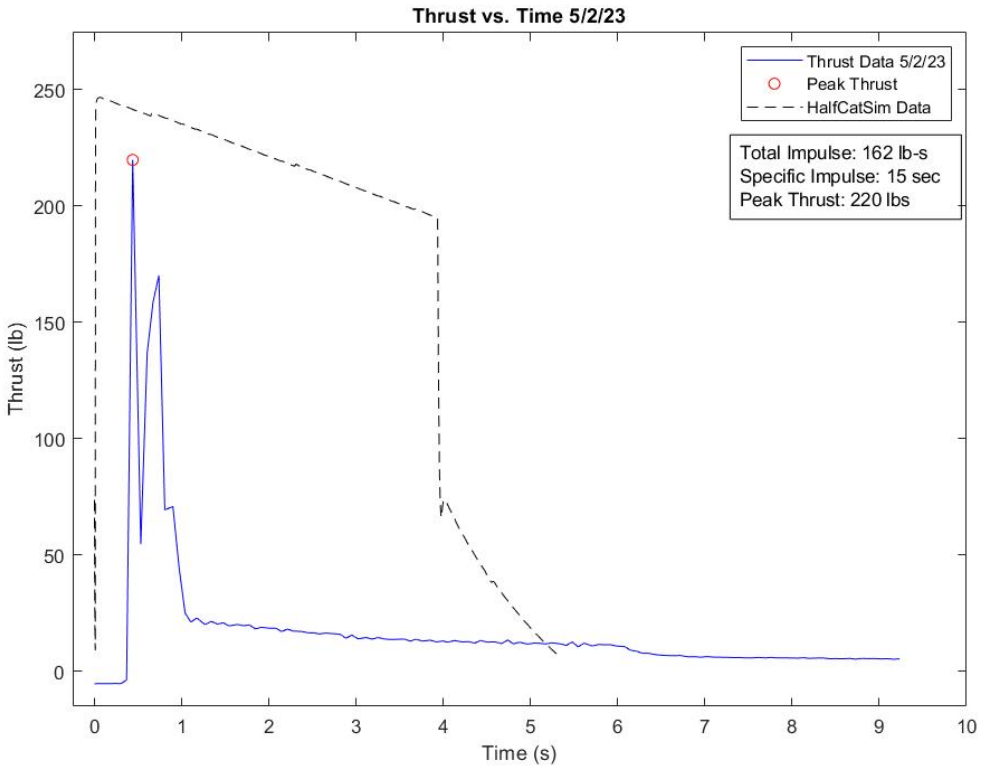


Figure 6.1: Engine Test Fire 5/2/23 Thrust vs. Time Data

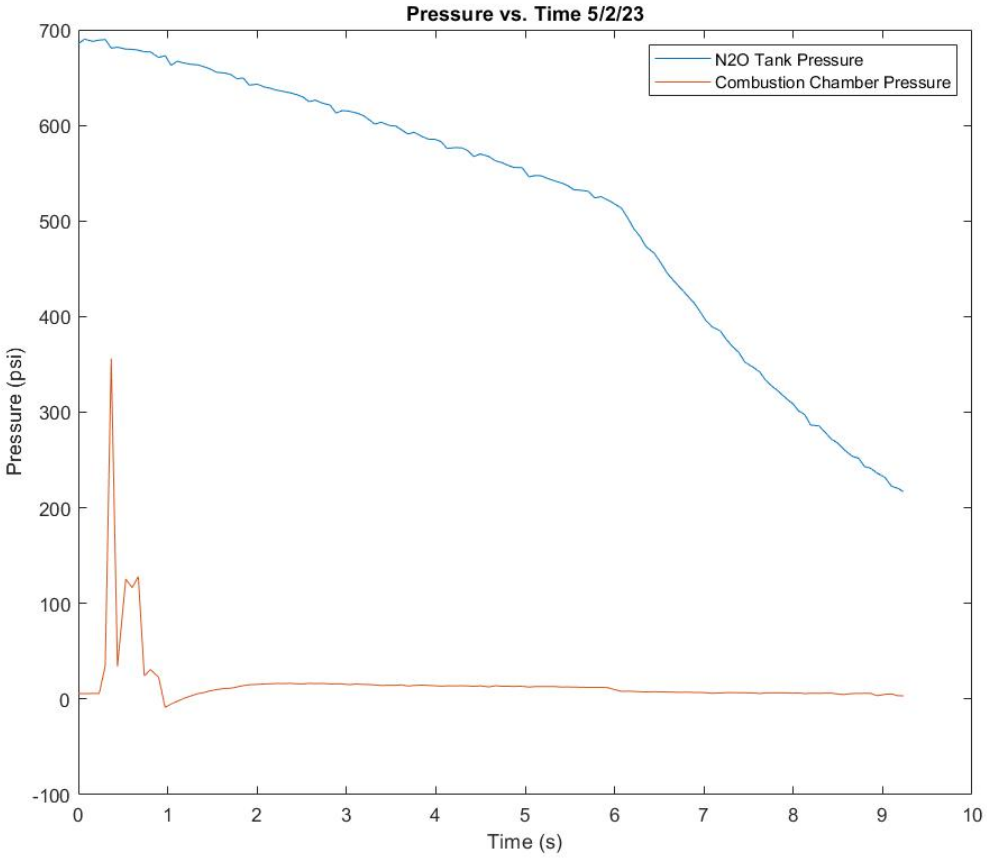


Figure 6.2: Engine Test Fire 5/2/23 Pressure vs. Time Data

fill lines to allow some flow of nitrous oxide into the combustion chamber, but it was clear that changes need to be made to the igniter so that the fill line would burn all the way through. It should also be noted that a large portion of the ABS igniter cup was found in the combustion chamber (Fig. B.1).

The culmination of these findings lead to changes in the design of the igniter that included: lengthening the overall igniter cup, making the walls thinner, and slightly adjusting the igniter compound. The igniter used in this test fire was Fig. A.4, and the igniter design that was driven from the findings can be seen here Fig. A.8. The decision was also made to not insert the full length of the plugs that were used in the ethanol and two of the N2O push-to-connects. The tab and cap of the plugs were much thicker than the walls, another potential point of failure for the first test fire. The theory behind this idea was that if the plug was not inserted all the way, there was a higher chance that the side walls would melt away allowing the proper flow of ethanol into the combustion chamber. A comparison of how the plugs were set up in the initial test fire and how they would be set up for the next test fire can be seen in Figures 6.3 and 6.4.

The small amount of data captured from the first test fire attempt can be seen in Fig. 6.1. A large dip in thrust, 220 lbs. to 55 lbs., can be seen just after ignition. This large dip in thrust may be attributed to the igniter being lit as there is a second peak, 170 lbs., in the thrust curve shortly after the initial peak.

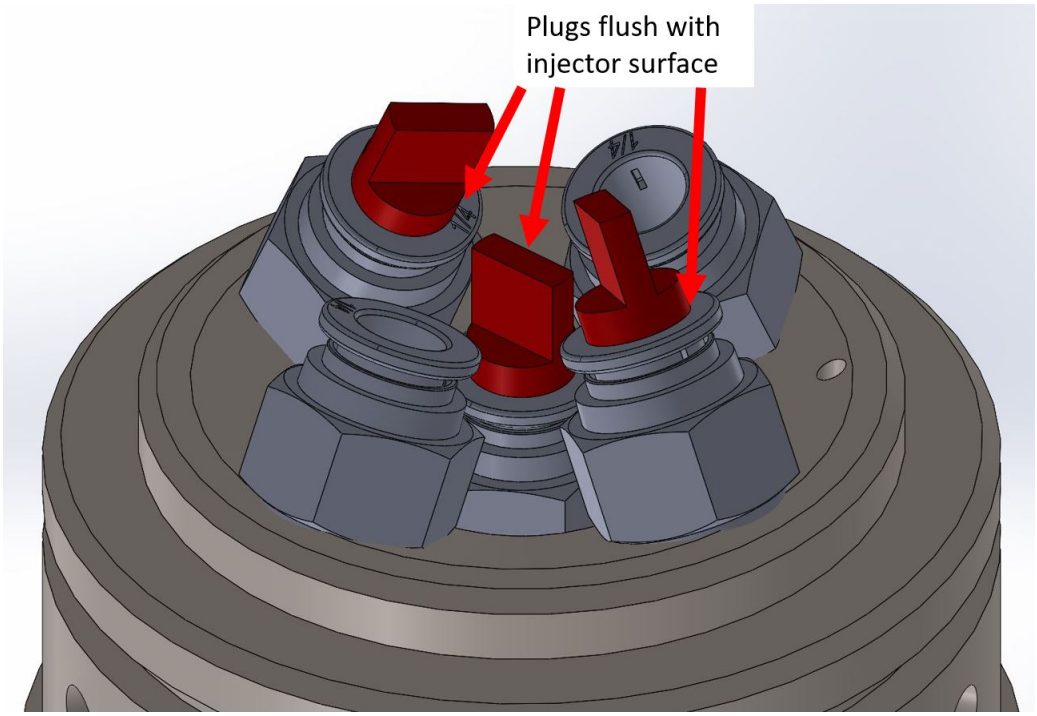


Figure 6.3: Injector Plug Configuration for 5/2/23 Test Fire

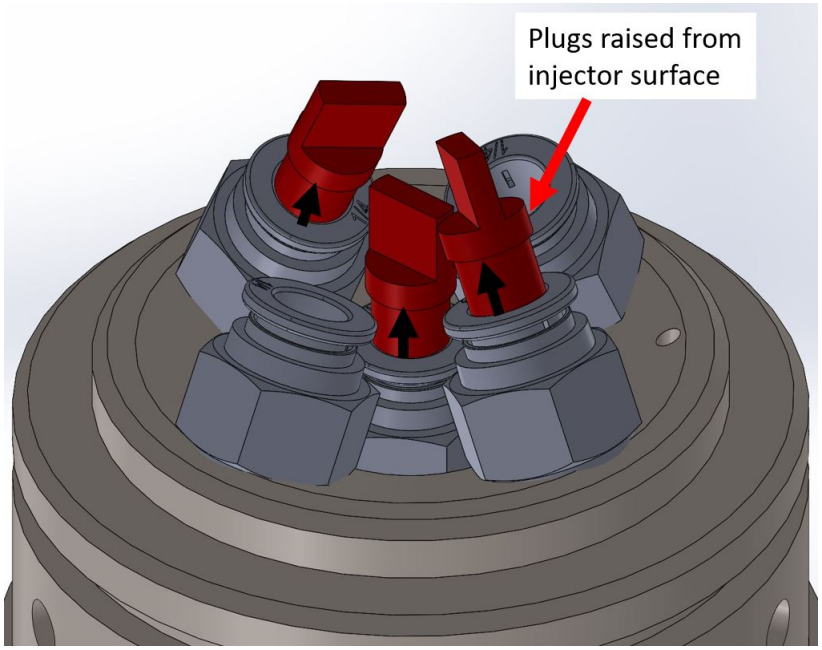


Figure 6.4: Injector Plug Configuration for 5/11/23 Test Fire

6.2.2 May 11, 2023 Test Fire

A second test fire was attempted on May 9th, 2023, but faulty push-to-connects on the inter-stage caused the nylon tubes on the inter-stage to bust during N2O loading. The nitrous oxide dumped overboard through the slots in the inter-stage section and the test was aborted. New push-to-connects were acquired and the inter-stage was disassembled and reassembled for another test fire.

The test fire on May 11th, 2023 was a partial success with another short duration burn. A peak thrust of 393 lbs. was recorded and the total impulse of the burn was calculated to be 170 lb.-s (Fig. 6.5). While the metrics of the second test fire were much more promising than that the first, more issues arose during this test fire. Almost immediately after the fire button was pressed on the control box the ethanol plug burst. Ethanol drained from the fuel tank for approximately four seconds, a majority of the ethanol, before the oxidizer lines had time to completely burn through. Six seconds into the test fire blue flames could be seen coming from the engine nozzle, indicating ethanol combustion. At seven and a half seconds a large pressure wave ejected from the nozzle (Fig. 6.6); the nitrous lines had finally burned away and oxidizer was entering the combustion chamber. The N2O very rapidly mixed with the small volume of ethanol left, and the motor truly ignited for the first time. For less than a second, the conical shape of rocket exhaust can be seen exiting the rocket motor before the mixture became too oxidizer rich and flaming out.

While the second test fire was in no way perfect, there was now proof that the Urbanski-Colburn Valve could be used to ignite a liquid bi-propellant rocket. The second key observation from the test fire was that the plugs used in the push-to-connects were unreliable and a different option should be explored. Other takeaways included: the igniter was still struggling to burn through the fill lines fast enough to introduce oxidizer into the combustion chamber in a timely manner, the thrust output of the engine may be much higher than it was originally designed for, the nozzle was degrading at a much faster rate than expected and its material composition would

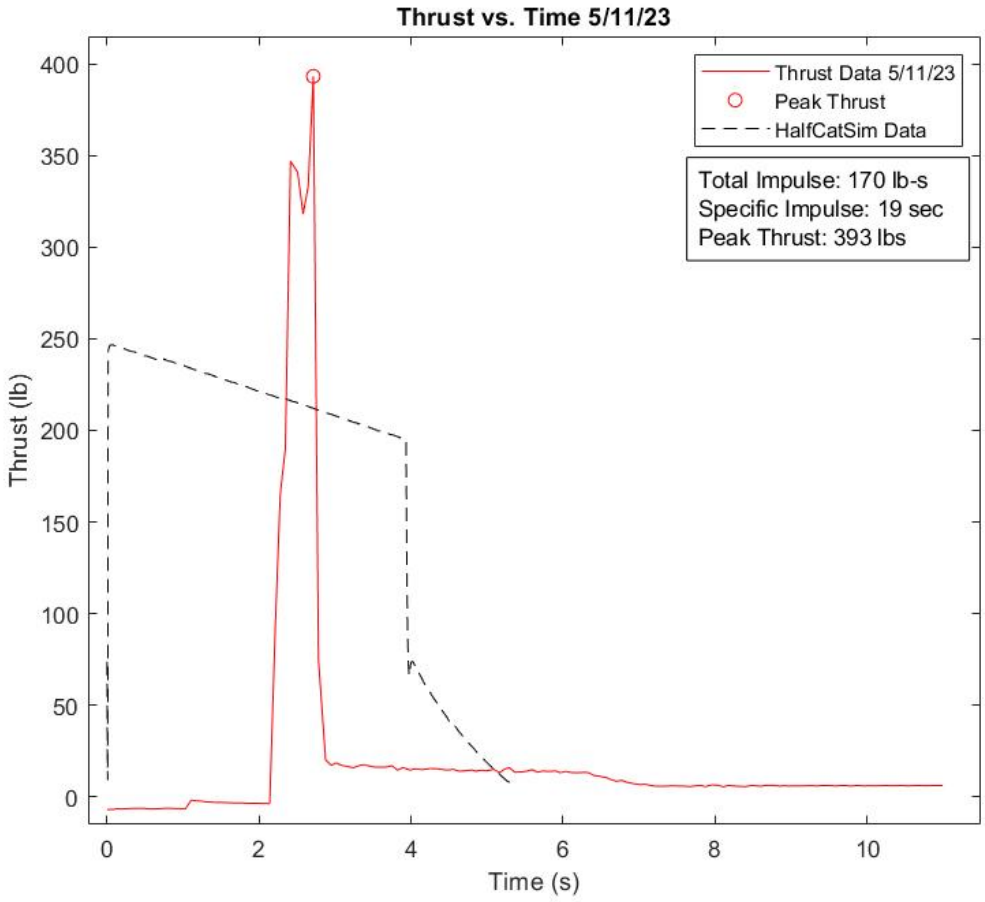


Figure 6.5: Engine Test Fire 5/11/23 Thrust vs. Time Data

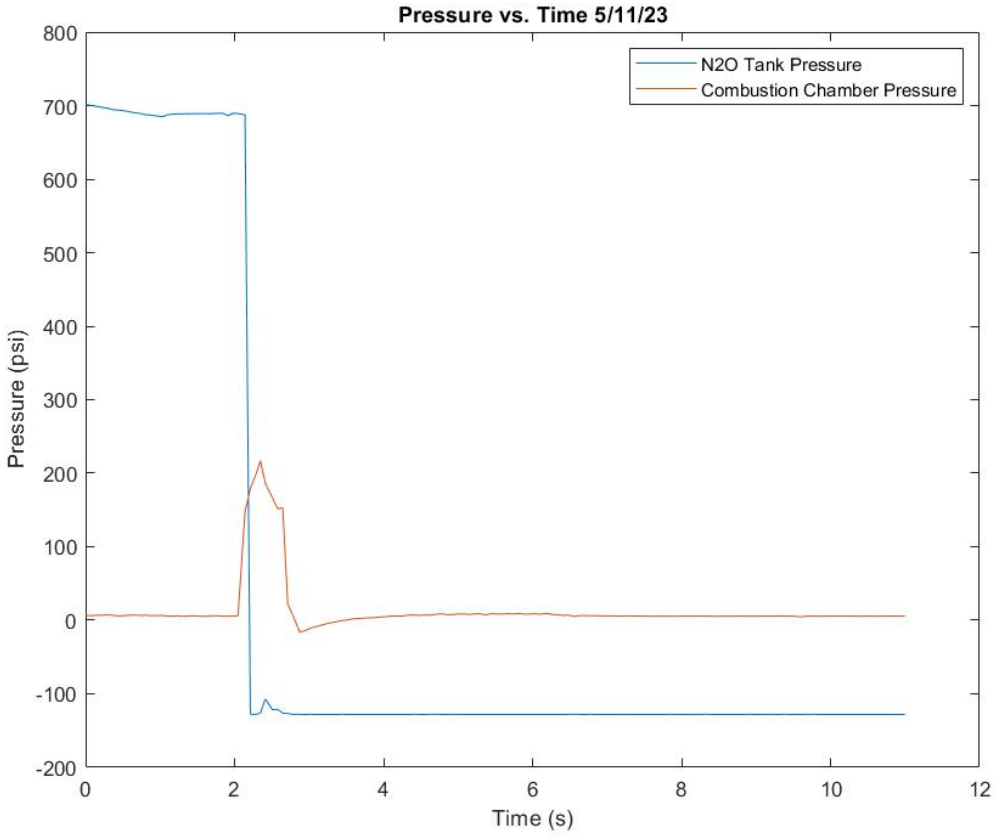


Figure 6.6: Engine Test Fire 5/11/23 Pressure vs. Time Data

need to be changed. Even though this test fire was much shorter than the expected nominal burn, the CHAMBERSAFE nozzle was nearly destroyed (Fig. 4.6 and Fig. 4.7). Chapter 4 Subsection 4.3 discusses the redesign of the nozzle. Pictures of the engine after the test fire can be seen in Appendix B.

6.2.3 February 27, 2024 Test Fire

Conducted by students in the spring 2024 senior design class, the third test fire of the liquid rocket engine implemented many of the lessons learned from the previous failed attempts. In an attempt to ensure the fuel and oxidizer entered the combustion chamber simultaneously nylon tubes were used to plug all of the push-to-connects on the injector. This was accomplished by utilizing a technique used in previously successful hybrid rocket motors developed at UTK. The N2O fill lines would remain unchanged, but the remaining oxidizer push-to-connects would have a single nylon tub inserted into both of them looping one to the other. Another section of nylon tube that extended out of the nozzle was inserted into the ethanol push-to-connect and plugged (Fig. 6.7). To help mitigate the issue of the nylon tubes not burning through, a small section of each tube, just above the push-to-connect, was covered in igniter compound. This set up bolstered the chance that all of the nylon tubes would burn through, and reduced the chance that one push-to-connect would initiate flow before another. Another upgrade that came with this test fire was the use of a machined Delrin® nozzle.

On February 27th, 2024 the third test fire of the rocket engine took place and resulted in a nearly completely successful test. The engine burned for five seconds outputting thrust in the 90 to 150 lb. range (Fig. 6.8). A peak thrust of 154 lbs. was measured, and the total impulse was calculated to be 567.3 lb.-s. The specific impulse of the engine was calculated to be 109 seconds. These results were extremely promising in proving that the Urbanski-Colburn valve could be used to ignite a liquid rocket engine. While this test fire was a near complete success, issues

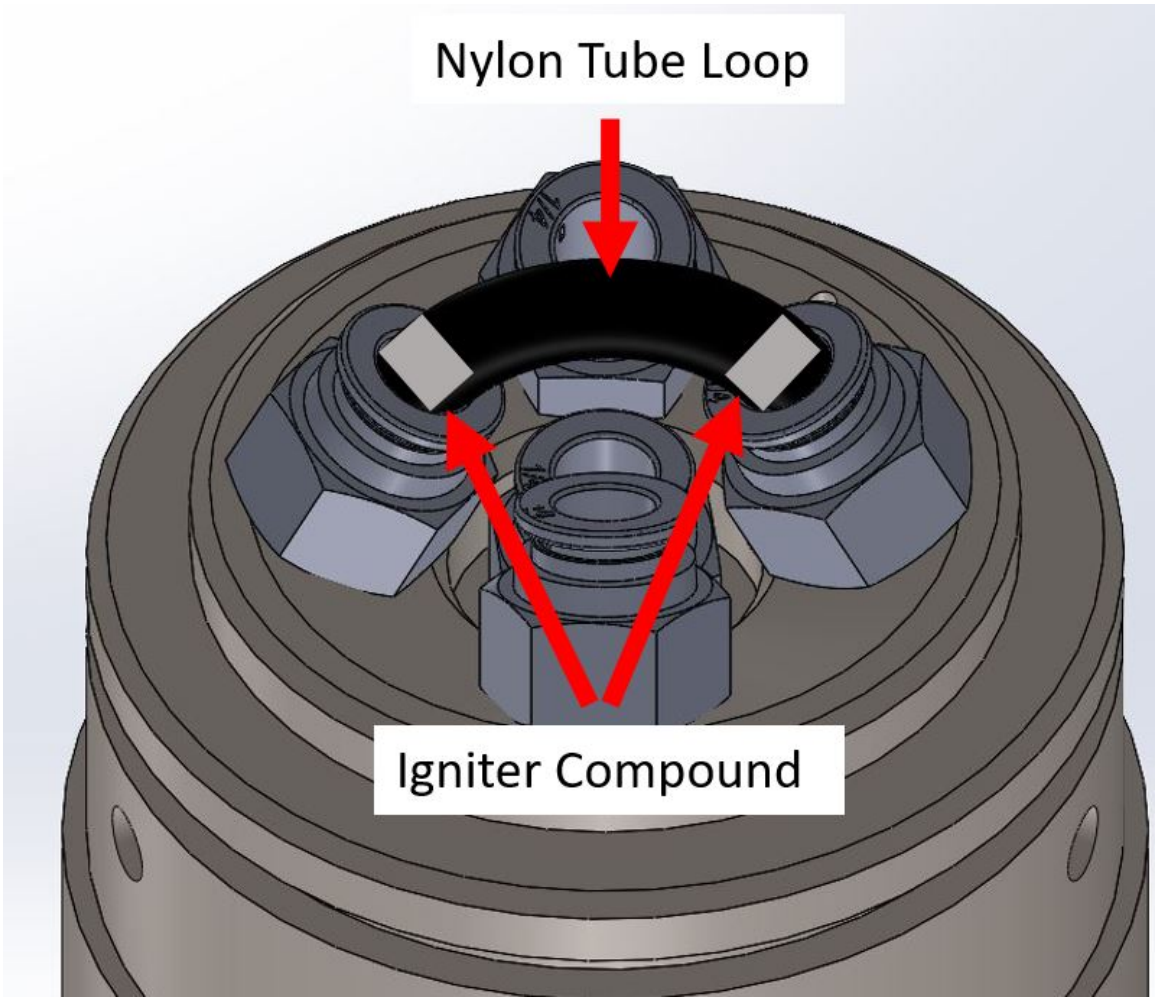


Figure 6.7: Injector with Nylon Tube Plugging Unused Oxidizer Lines (not to scale)

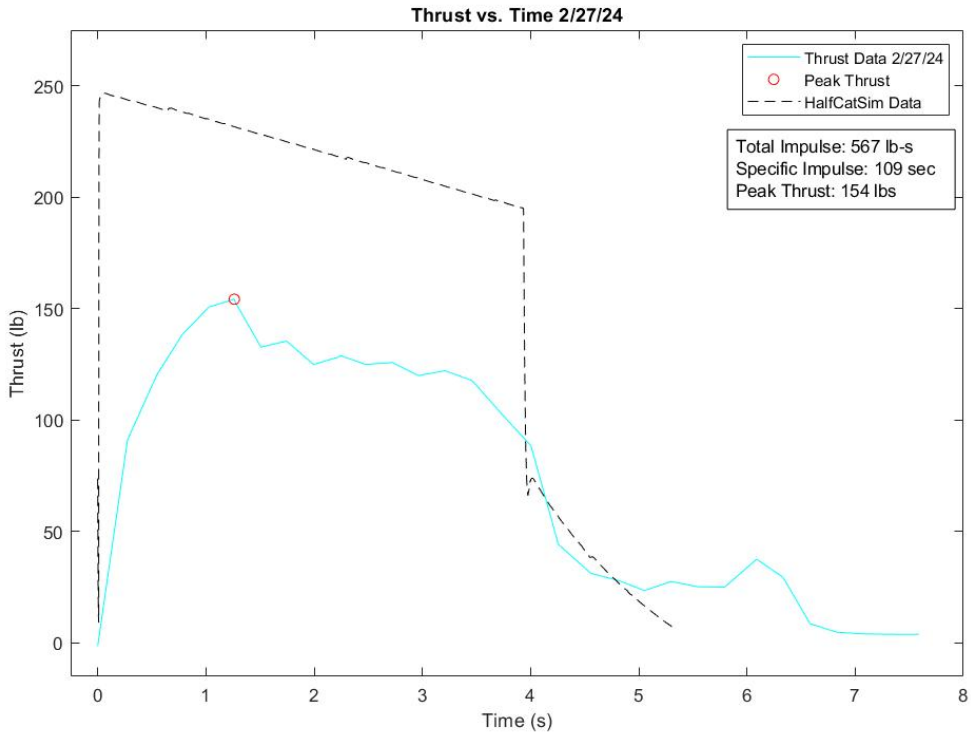


Figure 6.8: Engine Test Fire 2/27/24 Thrust vs. Time Data

still arose with the initial ignition of the motor and severing of the nylon tubes.

Fire could be seen in the nozzle for about one second after igniter ignition, and shortly after, the loop connected to one of the nitrous oxide injectors was burned away. With only one side of the loop released, N2O began spewing out of the nylon tube outside of the nozzle. However, there was evidence that the ethanol line had also been burned away; the nitrous was burning with a green-blue tint to it. Shortly after ignition of the igniter, all five nylon lines were completely severed and complete combustion was initiated in the combustion chamber. A bright blue flash could be seen and then the standard rocket exhaust profile appeared from the nozzle of the rocket engine. The exhaust shone a bright blue changing to a light green as the ethanol tank was emptied (Fig. 6.9).

When dissembling the engine special attention was given to the nozzle and the phenolic liner of the combustion chamber. There was little concern of the phenolic liner burning through as this recipe had been used in multiple much more powerful rockets that the university had built and test fired, but it is always good practice to ensure no burn throughs. The phenolic liner was charred as expected and the thickness had been reduced, as expected in an ablative liner. The nozzle was inspected and it was noted that the throat of the nozzle had still degraded, but the degradation was less than the CHAMBERSAFE nozzles. After reviewing the video of the test fire, the shape of the exhaust can be seen changing as the throat of the nozzle degrades. This could also explain the less than expected performance of the engine. As the throat area increases the engine loses the ability to choke the flow, and the area ratio decreases. As the area ratio decreases, the exit Mach number decreases, which decreases the exit velocity of the exhaust, and thus, thrust decreases.



Figure 6.9: Engine Test Fire 2/27/24 Engine Firing

6.2.4 April 11, 2024 Test Fire

The fourth, and final, test fire of the liquid rocket engine was conducted by the 2024 spring senior design class on April 11th, 2024. The nylon lines were assembled the same as the third test fire, but this time more igniter compound was applied to the lines to ensure they burned through properly. A new Delrin nozzle was used for this test fire. The engine was taken to the test stand and loaded into the test cell.

When oxidizer loading was complete, the ignition button was pressed and the engine roared to life instantly (Fig. 6.10). The engine burned for 5.8 seconds, outputting a maximum thrust of 188 lbs. It can be seen in Figure 6.11 that after initial peak thrust, the engine continued to output thrust ranging from 178 to 105 lbs. The total and specific impulse of the fourth test fire were calculated to be 810 lb.-s. and 119 s., respectively. This test fire was an all-around massive improvement from the previous test fires.

After disassembling the engine it was found that the Delrin nozzle was not able to withstand the heat and pressure of combustion, and eroded away as the engine burned. However, the nozzle performed better than the previous version. Reviewing the video of the test fire shows fluctuations in the exhaust, but less than the previous test fire.

All of the test fire thrust plots can be seen compared to the HalfCatSim data in Figure 6.12. Specific data points of interest can be seen in Table 6.1. It should be noted that an unknown but significant fraction of the measured thrust and impulse is due to the igniter. Another note should be made that the 1000 PSI pressure transducers used have an accuracy of $\pm 1\%$ and the 500 lb. load cell has an accuracy of $\pm 0.3\%$.



Figure 6.10: Engine Test Fire 4/11/24 Engine Firing

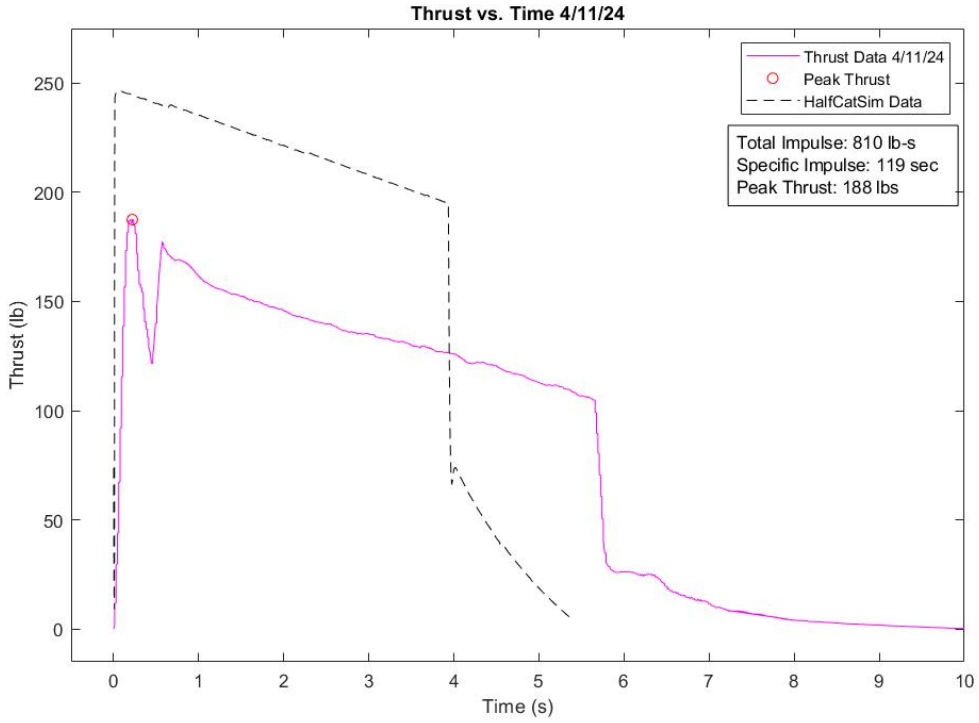


Figure 6.11: Engine Test Fire 4/11/24 Thrust vs. Time Data

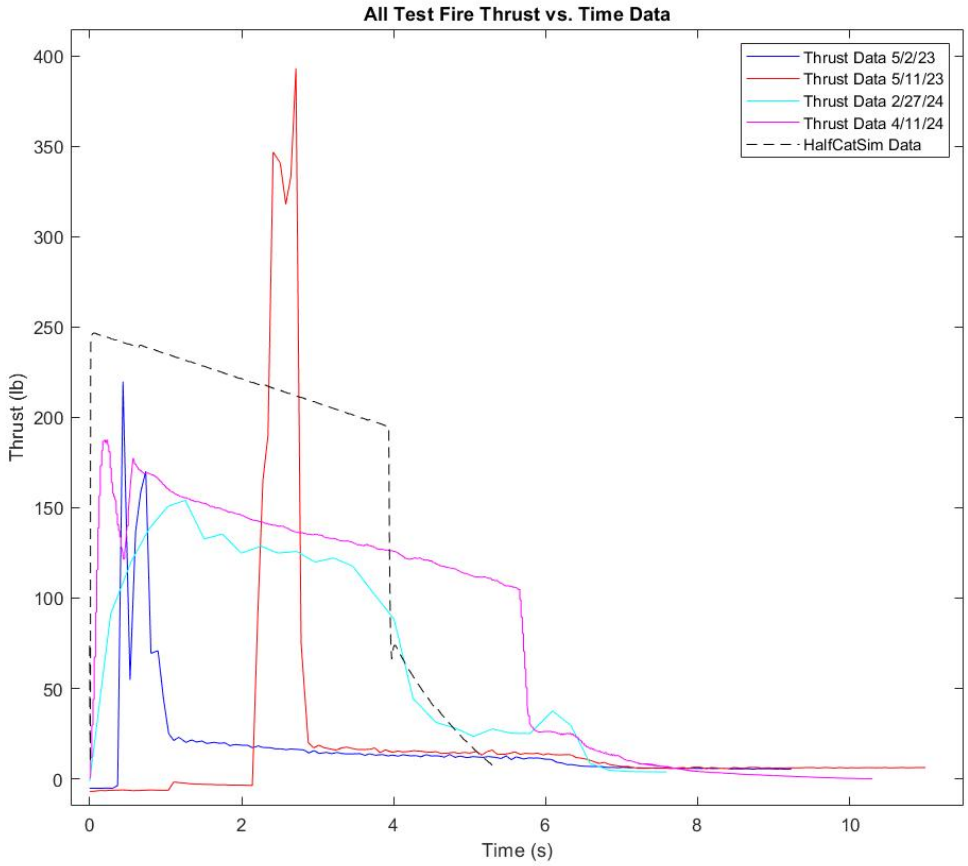


Figure 6.12: All Engine Test Fires Thrust vs. Time Data

Table 6.1: Sim Data vs. Test Fire Data

Data Set	Peak Thrust (lbs.)	ISP (sec.)	Total Impulse (lb-sec.)	C* (ft/s)	$\dot{m}$ (lb/sec.)
HalfCatSim 2	246	114	910	3415	2.1
RPA 2	248	209	No data	5085	No data
5/2/23 Test Fire	220	15	162	4970	1.2
5/11/23 Test Fire	393	19	170	4280	0.8
2/27/24 Test Fire	154	109	567	No data	0.7
4/11/24 Test Fire	188	119	810	No data	0.7

Chapter 7

Conclusion

7.1 Summary

Liquid propellant rockets have been used for nearly a century, and with recent revelations in re-usability, specifically the ability to land the first stage of a rocket, they will continue to be used for the foreseeable future. However, the barrier of entry for liquid rocketry can be daunting even for the programs with considerable funding. Hundreds of subsystems with thousands of moving parts must work in unison for a liquid rocket to perform nominally. While still extremely complex at the highest levels, hybrid rockets offer a simpler approach to rocketry. Incorporating knowledge from hybrid rocketry into liquid rockets can help to vastly simplify the fuel and oxidizer loading, injection, and ignition of liquid rockets.

Studying previously designed, tested, and implemented oxidizer loading systems used in hybrid rockets, it is clear that the same style of system can be used for a liquid rocket. Fuel and oxidizer can both be loaded through the nozzle and injector and into their respective tanks via nylon tubing. A new design for concentric fuel and oxidizer tanks allowed this engine to capitalize on nitrous oxide's autogenous property. This property allowed for a simple, yet effective, way to fill the oxidizer tank and pressurize both the fuel and oxidizer tank to desired levels. The pressure in the oxidizer tank

was monitored via pressure transducer to ensure it did not overcome the friction force of the push-to-connects holding in the fuel and oxidizer lines.

The final piece of the puzzle is the igniter. This liquid rocket engine has a smaller diameter and, therefore, less space for the igniter than the hybrid rockets studied. While the lack of a hybrid fuel grain allows for more space in the combustion chamber, it also means that the igniter must burn longer. There is no longer a crutch if the igniter does not perform exactly as intended. In hybrid rockets, if the igniter only partially severs the oxidizer lines, but the fuel grain begins to burn from the heat of the igniter, there is a high chance that the combustion process will begin. Once the combustion process has started, it is likely that the oxidizer lines will be completely severed and the total burn of the hybrid motor can be realized. However, in the case of a liquid rocket, this is not an option. The igniter must sever the fuel and oxidizer lines at the same time to allow the correct mixture ratio enter the combustion chamber while also burning long and hot enough to start the combustion process. If only the fuel or oxidizer line is severed and begins to discharge into the combustion chamber, there will be little to no reaction. Thus, engine performance will be greatly reduced. The results of the fuel and oxidizer lines not being severed at the same time can be seen in the first three test fires.

For the reasons stated above, the igniter had to be completely redesigned. The design had to move away from the previously used half-doughnut style, which allowed the heat of the igniter to ignite the hybrid grain, to an extended cylindrical design that would start by burning the fill lines away and last long enough to begin the combustion process in the combustion chamber. As stated in chapter four, the igniter went through many different iterations. The final design was a simple cylinder with ribs that allowed for increased packing density of the igniter compound. The additional application of igniter compound on the nylon lines allowed the fourth test fire to be a complete success.

A new liquid bi-propellant rocket engine was designed and built to prove the viability of the Urbanksi-Colburn valve in liquid rockets. After multiple complete

failures and semi-successful attempts, the liquid rocket engine ignited and burned for nearly six seconds on April 11th, 2024. A peak thrust of 187.5 lbs. and a nominal thrust range between 176 and 105 lbs. were measured. The total impulse was calculated to be 809 lb.-s. and the specific impulse was calculated to be 119 s. Although the results of the successful test fire do not reflect the expected design conditions of the engine, they prove that the Urbanksi-Colburn valve can be used to load and ignite a liquid rocket engine.

7.2 Future Work

Budget constraints and design complexities prevented the implementation of a fuel loading system for this engine. The possibility of overfilling the fuel tank and causing the nylon tubing to burst in the presence of an oxidizer also played a role in the decision to pre-load the ethanol into the fuel tank. Future work on the engine would include a ground side pump that would allow for the loading of ethanol simultaneously with, but separately from, the nitrous oxide. In order to implement the pump system, the forward closure could be redesigned to include a captured vent that would allow for any excess ethanol to be captured and contained in a safe manner. Another viable option would be to limit the total supply of ethanol to less than the total available volume in the fuel tank, mitigating the possibility of overloading the fuel tank.

A simpler solution to this problem would be to use a fuel that is either gaseous or self-pressurizing. Cryogenic fuels, such as liquid hydrogen or liquid natural gas, are currently very popular among leading launch providers, but these fuels can be extremely dangerous if not handled properly and require very complex ground systems to properly utilize. The solution to this problem is to use propane or butane.

Both propane and butane are typically stored in a liquid state and transition to a gaseous state when introduced to standard atmospheric conditions. In this sense, they have the same autogenous property as the oxidizer used in the experiments discussed above. Propane and butane are also easily purchased in containers large enough to fuel

this liquid rocket while also providing similar combustion characteristics to ethanol. Another upside to using propane or butane is that both aerosolize extremely easily, unlike ethanol. The current push-to-connect injector design would mix propane or butane extremely well with nitrous oxide.

The simplest and most practical way to alleviate the issues that arose from the use of different nozzles throughout the test fire campaign is to use a machined graphite nozzle. Graphite has the mechanical and chemical properties to withstand the heat and pressures that this engine is capable of generating. Using a graphite nozzle would allow the flow to remain choked at the throat, maintaining the area ratio and overall engine performance.

Bibliography

[1] Dunbar B. A pictorial history of rockets. https://www.pcsb.org/cms/lib/FL01903687/Centricity/Domain/4681/Rockets_History.pdf, year unknown. 1

[2] K. Mars. 95 years ago: Goddard's first liquid-fueled rocket. https://www.nasa.gov/feature/95-years-ago-goddard-s-first-liquid-fueled-rocket, year unknown. 1

[3] National Air and Space Museum. Missile, surface-to-surface, v-2 (a-4). https://airandspace.si.edu/collection-objects/missile-surface-surface-v-24/nasm_A19600342000#:~:text=Brief%20Description,ancestors%20of%20today's%20launch%20vehicles, year unknown. 1

[4] Gosselin A. M. Technical paper session 1-a - automated ground umbilical systems (agus) project. https://commons.erau.edu/cgi/viewcontent.cgi?referer=https://www.google.com/&httpsredir=1&article=3435&context=space-congress-proceedings, year unknown. 3, 4

[5] United States Department of Education. Science, technology, engineering and math (stem) education. https://www.ed.gov/sites/ed/files/about/overview/budget/budget15/crosscuttingissues/stem.pdf, 2014. 3

[6] Ambrose M. Schwarber A. Final fy20 appropriations: Stem education. https://ww2.aip.org/fyi/2020/final-fy20-appropriations-stem-education, 2020. 3

[7] Rocket Proejct at UCLA. Project ares. https://www.rocketproject.seas.ucla.edu/ares.html, 2025. 3

[8] MIT Rocket Team. Project. https://rocketry.mit.edu/projects, 2025. 3

[9] Yellow Jacket Space Program. Programs. https://www.gtspaceprogram.com/programs, 2025. 3

[10] Knights Experimental Rocketry. Far dollar-per-foot liquid bipropellent. https://www.kxrucf.com/dpf, 2025. 3

[11] Experimental Sounding Rocket Assosciation. The space shuttle. https://www.soundingrocket.org/, 2025. 3

[12] Eckhart J. Goodwin J. Nasa student launch. https://www.nasa.gov/learning-resources/nasa-student-launch/, 2025. 3

[13] Kloudbusters. The argonia cup challenge. https://www.nasa.gov/learning-resources/nasa-student-launch/, 2025. 3

[14] Friends of Amatuer Rocketry. Dpf and tcpf challenge. https://friendsofamateurrocketry.org/dpf-challenge/, 2024. 3

[15] NASA. The space shuttle. https://www.nasa.gov/reference/the-space-shuttle/#:~:text=An%20idea%20born%20in%20unsettled,the%20road%20to%20space%20exploration., 2023. 5

[16] Colburn B. The urbanski-colburn valve for hybrid motors. https://aeroconsystems.com/cart/the-urbanski-colburn-valve-for-hybrid-motors, year unknown. 6, 7

[17] Sanders T. 54mm complete motor system. https://contrailrockets.com/product-category/75mm-mono-motor/75mm-mono-compete-set, 2022. 7, 9

[18] MacMillen A. hybrid rocket motor tutorial. https://www.macmillen.com/rockets/hybrid_tutorial.html, 2006. 8

[19] Lyne J.E Naoumov V.Scoles J. Dodge M. Elton B. Wozniak P. Austin D. Combs C. First steps in the development and testing of nontoxic, bioderived fuels for hybrid rocket motors. https://arc.aiaa.org/doi/abs/10.2514/6.2005-741, 2005. 9

[20] Scholes J.D. Bio-derived fuels for hybrid rocket motors. https://trace.tennessee.edu/utk_gradthes/4571, 2005. 9

[21] Pfeffer D.L. Lard used as a fuel for hybrid rocket motors. https://trace.tennessee.edu/utk_gradthes/313, 2007. 9

[22] Quigley N. Lyne J.E. Development of a three-dimensional printed, liquid-cooled nozzle for a hybrid rocket motor. http://dx.doi.org/10.2514/1.B354553, 2014. 9

[23] Lyne J.E. et al. The use of a 3-d printed, polymer matrix containing pulverized fuel in a hybrid rocket. http://dx.doi.org/10.2514/6.2018-4597, 2018. 9

[24] Aarant T. et al. The development of a powder-filled, abs matrix for use as fuel in a hybrid rocket motor. http://dx.doi.org/10.2514/6.2019-4417, 2019. 9

[25] Barnhil et al.. Design and development of hybrid rocket for spaceport america cup. https://trace.tennessee.edu/utk_chanhonoproj/2307, 2019. 9

[26] White F. M. *Fluid Mechanics Eighth Edition*. McGraw-Hill, 2016. 15

[27] Sutton G. P. and O. Bilbarz. *Rocket Propulsion Elements*. John Wiley & Sons, Inc, 2017. 17, 19

[28] Airgas an Air Liquide company. Safety data sheet nitrous oxide. https://www.airgas.com/msds/001042.pdf, 2021. 25

[29] Airgas an Air Liquide company. Safety data sheet oxygen, refrigerated liquid. https://www.airgas.com/msds/001190.pdf, 2021. 25

[30] Thermo Fisher Scientific. Safety data sheet hydrogen peroxide (30% in water). https://www.fishersci.com/store/msds?partNumber=BP2633500&productDescription=HYDROGEN+PEROXIDE+30%25%2C+500ML&vendorId=VN00033897&countryCode=US&language=en, 2021. 25

[31] HalfCat Rocketry. Chambersafe. https://www.halfcatrocketry.com/chambersafe, 2022. 27, 29

[32] Gill G. S. and Nurick W. H. Liquid rocket engine injectors. https://contrailrockets.com/product/54mm-complete-motor-system-2, 1976. 32

[33] Phillip J. et. al. Development and testing of a nitrous-oxide/ethanolbi-propellant rocket engine. https://doi.org/10.2514/6.2016-5092, 2016. 32, 34

[34] Xie Y. et. al. Review on spray characteristics of liquid–liquid injectors in liquid rocket engines. 10.1063/5.0223894, 2024. 33

[35] Youngblood S.H. Design and testing of a liquid nitrous oxide and ethanol fueled rocket engine. https://www.nmt.edu/academics/mecheng/faculty/mhargather/docs/Youngblood2015.pdf, 2015. 34

[36] Weismiller M.R. Lee J.G. Yetter R.A. Temperature measurements of al containing nano-thermite reactions using multi-wavelength pyrometry. https://www.sciencedirect.com/science/article/pii/S1540748910001616?via%3Dihub, 2010. 37, 50

[37] Naud D. et al. Feasibility study on the use of nanoscale thermites for lead-free electric matches. https://www.jpyro.co.uk/wp-content/uploads/K07_016_vy4n.pdf, 2003. 38

[38] NASA Technical Report. Solid rocket motor igniters. https://ntrs.nasa.gov/citations/19710020870, 1971. 39

[39] Rae P.J Dickson P.M. A review of the mechanism bywhich exploding bridge-wiredetonators function. https://doi.org/10.1098/rspa.2019.0120, 2019. 39

[40] Dreizin E.L. Berman C.H. Vicenzi E.P. Condensed-phase modifications in magnesium particle combustion in air. https://www.sciencedirect.com/science/article/pii/S0010218000001012, 2000. 39

[41] Ponomarenko A. Rocket propulsion analysis sowftware+engineering ug. https://www.rocket-propulsion.com/index.htm, 2025. 44

[42] HalfCatRocketry. Halfcatsim. https://www.halfcatrocketry.com/halfcatsim, 2025. 44

[43] Simpson D. A. Comparative risks of hydrostatic and pneumatic pipeline testing. asme. j. pressure vessel technology. https://doi.org/10.1115/1.4046981, 2020. 52

Appendix A

Igniter Designs

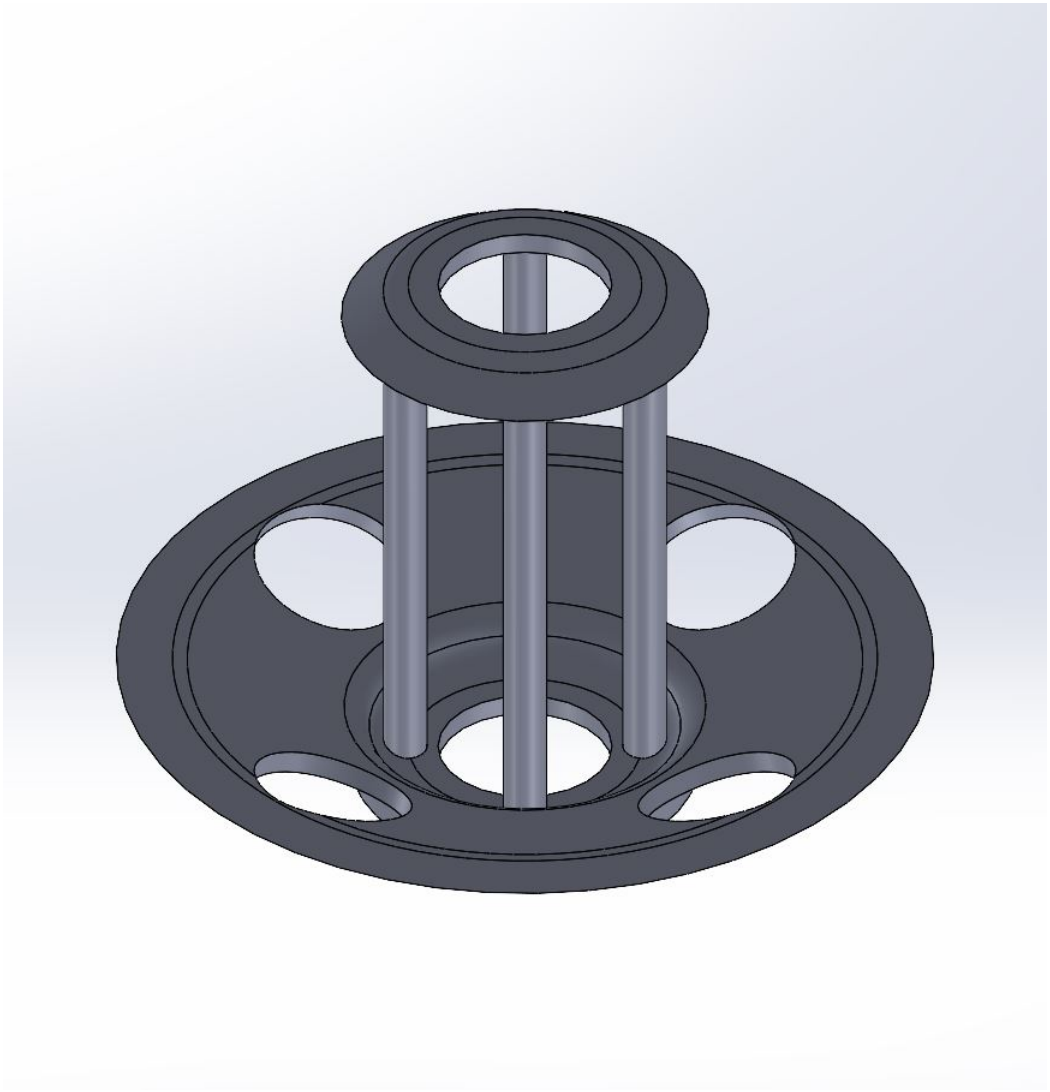


Figure A.1: Igniter 1 Design, OD = 1.88 in., Height = 1.35 in.

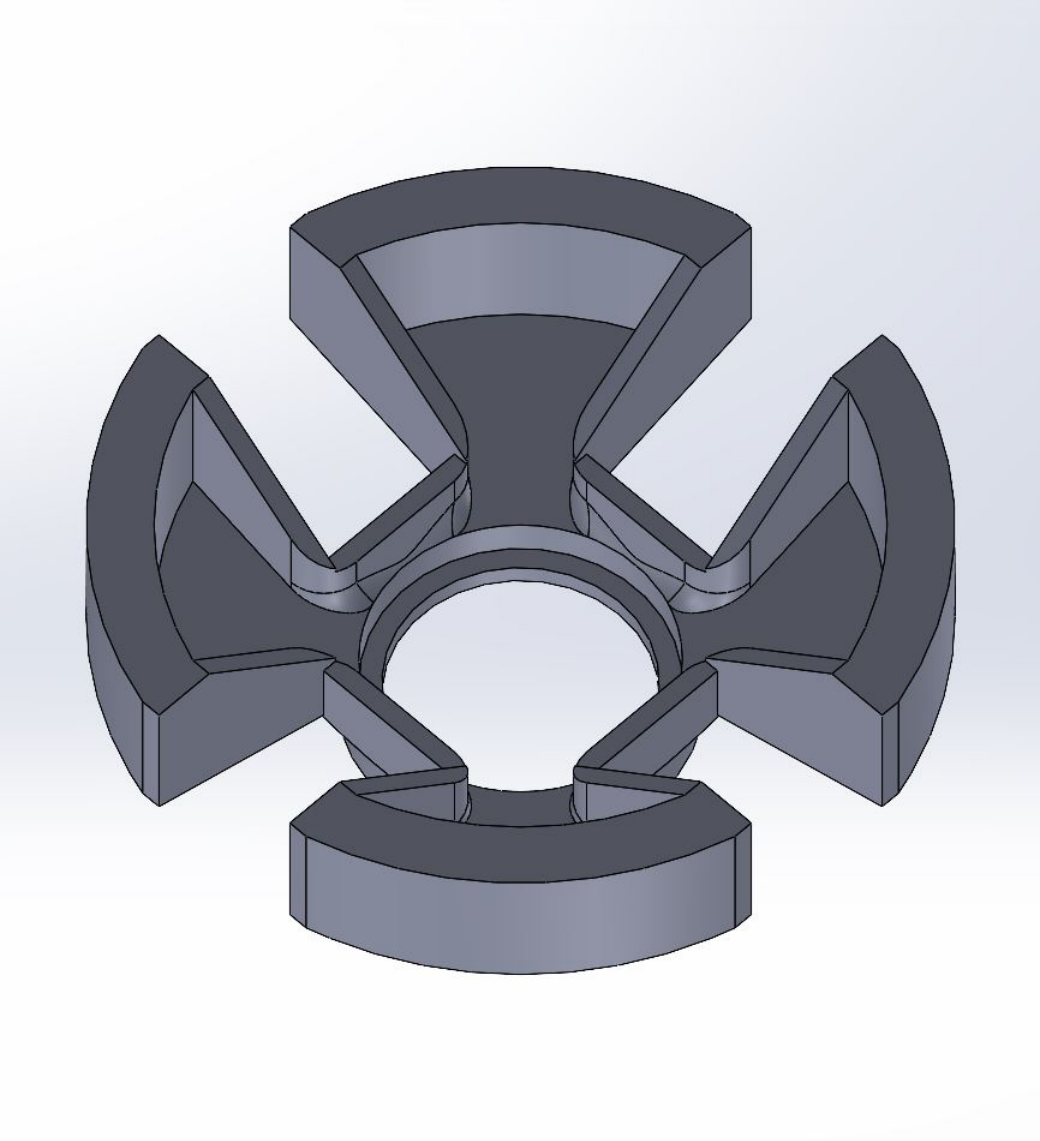


Figure A.2: Igniter 2 Design, OD = 1.88 in., Height = 0.65 in.

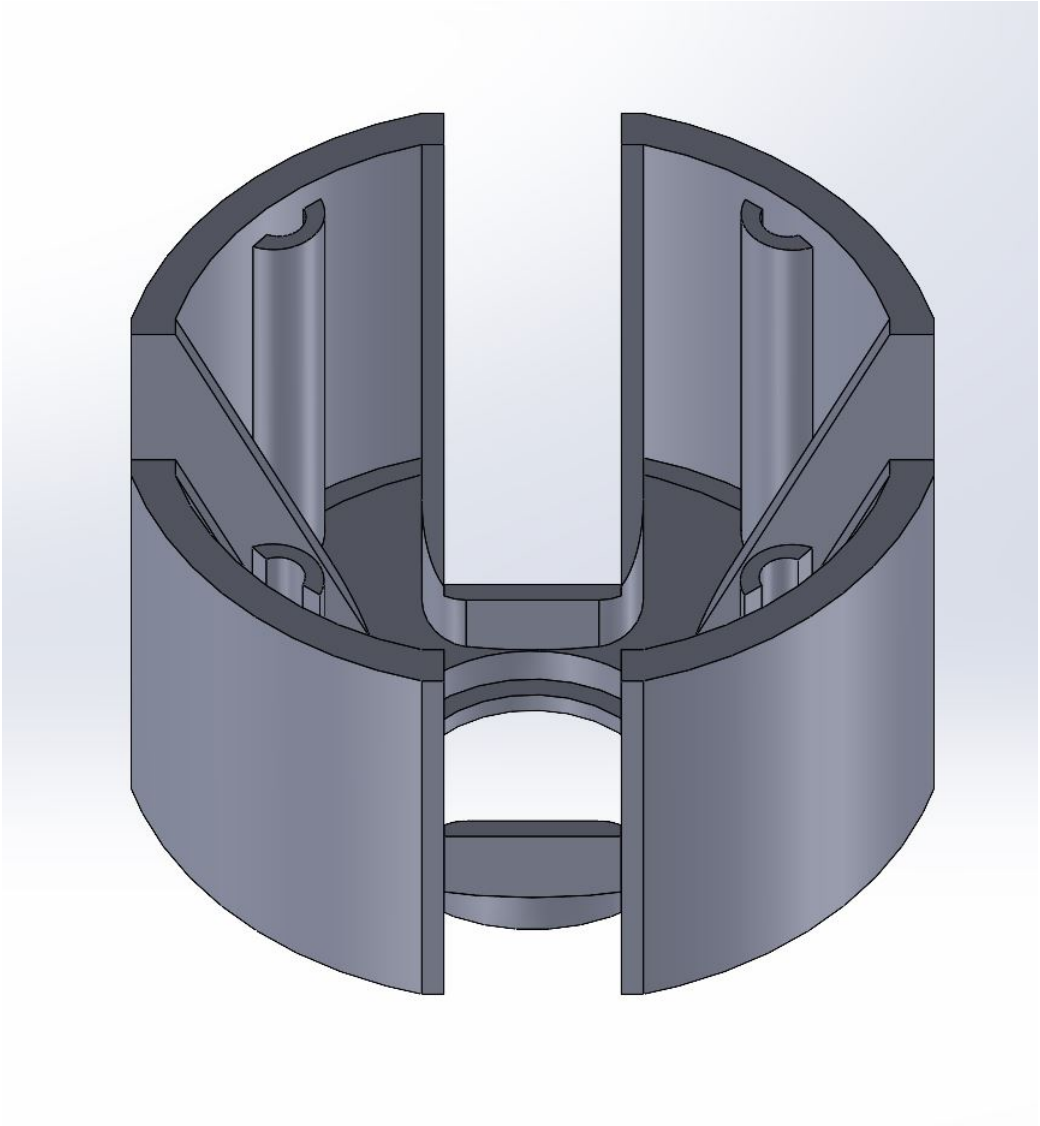


Figure A.3: Igniter 3 Design, OD = 1.88 in., Height = 1.30 in.

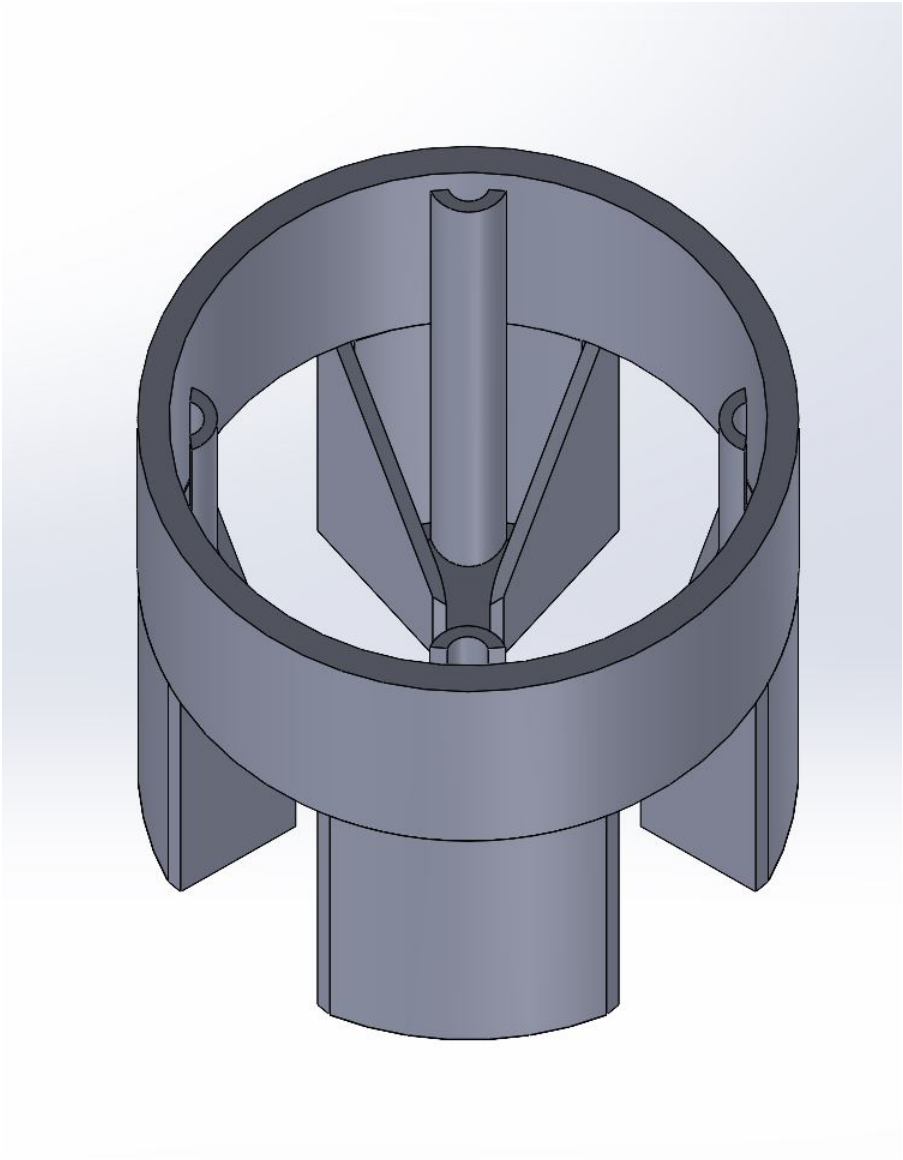


Figure A.4: Igniter 7 Design, OD = 1.88 in., Height = 1.91 in.

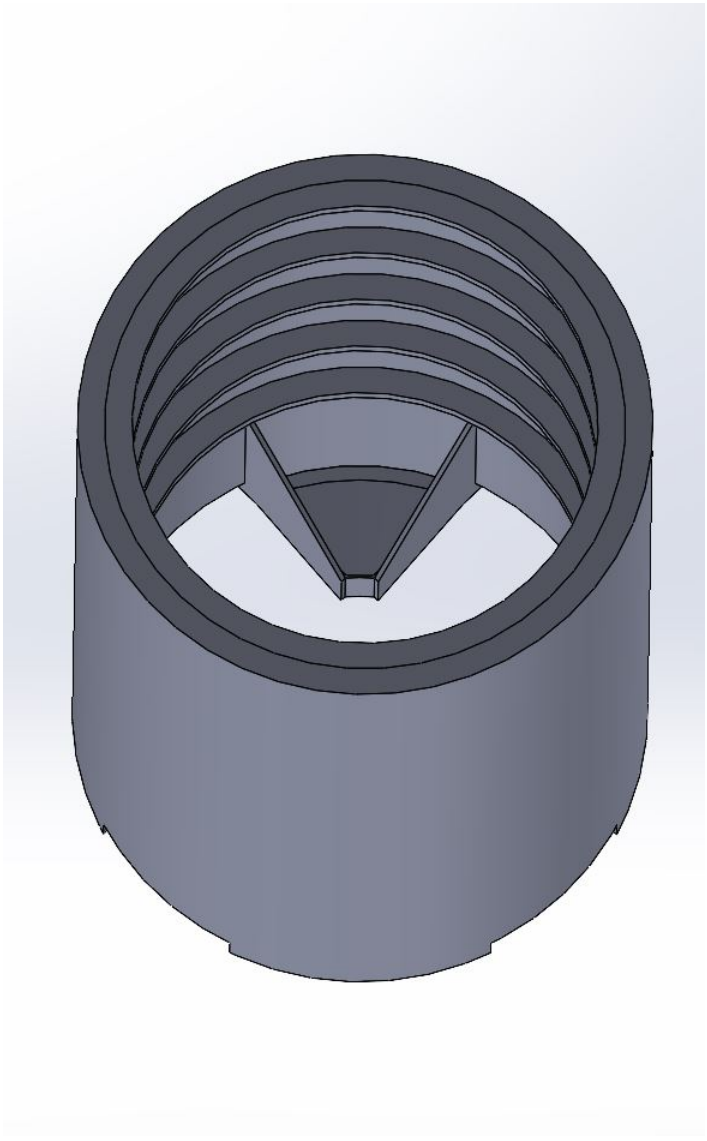


Figure A.5: Igniter 8 Design, OD = 2.1 in., Height = 3.2 in.

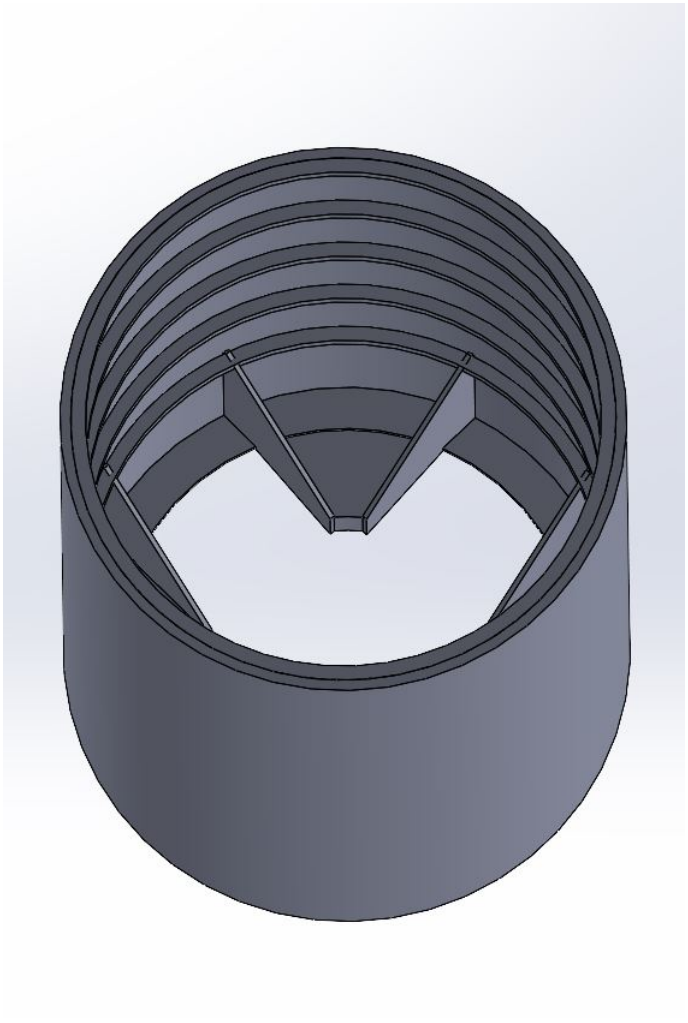


Figure A.6: Igniter 9 Design, OD = 2.1 in., Height = 3.2 in.

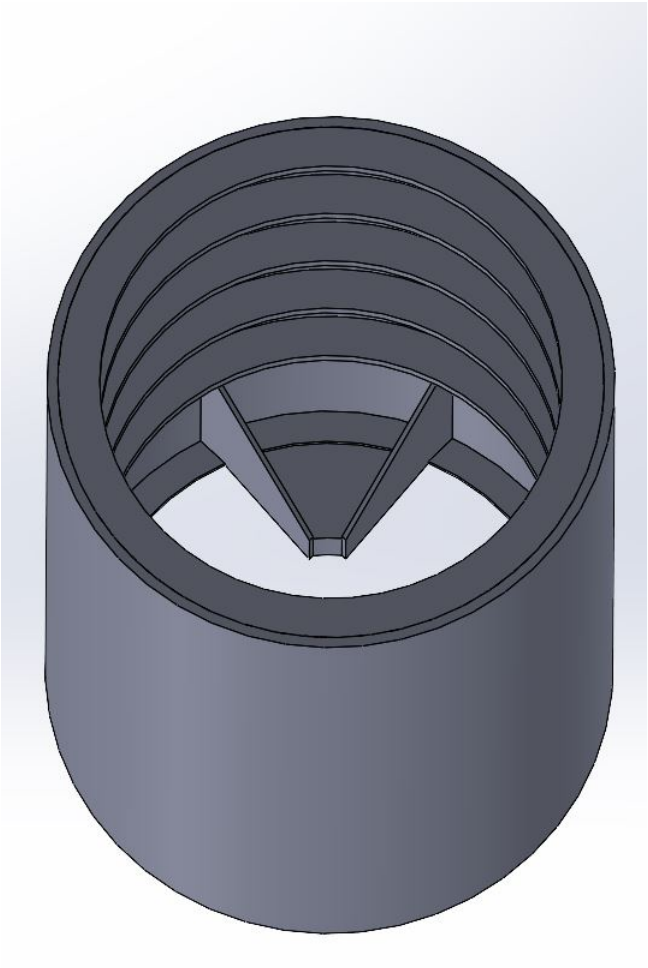


Figure A.7: Igniter 10 Design, OD = 2.1 in., Height = 3.2 in.

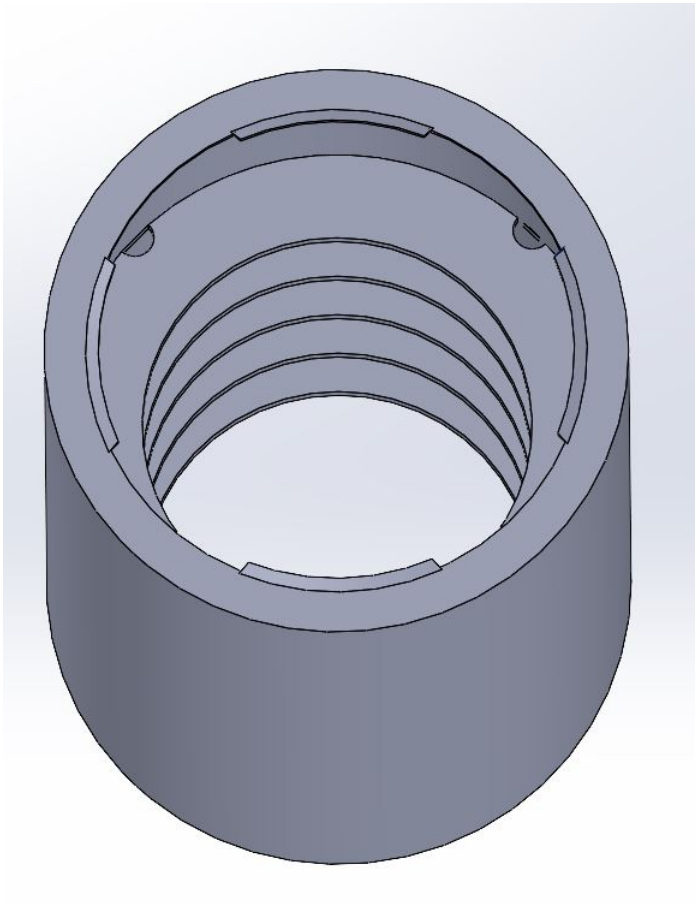


Figure A.8: Igniter 11 Design, OD = 2.1 in., Height = 3.02 in.

Appendix B

Post Test Fire Engine Disassembly Pictures

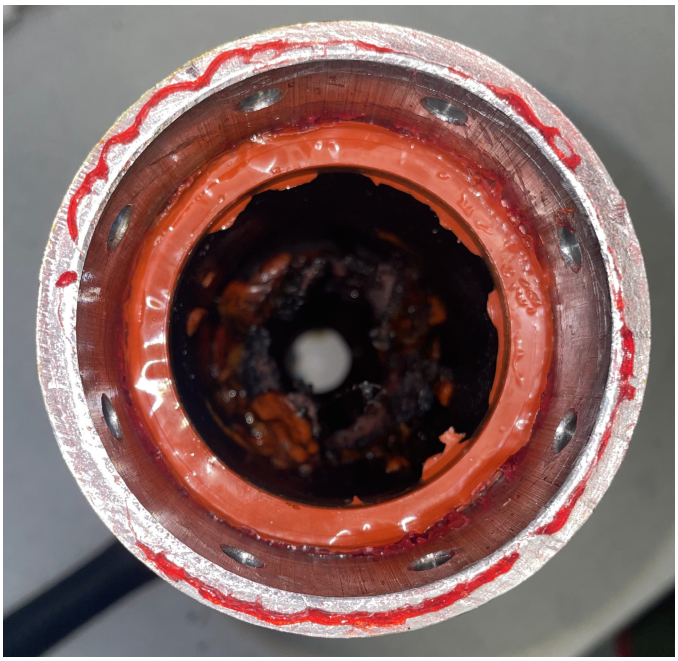


Figure B.1: Combustion Chamber post 5/2/23 Test Fire



Figure B.2: Injector Post 5/2/23 Test Fire



Figure B.3: Oxidizer Tank Post 5/2/23 Test Fire



Figure B.4: Combustion Chamber Post 5/11/23 Test Fire



Figure B.5: Combustion Chamber Alternate View Post 5/11/23 Test Fire



Figure B.6: Injector Post 5/11/23 Test Fire



Figure B.7: Oxidizer Tank Post 5/11/23 Test Fire



Figure B.8: Nozzle Inlet Post 5/11/23 Test Fire



Figure B.9: Nozzle Outlet Post 5/11/23 Test Fire



Figure B.10: Nozzle Carrier Inlet Post 5/11/23 Test Fire



Figure B.11: Nozzle Carrier Inlet Post 5/11/23 Test Fire

Appendix C

Liquid Engine Data Analysis Code

The following is the MATLAB^{TM} code used to analyze and plot the data received from the liquid rocket engine tests.

```
1
2  % Data and Calculations for Vega Rocket Engine
3  % Matthew Dale Thesis "The Novel Use of the Urbanski-
       Colburn Valve for
4  % Liquid Bi-Propellant Rocket Engines"
5
6  clc, close all,clear all, format long g
7
8  load Engine_Data.mat
9
10 g = 32.2; %ft/s^2
11 At = pi*0.4^2; % Throat Area of nozzle, in
12
13 Time_Data_Ideal = Ideal_Thrust(:,1);
14 Thrust_Data_Ideal = Ideal_Thrust(:,2);
15
```

```
Time_Data_5_2_23 = Data_5_2_23(:,1);
Thrust_Data_5_2_23 = Data_5_2_23(:,2);
Bottle_Pressure_Data_5_2_23 = Data_5_2_23(:,3);
Chamber_Pressure_Data_5_2_23 = Data_5_2_23(:,4);
m_dot_5_2_23 = ((Thrust_Data_5_2_23(end) -
   Thrust_Data_5_2_23(1))/(Time_Data_5_2_23(end) -
   Time_Data_5_2_23(1)))
%fuel_diff_5_11_23 = Thrust_Data_5_11_23(1) +
   m_dot_5_11_23 *(Time_Data_5_11_23 - Time_Data_5_11_23
   (1));
%adjusted_thrust_5_11_23 = Thrust_Data_5_11_23 -
   fuel_diff_5_11_23;
Tot_Impulse_5_2_23 = trapz(Time_Data_5_2_23,
   Thrust_Data_5_2_23)
Isp_5_2_23 = Tot_Impulse_5_2_23/(Time_Data_5_2_23(end)*(
   m_dot_5_2_23))
c_5_2_23 = Isp_5_2_23*g; %effective exhaust velocity
C_Star_5_2_23 = (Chamber_Pressure_Data_5_2_23(6)*At)/(
   m_dot_5_2_23/g) %Characteristic Velocity
CF_5_2_23 = c_5_2_23/C_Star_5_2_23; % Thrust Coefficient

Time_Data_5_11_23 = Data_5_11_23(:,1);
Thrust_Data_5_11_23 = Data_5_11_23(:,2);
Bottle_Pressure_Data_5_11_23 = Data_5_11_23(:,3);
Chamber_Pressure_Data_5_11_23 = Data_5_11_23(:,4);
Tot_Prop_5_11_23 = 9.0313; % from raw data and knowing 2
   lbs of ethanol were used
```

```
m_dot_5_11_23 = (Tot_Prop_5_11_23/(Time_Data_5_11_23(end)-
    Time_Data_5_11_23(1)))
%(Thrust_Data_5_23_23(end) - Thrust_Data_5_23_23(1))/(
    Time_Data_5_23_23(end) - Time_Data_5_23_23(1))
%fuel_diff_5_23_23 = Thrust_Data_5_23_23(1) +
    m_dot_5_23_23 *(Time_Data_5_23_23 - Time_Data_5_23_23
    (1));
%adjusted_thrust_5_23_23 = Thrust_Data_5_23_23 -
    fuel_diff_5_23_23;
Tot_Impulse_5_11_23 = trapz(Time_Data_5_11_23,
    Thrust_Data_5_11_23);
Isp_5_11_23 = Tot_Impulse_5_11_23/(Time_Data_5_11_23(end)
    *(m_dot_5_11_23))
c_5_11_23 = Isp_5_11_23*g; %effective exhaust velocity
C_Star_5_11_23 = (Chamber_Pressure_Data_5_11_23(33)*At)/(
    m_dot_5_11_23/g) %Characteristic Velocity
CF_11_23 = c_5_11_23/C_Star_5_11_23; % Thrust Coefficient

Time_Data_2_27_24 = Data_2_27_24(:,1);
Thrust_Data_2_27_24 = Data_2_27_24(:,2);
m_dot_2_27_24 = (Thrust_Data_2_27_24(end) -
    Thrust_Data_2_27_24(1))/(Time_Data_2_27_24(end) -
    Time_Data_2_27_24(1))
Tot_Impulse_2_27_24 = trapz(Time_Data_2_27_24,
    Thrust_Data_2_27_24);
Isp_2_27_24 = Tot_Impulse_2_27_24/(Time_Data_2_27_24(end)*
    m_dot_2_27_24);
c_2_2_24 = Isp_2_27_24*g %effective exhaust velocity
```

```
50
51 Time_Data_4_11_24 = Data_4_11_24(:,1);
52 Thrust_Data_4_11_24 = Data_4_11_24(:,2);
53 Tot_Prop_4_11_24 = 6.8; %lbs
54 m_dot_4_11_24 = (Tot_Prop_4_11_24/(Time_Data_4_11_24(end)-
     Time_Data_4_11_24(1)))
55 Tot_Impulse_4_11_24 = trapz(Time_Data_4_11_24,
     Thrust_Data_4_11_24);
56 Isp_4_11_24 = Tot_Impulse_4_11_24/(Time_Data_4_11_24(end)
     *(m_dot_4_11_24));
57 c_4_11_24 = Isp_4_11_24*g %effective exhaust velocity
58
59 figure ()
60 plot(Time_Data_5_2_23, Thrust_Data_5_2_23, 'Color', 'blue'
     )
61 hold on
62 plot(0.438,219.848, 'ko', 'Color', 'red')
63 hold on
64 plot(Time_Data_Ideal, Thrust_Data_Ideal, "--", 'Color', '
     black')
65 hold off
66 xlabel('Time (s)')
67 ylabel('Thrust (lb)')
68 xlim([-0.25 10])
69 ylim([-15 275])
70 title('Thrust vs. Time 5/2/23')
```

```
71 str = {['Total Impulse: ', num2str(round(
      Tot_Impulse_5_2_23)), ' lb-s'], ['Specific Impulse: ',
      num2str(round(Isp_5_2_23)), ' sec'],...
72 ['Peak Thrust: ', num2str(round(max(Thrust_Data_5_2_23))),
       ' lbs']};
73 dim = [.7 .5 .3 .3];
74 annotation('textbox', dim, 'String', str, 'FitBoxToText',
      'on');
75 legend('Thrust Data 5/2/23','Peak Thrust', 'HalfCatSim
      Data')
76
77 figure ()
78 plot(Time_Data_5_2_23, Bottle_Pressure_Data_5_2_23)
79 hold on
80 plot(Time_Data_5_2_23,Chamber_Pressure_Data_5_2_23)
81 title('Pressure vs. Time 5/2/23')
82 xlabel('Time (s)')
83 ylabel('Pressure (psi)')
84 legend('N2O Tank Pressure', 'Combustion Chamber Pressure')
85
86 figure()
87 plot(Time_Data_5_11_23, Thrust_Data_5_11_23, 'Color', 'red
      ')
88 hold on
89 plot(2.714,393.264, 'ko', 'Color', 'red')
90 hold on
91 plot(Time_Data_Ideal, Thrust_Data_Ideal, "--", 'Color', '
      black')
```

```
92  hold off
93  xlabel('Time (s)')
94  ylabel('Thrust (lb)')
95  xlim([-0.25 11.5])
96  ylim([-15 415])
97  title('Thrust vs. Time 5/11/23')
98  str = {['Total Impulse: ', num2str(round(
       Tot_Impulse_5_23_23)), ' lb-s'], ['Specific Impulse: ',
        num2str(round(Isp_5_23_23)), ' sec'],...
99  ['Peak Thrust: ', num2str(round(max(Thrust_Data_5_23_23)))
       , ' lbs']};
100 dim = [.65 .5 .3 .3];
101 annotation('textbox', dim, 'String', str, 'FitBoxToText',
       'on');
102 legend('Thrust Data 5/11/23','Peak Thrust', 'HalfCatSim
       Data')
103
104 figure ()
105 title('Pressure vs. Time 5/11/23')
106 plot(Time_Data_5_11_23, Bottle_Pressure_Data_5_11_23)
107 hold on
108 plot(Time_Data_5_11_23,Chamber_Pressure_Data_5_11_23)
109 title('Pressure vs. Time 5/11/23')
110 xlabel('Time (s)')
111 ylabel('Pressure (psi)')
112 legend('N2O Tank Pressure', 'Combustion Chamber Pressure')
113
114
```

```
figure()
plot(Time_Data_2_27_24, Thrust_Data_2_27_24, 'Color', '
    cyan')
hold on
plot(1.262,154.24, 'ko', 'Color', 'red')
hold on
plot(Time_Data_Ideal, Thrust_Data_Ideal, "--", 'Color', '
    black')
hold off
xlabel('Time (s)')
ylabel('Thrust (lb)')
xlim([-.25 8])
ylim([-15 275])
title('Thrust vs. Time 2/27/24')
str = {['Total Impulse: ', num2str(round(
    Tot_Impulse_2_27_24)), ' lb-s'], ['Specific Impulse: ',
     num2str(round(Isp_2_27_24)), ' sec'],...
['Peak Thrust: ', num2str(round(max(Thrust_Data_2_27_24)))
    , ' lbs']};
dim = [.7 .5 .3 .3];
annotation('textbox', dim, 'String', str, 'FitBoxToText',
    'on');
legend('Thrust Data 2/27/24','Peak Thrust', 'HalfCatSim
    Data')

figure()
plot(Time_Data_4_11_24, Thrust_Data_4_11_24, 'Color', '
    magenta')
```

```
135 hold on
136 plot(0.22,187.53, 'ko', 'Color', 'red')
137 hold on
138 plot(Time_Data_Ideal, Thrust_Data_Ideal, "--", 'Color', '
    black')
139 hold off
140 xlabel('Time (s)')
141 ylabel('Thrust (lb)')
142 title('Thrust vs. Time 4/11/24')
143 xlim([-0.5 10]);
144 ylim([-15 275])
145 str = {['Total Impulse: ', num2str(round(
    Tot_Impulse_4_11_24)), ' lb-s'], ['Specific Impulse: ',
     num2str(round(Isp_4_11_24)), ' sec'],...
146 ['Peak Thrust: ', num2str(round(max(Thrust_Data_4_11_24)))
    , ' lbs']};
147 dim = [.7 .5 .3 .3];  % position of the annotation in
    normalized figure units
148 annotation('textbox', dim, 'String', str, 'FitBoxToText',
    'on');
149 legend('Thrust Data 4/11/24','Peak Thrust', 'HalfCatSim
    Data')
150
151 figure ()
152 plot(Time_Data_5_2_23, Thrust_Data_5_2_23, 'Color', 'blue'
    )
153 hold on
```

```
154 plot(Time_Data_5_11_23, Thrust_Data_5_11_23, 'Color', 'red
    ')
155 hold on
156 plot(Time_Data_2_27_24, Thrust_Data_2_27_24, 'Color', '
    cyan')
157 hold on
158 plot(Time_Data_4_11_24, Thrust_Data_4_11_24, 'Color', '
    magenta')
159 hold on
160 plot(Time_Data_Ideal, Thrust_Data_Ideal, "--", 'Color', '
    black')
161 xlabel('Time (s)')
162 ylabel('Thrust (lb)')
163 xlim([-.25 11.5]);
164 ylim([-15 415])
165 legend('Thrust Data 5/2/23', 'Thrust Data 5/11/23', '
    Thrust Data 2/27/24', 'Thrust Data 4/11/24', '
    HalfCatSim Data')
166 title('All Test Fire Thrust vs. Time Data')
```

Vita

Matthew Dale grew up in Germantown, Tennessee before pursuing a Bachelor's Degree in Aerospace Engineering at the University of Tennessee. After graduating, he began his Master's in Aerospace Engineering at the University of Tennessee. When Matthew completed his academic course work, he accepted a job at Blue Origin in Cape Canaveral, Florida. While supporting the activation of pad systems, hot fires of the first and second stages, and the inaugural launch of Blue Origin's New Glenn launch vehicle, he continued his work on this thesis. After graduation, Matthew will continue his work at Launch Complex 36 supporting the launch of New Glenn and the many exciting things to come. He is grateful for all the support he has received throughout this journey and looks forward to what the next chapter of life brings him.